THERMODYNAMIC AND STRUCTURAL STUDIES OF AQUEOUS CHELATING AGENTS AND THEIR METAL COMPLEXES AT VARIOUS TEMPERATURES AND PRESSURES

DIETHYLENETRIAMINEPENTAACETIC ACID (DTPA) AND TARTARIC ACID

WEI XIE

THERMODYNAMIC AND STRUCTURAL STUDIES OF AQUEOUS CHELATING AGENTS AND THEIR METAL COMPLEXES AT VARIOUS TEMPERATURES AND PRESSURES

DIETHYLENETRIAMINEPENTAACETIC ACID (DTPA) AND TARTARIC ACID

by

Wei Xie

A thesis submitted to the
School of Graduate Studies
in partial fulfilment of the
requirements for the degree of
Master of Science

Department of Chemistry
Memorial University of Newfoundland

May, 1999

St John's Newfoundland

Abstract

Chelating agents are used in many industrial applications including cleaning conventional boilers, decontaminating nuclear power systems and treating oil wells to remove scales and certain clay minerals. Standard partial molar heat capacities C_p° and volumes V° are important in this context because they define the temperature- and pressure-dependence of the stability constants, respectively. They are also of considerable interest in the development of semi-empirical models and simulations of ionic solvation, because both are sensitive indicators of hydration effects. In this research, we have studied the thermodynamic and structural properties of (i) aqueous diethylenetriamine-pentaacetic acid (DTPA) and its metal complexes, and (ii) aqueous tartaric acid and its sodium salts, to examine the effects of temperature and pressure.

The apparent molar heat capacities and volumes of aqueous DTPA species, Na_3H_2DTPA (aq) and Na_5DTPA (aq), and metal complexes, $Na_3CuDTPA$ (aq), $NaCu_2DTPA$ (aq), $Na_3NiDTPA$ (aq), $Na_2FeDTPA$ (aq) and NaFeHDTPA (aq) were determined over a range of temperatures between 283 to 328 K by a Sodev Picker flow micro-calorimeter and vibrating-tube densimeter at a pressure of 0.1 MPa. The experimental results were analyzed by means of the Guggenheim form of the extended Debye-Hückel equation to obtain C_p°, V° and expressions for the excess properties. The revised Helgeson-Kirkham-Flowers (HKF) model has been used to represent the

temperature-dependence of these standard partial molar properties within the experimental uncertainty. It was found that, while the values of C_p^o and V^o of DTPA species and metal complexes are charge dependent, the metal complexes show regular behavior despite the complexity in their structures and charge distribution. Widely applicable predictive methods to estimate the "non-Born" contributions to the partial molar heat capacities and volumes of the complexes of metal ions (M^{Z+}) with the chelating agents, $EDTA^{4-}$ (aq), and $DTPA^{5-}$ (aq) over a wide range of temperature were developed using the Cu^{2+} complex as a model system. The results may also be applicable to nitrilotriacetic acid (NTA) complexes.

The apparent molar heat capacity of L-tartaric acid (H_2Tar,aq) and its sodium salts, NaHTar (aq) and Na_2Tar (aq), at temperatures from 283 to 328 K, and the apparent molar volume of H_2Tar(aq) and sodium tartrate (Na_2Tar, aq) at temperatures 283 to 530 K, and pressures up to 10MPa were determined. The behavior of V_2^o (Na_2Tar, aq) over the whole temperature range is typical of most electrolytes. Unusual behavior observed for V^o (H_2Tar, aq) at temperatures above 473 K reflects the attractive interactions between tartaric acid molecules and water because of the strong hydrogen-bonding. Various semi-empirical solvation models were used to extrapolate standard partial molar properties of tartaric acid and sodium tartrate to elevated temperatures.

Acknowledgments

During the course of my graduate studies at Memorial University, many people helped me, both formally and informally, and it is my great pleasure to acknowledge their help here.

I want to express my sincere appreciation and gratitude to my supervisor, Dr. Peter R. Tremaine for his guidance, inspiration and patience throughout the course of this work, and my thanks to Dr. M. H. Brooker and Dr. R. A. Poirier, my supervisory committee, for contributing their time, ideas, lab equipment and friendship during my project and thesis. I also want to thank Dr. F. R. Smith for his help and encouragement in my instrumental analysis course.

For the good times and help of many different kinds, special thanks are extended to my wonderful group colleagues: Dr. D. Chvedov, Dr. C. Xiao, Dr. L. Trevani, Mr. Zhongning Wang, Mr. Rodney Clarke, Mr. Brent Hawrylak, Mr. Chris Collins, and Miss Tram Pham. This list would certainly be incomplete without acknowledging Dr. John Bridson and Mr. David Miller for their assistance with the single crystal X-ray diffraction.

I want to thank Dr. Peter R. Tremaine and his family again for their great help to me and my family during a family emergency, and I thank my wife Bing Li and my son Lijia Xie for their support, understanding, and encouragement.

Financial support from the following is gratefully acknowledged: the Natural Science and Engineering Research of Canada (NSERC), an OLI/DuPont Unrestricted Grant, and Memorial University of Newfoundland.

Table of Contents

List of Tables

List of Figures

List of Abbreviations and Symbols

Abbreviations

aq	Aqueous
DHLL	Debye-Hückel limiting law
DTPA	Diethylenetriaminepentaacetic acid
exp	Experimental
HKF	Helgeson-Kirkham-Flowers (equation)
NTA	Nitrilotriacetic acid
rel	Chemical relaxation contribution

Symbols

a, b, c	Unit cell axial lengths
A_C, A_V	DHLL slope for apparent molar heat capacity and volume
Å	Angstrom (length, 1Å = 10^{-10} m)
c_p	Massic heat capacity
C_p^o	Standard partial molar heat capacity in water
C_p^o (I = 0.1)	Standard partial molar heat capacity in I = 0.1 mol kg^{-1} supporting electrolyte
$C_{p,\phi}$	Apparent molar heat capacity
D_c	Density of single crystal
F	Molality fraction

F(000)	The structure factor for the unit cell, which is equal to the total number of electrons in the unit cell
$\|F_o\|$, $\|F_c\|$	Amplitudes of structure factors observed ($\|F_o\|$), and calculated ($\|F_c\|$) from a postulated trial structure
G	Gibbs free energy
H	Enthalpy
I	Ionic strength; Intensity
K	Densimeter constant; Equilibrium constant
m	Molality
M	Molar mass
n_i	Number of moles of species i
p	Pressure
r_i	Radius of ion i
R	Gas constant, 8.314 $J \cdot K^{-1} \cdot mol^{-1}$; Discrepancy index
T	Temperature
V	Volume
$V°$	Standard partial molar volume in water
$V°$ (I = 0.1)	Standard partial molar volume in I = 0.1 mol kg^{-1} supporting electrolyte
V_ϕ	Partial molar volume
Z	Charge; Number of molecules in a unit cell
α	Degree of dissociation; Interaxial angles

α_l^*	Thermal expansivity of water
β	Degree of dissociation; Interaxial angles
$\beta^{(o)Y}$, $\beta^{(1)Y}$	Adjustable parameters in the Pitzer equation for apparent molar properties
β_l^*	Isothermal compressibility of water
γ	Average activity coefficient; Interaxial angles
δ	Excess mixing term in Young's rule
η	A constant defined in Born equations
Θ	Solvent temperature parameter, equal to 228 K in HKF equations
θ	The glancing angle (complement of the angle of incidence) of the X-ray beam to the "reflecting plane". 2θ is the deviation of the diffracted beam from the direct X-Ray beam
λ	Wavelength, usually that of the radiation used in the diffraction experiment
μ	Linear absorption coefficient
ν	Stoichiometry number
ρ	Density
ρ_l^*	Density of water
τ	Resonance period of the vibrating tube densitometer
ϕ	Practical osmotic coefficient
ω	Valence factor
ω_{Born}	Born coefficient
ε	Dielectric constant

List of Appendices

Chapter I. Introduction

Chelating agents are used in many industrial applications including environmental cleanup of heavy meals, boiler water treatment, nuclear reactor decontamination and oil well treatments. Chemical and geochemical equilibrium models of these processes require stability constant data over a range of temperatures and pressures. Standard partial molar heat capacities C_p^o and volumes V^o are important in this context because they define the temperature- and pressure-dependence of the stability constants, respectively. Standard partial molar heat capacities and volumes are also of considerable interest in the development of semi-empirical models and simulations of ionic solvation, because both are sensitive indicators of hydration effects.

This research consisted of two parts. The objective of the first part was to study the thermodynamic and structural properties of aqueous diethylenetriaminepentaacetic acid (DTPA) and its metal complexes by determining the apparent molar heat capacities and volumes of different DTPA and metal complexes in aqueous solutions, and to interpret the results by semi-empirical hydration models. Predictive methods for estimating "missing" values of C_p^o and V^o for complexes with other metals were developed. The objective of the second part was to determine the apparent molar heat capacities and volumes of tartaric acid and its sodium salts over a wide range of temperatures and pressures, as a means of examining the effect of ionization on hydration

and the success of various models used to extrapolate standard molar properties to elevated temperatures.

The standard partial molar heat capacity and volume were calculated from experimentally determined apparent molar heat capacities and volumes, obtained from measurements with a Picker flow micro-calorimeter and vibrating-tube densitometers. The excess properties were treated with activity coefficient models, and the resulting standard state partial molar properties were described by theoretical models, such as the Helgeson-Kirkham-Flowers (HKF) equations (Helgeson *et al.*, 1976, 1981), and the density model. Various calculations were required to obtain these fundamental thermodynamic properties. These include the determination of temperature-dependent equilibrium constants and enthalpies of related reactions, the hydrolysis or dissociation of ions in solutions containing mixed electrolytes and systems comprised of two or more coupled equilibria, and chemical relaxation effects to correct for the shift in the degree of dissociation caused by the temperature increment in the heat capacity measurement.

I.1 Thermodynamics of Aqueous Solutions

I.1.1 Apparent and Partial Molar Properties

An extensive thermodynamic property Y (such as Gibbs free energy, enthalpy, entropy, heat capacity or volume, etc) of a solution containing n moles of an electrolyte in 1 kg of water can be expressed as:

$$Y = n_1 Y_1^* + \sum_i n_i Y_i \tag{I.1}$$

where n_1 and n_i are the number of moles of the solvent and ion, respectively; and Y_1^* and Y_i are the partial molar properties of the pure solvent and ion, respectively, defined as:

$$Y_i = \left(\frac{\partial Y}{\partial n_i}\right)_{T,p,n_{j\neq i}} \tag{I.2}$$

Partial molar properties are often calculated from apparent molar properties, while the latter can be determined directly by the experiment. By definition, an apparent molar property is expressed as:

$$Y_\phi = \frac{Y - n_1 Y_1^*}{n_2} \tag{I.3}$$

where n_1 and n_2 are the number of moles of pure solvent and solute, respectively, Y is the value of the extensive property for the total quantity of the solution, and Y_1^* is the molar property of the pure solvent. The apparent molar volume V_ϕ of the solute is the change in the volume of the solution per mole of solute when n_2 moles of a solute are added to n_1 moles of water. Apparent molar properties are calculated from the quantities directly

measured, for example, the apparent molar volume V_ϕ and $C_{p,\phi}$ are given by the following equations, when molality is used as the composition variable:

$$V_\phi = \frac{1000(\rho_1^\bullet - \rho)}{m\rho_1^\bullet\rho} + \frac{M_2}{\rho} \tag{I.4}$$

and

$$C_{p,\phi} = \frac{c_p(1000 + mM_2) - 1000c_{p,1}^\bullet}{m} \tag{I.5}$$

where M_2 is the molar mass of the solute, $\rho_1^\bullet$ and $c_{p,1}^\bullet$ are the density ($g{\cdot}cm^{-3}$) and the specific heat capacity ($J{\cdot}K^{-1}{\cdot}g^{-1}$) of pure solvent, respectively; ρ and c_p are the density and the specific heat capacity of the solution, respectively.

Standard partial molar properties of aqueous electrolytes give insight into the nature of the ion-solvent interactions, and are experimentally accessible from volumetric, calorimetric, or emf studies. Usually, their determination requires the extrapolation of experimental data to infinite dilution, and consequently, their values are known with an accuracy which is limited, both by the experimental uncertainty and also by the reliability of the extrapolation procedure. Among the various standard state properties, the partial molar heat capacity and partial molar volume are the most important and extensively studied because they are directly related to changes of the Gibbs free energy with

temperature and pressure , as expressed in the following equations:

$$\left(\frac{\partial \Delta_r G^o}{\partial T}\right)_p = \Delta_r S^o \tag{I.6a}$$

$$\left(\frac{\partial \Delta_r S^o}{\partial T}\right)_p = \Delta_r C_p^o \tag{I.6b}$$

$$\left(\frac{\partial \Delta_r G^o}{\partial p}\right)_T = \Delta_r V^o \tag{I.6c}$$

$$\begin{aligned}\Delta_r G^o &= \Delta_r G^o(T_r, p_r) - \Delta_r S^o(T_r, p_r) \\ &+ \int_{T_r}^{T} \Delta_r C_p^o dT - T\int_{T_r}^{T} \frac{\Delta_r C_p^o}{T} dT + \int_{p_r}^{p} \Delta_r V_T^o dp\end{aligned} \tag{I.6d}$$

Here $\Delta_r C_p^o$, $\Delta_r V^o$ and $\Delta_r S^o$ are the standard heat capacity, volume, and entropy of reaction, respectively; and T_r and p_r are the reference temperature and pressure, respectively.

I.1.2 Standard State and Excess Properties

All apparent molar properties can be expressed in terms of ideal properties and

excess properties:

$$Y_\phi = Y_i^{id} + Y_i^{ex} \tag{I.7}$$

where Y_i^{id} is the infinite dilution value according to ideal Henry's law behaviour, and Y_i^{ex} is the excess partial molar property that accounts for the ion-ion interactions in aqueous electrolyte solutions. Y_i^{ex} is related to $RT\ln\gamma_i$ or the temperature and pressure derivatives of this quantity.

If the apparent molar properties are determined for a range of composition, the partial molar properties can be calculated by differentiation. By differentiating equation (I.3) partially with respect to n_2, we have:

$$\left(\frac{\partial Y}{\partial n_2}\right)_{T,p,n_1} = \overline{Y}_2 = n_2\left(\frac{\partial Y_\phi}{\partial n_2}\right)_{n_1} + Y_\phi \tag{I.8}$$

and since the molality m is defined for constant n_1, equation (I.8) becomes:

$$\overline{Y}_2 = m\left(\frac{\partial Y_\phi}{\partial m}\right) + Y_\phi \tag{I.9}$$

By definition, a standard state property Y^o is equal to the partial molar property at infinite dilution:

$$Y^o = \lim_{m \to 0} \overline{Y} = \lim_{m \to 0} Y_\phi \tag{I.10}$$

For electrolytes, the Debye-Hückel equation has been found to be an effective tool for extrapolation:

$$Y_\phi = Y^o + \omega A_Y I^{1/2} \tag{I.11}$$

where the Debye-Hückel limiting slope ωA_Y is known from theory.

By convention, the standard partial molar properties of ions are defined in relation to the corresponding standard partial molar quantity of the hydrogen ion. These "conventional" single ion properties are defined as:

$$Y_i^{o*} = Y_i^o - Z_i Y_{H^+}^o \tag{I.12}$$

where $Y_{H^+}^o \equiv 0$. Any standard partial molar property of the ith aqueous electrolyte is

related to the corresponding absolute standard partial properties of its constituent ions by:

$$Y_i^o = \sum \nu_{i,j} Y_j^{oabs} \tag{I.13}$$

where the subscripts i and j refer to the electrolyte and ion, respectively. The conventional standard partial molar properties of the jth ion can also be defined by:

$$Y_j^o = Y_j^{oabs} - Z_j Y_{H+}^{oabs} \tag{I.14}$$

where $Y_{H^-}^{oabs}$ refers to the absolute standard partial molar property of the H^- ion. There are many proposed routes for the determination of the absolute standard partial molar heat capacity and volume of hydrogen ion. In the current study we chose C_p^{oabs} (H^-, aq) = -71 J K^{-1} mol^{-1} and V^{oabs} (H^-, aq) = -6.4 cm^3 mol^{-1}, based on the assumption of Y^o (Ph_4As^-, aq) = Y^o (Ph_4B^-, aq) (Marcus, 1985; Abraham and Marcus, 1986).

There are many statistical mechanical approaches to calculate the excess thermodynamic properties of electrolyte systems. Two of these, an extended Debye-Hückel theory and the Pitzer ion interaction model, are presented in section I.2.4.

I.2 Thermodynamic Models for Standard Partial Molar Properties

As mentioned above, aqueous electrolyte systems are present in many industrial processes as well as in natural environments and the need for thermodynamic information under extreme conditions of temperature and pressure is still growing. Generally, there are two ways to satisfy these demands: direct experimental measurements, or semi-empirical and theoretical predictions of the desired property. Despite the rapid increase in recent years of experimental data for the thermodynamic properties of aqueous electrolytes at high temperature and pressure, the amount of available data is still small compared to the actual requirements, because of the technical difficulties in the design and operation of equipment. Therefore, it is very necessary to develop reliable estimation and extrapolation techniques for the prediction of the thermodynamic properties that have not been studied experimentally. In this section, several theoretical models used in the current study will be described.

I.2.1 Solvation Effects

In electrolyte solution theory, it is quite common to consider the solvent as a continuum characterized only by its dielectric constant and density, while ions are viewed as charged spheres. In the solvation process, these charged spheres are transferred from a fixed point in a vacuum to a cavity in the dielectric, and the difference in the work necessary to charge the spheres in vacuum and in the dielectric is associated with the electrostatic Gibbs free energy of transfer. The first crude and approximate model to

calculate ion-solvent interactions was suggested by Born (1920). According to the Born model, the change in Gibbs free energy corresponding to the difference between charging a sphere of radius r_i to $Z_i e$ in the incompressible dielectric continuum and in vacuum is given by:

$$\Delta_s G^o_{Born} = \frac{-\eta Z_i^2}{r_i}\left(1-\frac{1}{\varepsilon}\right)$$
$$\eta = \frac{e^2 N_A}{8\pi\varepsilon_o} \tag{I.15}$$

where N_A is Avogadro's constant, ε_o is the permittivity of a vacuum, ε is the static dielectric constant of the solvent, and e is the charge of one electron.

Other thermodynamic properties can be derived from the expression for $\Delta_s G^o_{Born}$. For example:

$$\Delta_s V^o_{Born} = \left(\frac{\partial \Delta_s G^o}{\partial T}\right)_T = \frac{\eta Z_i^2}{r_i}\left(\frac{\partial \ln \varepsilon}{\partial p}\right)_T \tag{I.16}$$

and

$$\Delta_s C^o_{p,Born} = T\left(\frac{\partial \Delta_s S^o}{\partial T}\right)_p = \frac{\eta Z_i^2 T}{r_i}\left[\left(\frac{\partial^2 \ln \varepsilon}{\partial T^2}\right)_p - \left(\frac{\partial \ln \varepsilon}{\partial T}\right)_p^2\right] \tag{I.17}$$

The practical application of the Born model is based largely on the use of an "effective radius" for the solvated ion (Tanger and Helgeson, 1988). Because of the dielectric saturation caused by the high electric field of the ions and the presence of a localized "first" hydration sphere, it is expected that the dielectric constant in the vicinity of ions is much lower than that of bulk water. While this effect was not taken into consideration in the primitive Born model, its approach to ion-solvent interactions, and the fact that it gave answers of the same order of magnitude as experiment, helped to confirm the hypothesis that ions exist in solution. Moreover, the Born model provides a simple and important equation for calculating the role of long-range solvent polarization in the hydration of simple ions (Cobble and Murray, 1977).

I.2.2 The Helgeson Kirkham Flowers Model

Helgeson *et al.* (1981) developed an equation of state for the standard partial molar properties of aqueous ions and electrolytes based on the assumption that the standard partial molar properties consist of two parts: (i) an electrostatic part, which is expressed in terms of a modified Born equation in which the effective electrostatic radius of the aqueous ion is regarded as a function of pressure and temperature, (ii) a non-electrostatic part, which was assumed to be composed of an intrinsic part, that decreases in magnitude with increasing temperature and pressure.

In the Helgeson-Kirkham-Flowers (HKF) model, the standard partial molar volume of species i was given by:

$$V_i^o = a_{1,i} + a_{2,i}p + \frac{a_{3,i} + a_{4,i}pT}{T - \Theta} - \omega_{Born,i}Q \tag{I.18}$$

where p and T refer to the pressure in bars and temperature in K. The terms a_{ij} are adjustable parameters that are independent of temperature and pressure, and Θ = 228 K is a solvent-dependent parameter associated with the anomalous behaviour of supercooled water (Angell, 1982). The terms Q and ω_{Born} in equation are derived from the Born equation and given by:

$$Q = \frac{1}{\varepsilon}\left(\frac{\partial \ln \varepsilon}{\partial p}\right)_T \tag{I.19}$$

$$\omega_{Born,i} = \frac{\eta Z_i^2}{r_{e,i}} \tag{I.20}$$

where Z_i is the charge of the ith ion and $\eta = 6.9466\times10^6$ nm·J·mol^{-1} = 6.9466×10^5 nm·cm^3·bar·mol^{-1}; $r_{e,i}$ is an effective electrostatic radius of the ion: $r_{e,i} = r_{cryst} + 0.94\ Z_i$ for cations; and $r_{e,i} = r_{cryst}$ for anions.

The isobaric temperature dependence of the standard partial molar heat capacity was represented by:

$$C^{o}_{p,i} = c_{1,i} + \frac{c_{2,i}T}{(T-\Theta)^2} + \omega_{Born,i}TX \tag{I.21}$$

where c_{ij} is a temperature and pressure independent adjustable parameter, and X is given by:

$$X = \frac{1}{\varepsilon}\left[\left(\frac{\partial^2 \ln\varepsilon}{\partial T^2}\right)_p - \left(\frac{\partial \ln\varepsilon}{\partial T}\right)_p^2\right] \tag{I.22}$$

The parameters for the HKF equation were obtained for many electrolytes by regression analysis from experimental values of C^{o}_{p} and V^{o} of electrolytes with prototypical ions over a wide range of temperature and pressure (Shock and Helgeson, 1988). A computer code for calculating the standard state thermodynamic properties of aqueous electrolytes over a temperature range of 273 to 1000K and pressures up to 500 MPa according to HKF theory is now available (Johnson *et al.*, 1992). Despite the fact that the physical interpretation of the non-electrostatic contribution to these quantities has not been clearly established, the HKF equations reproduce the experimental results of the

standard state properties of aqueous electrolytes quite well, and the HKF approach has been widely used in the modelling of geochemical systems and in some industrial applications.

I.2.3 The Density Model

Analysing the dissociation constant of aqueous electrolytes which behave as strong electrolytes at room temperature, Franck (1956, 1961) showed that at constant temperature there was a linear relationship between the logarithm of their dissociation constants and the logarithm of the solvent density. Based on this observation, Mesmer *et al.* (1985) suggested an equation to calculate ln K at high temperature and pressure:

$$\log K = a + \frac{b}{T} + \frac{c}{T^2} + \frac{d}{T^3} + \left(e + \frac{f}{T} + \frac{g}{T^2}\right) \log \rho_l^* \qquad \text{(I.23)}$$

where ρ_l^* is the density of water. Using only the a, b, and f terms and natural logarithms, equation (I.23) can be rewritten as:

$$\ln K = p_1 + p_2 / T + (p_3 \cdot \ln \rho_l^*) / T \qquad \text{(I.24)}$$

where p_1, p_2, and p_3 are constants, independent of T and p.

Equation (I.24), which gives K as a function of ρ_1^* (T,p), is thermodynamically equivalent to an equation which gives the Gibbs free energy of reaction $\Delta_r G^\circ$, as a function of T and p. Therefore, there are implicit relationships between the parameters p_1, p_2, and p_3 and all other standard state thermodynamic parameters. For example, the partial molar enthalpy of reaction could be obtained from the following relationships:

$$\Delta G^\circ = -RT \ln K \tag{I.25}$$

and

$$\Delta H^\circ = \left(\frac{\partial(\Delta G^\circ / T)}{\partial(1/T)} \right)_p \tag{I.26}$$

so that

$$\Delta H^\circ = -R(p_2 + p_3(T\alpha + \ln \rho_1^*)) \tag{I.27}$$

where α_1^* is the coefficient of thermal expansion of water. Similarly ΔC_p° can be obtained by:

$$\Delta C_p^\circ = \left(\frac{\partial \Delta H^\circ}{\partial T} \right)_p = -RTp_3 \left(\frac{\partial \alpha_1^*}{\partial T} \right)_p \tag{I.28}$$

or

$$p_3 = -\frac{\Delta C^{o}_{p_r}}{RT_r(\partial\alpha^{*}_{l} / \partial T)_{p_r}} \tag{I.29}$$

Here r refers to the reference state (T_r = 298.15 K, p_r = 0.1MPa). A similar expression could be obtained for partial molar volume:

$$\Delta V^{o} = \frac{\Delta C^{o}_{p_r} \cdot \beta^{*}_{l}}{T_r(\partial\alpha^{*}_{l} / \partial T)_{p_r}} \tag{I.30}$$

where β^{*}_{l} is the coefficient of the compressibility of water.

The complete expression for ln K is:

$$\begin{aligned} \ln K = \ln K_r &- \frac{\Delta H^{o}_{r}}{R}\left(\frac{1}{T} - \frac{1}{T_r}\right) \\ &+ \frac{\Delta C^{o}_{p_r}}{RT_r(\partial\alpha^{*}_{l} / \partial T)_{p_r}}\left(\frac{1}{T}\ln\frac{\rho^{*}_{l,r}}{\rho^{*}_{l}} - \frac{\alpha^{*}_{l,r}}{T}(T - T_r)\right) \end{aligned} \tag{I.31}$$

To use this equation, one needs only the values of ln K, ΔH^{o}, and ΔC^{o}_{p} for the reaction at 298.15 K and 0.1 MPa, or any other reference state, as well as the density of

the solvent at the desired T, p conditions. To obtain the values of ΔC_p° and ΔV° for the reaction at T, p, values of α_1^* and β_1^* for the solvent are also required. For reactions for which ln K, ΔH°, and ΔC_p° at 298.15 K are available but little else, the density model is one of the best ways to obtain estimates of ln K and other parameters at higher temperatures and pressures.

I.2.4 The Activity Coefficient Models

I.2.4.1 The Debye-Hückel Equation

One of the major breakthroughs in electrolyte solution theory was the derivation of the well-known Debye-Hückel theory (Debye and Hückel, 1923), which described the limiting law behaviour of the activity coefficients of electrolyte solutions.

The Debye-Hückel equation for mean molar stoichiometric ion activity coefficients is:

$$\log \gamma_{\pm} = \frac{-|Z_+ Z_-| A_\phi I^{1/2}}{1 + \sigma B I^{1/2}} \tag{I.32}$$

where Z_+ and Z_- are the valences of the cation and anion constituents of the salt, A_ϕ is the Debye-Hückel limiting law (DHLL) slope for the activity coefficient, I is the ionic strength, σ is the D-H distance of closest approach in units of angstroms, and B equals $50.29\rho_1^{*1/2}/(T\varepsilon)^{1/2}$. Here ρ_1^* and ε refer to the density and dielectric constant of pure water

at the T and p of interest, the product of σB usually approximates unity. The ionic strength I is defined by the following sum over all anions and cations:

$$I = \frac{1}{2}\sum_i m_i Z_i^2 \tag{I.33}$$

Because the Debye-Hückel equation considers only long-range electrostatic interactions between ions, it can not be expected to be accurate for solutions above a certain limiting concentration. It may easily be calculated that only 2 or 3 solvent molecules separate individual ions in a 1 molar solution. At very low concentrations, the second term in the denominator of (I.32) becomes insignificant and the equation (I.32) reduces to:

$$\log \gamma_{\pm} = -|Z_+ Z_-| A_\phi I^{1/2} \tag{I.34}$$

This is called the Debye-Hückel limiting law and has the advantage of being simpler because it dose not include the adjustable σ parameter; however, because of this, it can not be used at concentrations above approximately 10^{-3} m.

It is well known that the Debye-Hückel theory gives correct limiting behaviour for electrolytes at infinite dilution, and that it is also useful at finite but very low

concentrations. Because of this, many attempts have been made to extend the range of the validity of the D-H theory. For example, for the apparent molar heat capacity and volume, the extended Debye-Hückel equations in Guggeheim's form are often used:

$$C_{p,\phi} = C_p^o + 1.5|Z_+Z_-|A_J[I - 2I^{1/2} + 2\ln(1 + I^{1/2})]/I + B_J I \qquad (I.35)$$

$$V_\phi = V^o + 1.5|Z_+Z_-|A_v[I - 2I^{1/2} + 2\ln(1 + I^{1/2})]/I + B_v I \qquad (I.36)$$

I.2.4.2 The Pitzer Ion Interaction Model

In the 1970s, Pitzer and coworkers developed a theoretical model for electrolyte solutions which combined the Debye-Hückel equation with additional terms in the form of a virial equation. This has proven to be extraordinarily successful at fitting the behaviour of both single- and mixed-salt solutions to high concentrations.

The Pitzer model adds a simple extended version of the Debye-Hückel limiting law to a virial expansion representing ion-ion interactions and begins by describing the total excess free energy of an electrolyte solution as:

$$\frac{G^{EX}}{RT} = w_w f(I) + \frac{1}{w_w}\sum_{ij}\lambda_{ij}(I)n_i n_j + \frac{1}{w_w}\sum_{ijk}\mu_{ijk}n_i n_j n_k + \cdots, \qquad (I.37)$$

where w_w is the mass of water in kg, and n_i, n_j, and n_k are the moles of solute i, j, and k. The term f(I) is a version of the DHLL dependent only on ionic strength. The quantities $\lambda_{ij}(I)$ and μ_{ijk} are second and third virial coefficients added to account for short-range interactions at higher concentrations. $\lambda_{ij}(I)$ applies to interactions of pairs of ions i and j, and μ_{ijk} to interactions of the ions i, j, k three at a time.

For a single ionic solute, $M^{z_{M^+}}_{\nu_M} X^{z_{X^-}}_{\nu_X}$, equation (I.37) simplifies to:

$$\frac{G^{EX}}{RT} = w_w f(I) + \frac{2}{w_w} n_M n_X \left(B_{MX} + \frac{1}{w_w} n_M z_M C_{MX} \right) \tag{I.38}$$

where the expressions for f(I) and B_{MX} are described as:

$$f = -\frac{4IA_\phi}{b} \ln(1 + bI^{1/2}) \tag{I.39}$$

$$B_{MX} = \beta^{(0)}_{MX} + \beta^{(1)}_{MX} g(\alpha_1 I^{1/2}) + \beta^{(2)}_{MX} g(\alpha_1 I^{1/2}) \tag{I.40}$$

$$g(x) = \frac{2[1 - (1 + x)\exp(-x)]}{x^2} \tag{I.41}$$

From the relationship of the osmotic coefficient to the excess Gibbs free energy, one

could derive the following expressions:

$$\phi - 1 = -(\sum_i m_i)^{-1}\left(\frac{\partial G^{EX}/RT}{\partial w_w}\right)_{T,p,n_i}$$
$$= |z_+ z_-| f^{\phi} + m\left(\frac{2\nu_M \nu_X}{\nu}\right) B^{\phi}_{MX} + m^2\left[\frac{2(\nu_M \nu_X)^{3/2}}{\nu}\right] C^{\phi}_{MX} \qquad \text{(I.42)}$$

then the mean activity coefficient for the pure electrolyte is obtained by differentiation of equation (I.38) followed by an appropriate combination of γ_M with γ_X to yield $\gamma\pm$:

$$\ln \gamma_i = \left(\frac{\partial(G^{EX}/RT)}{\partial n_i}\right)_{T,p,w_w,n_{j\neq i}} \qquad \text{(I.43)}$$

$$\ln \gamma_{\pm} = |z_M z_X| f^{\gamma} + m\left(\frac{2\nu_M \nu_X}{\nu}\right) B^{\gamma}_{MX}$$
$$+ m^2\left[\frac{2(\nu_M \nu_X)^{3/2}}{\nu}\right] C^{\gamma}_{MX} \qquad \text{(I.44)}$$

Many summaries and detailed reviews of the Pitzer ion interaction model have been provided by Pitzer (1979, 1987, 1991), Harvie and Weare (1980), and Weare (1987). In this current study, we only used the expressions for heat capacity and volume from the Pitzer model. The detailed calculations are discussed in Chapter III.

The most remarkable thing about the Pitzer model is that the parameters derived from one- and two-salt systems can be used with success to predict behaviour in systems containing many more ionic components. For example, the Pitzer model has been used to successfully represent the thermodynamic properties of systems such as Na^+-HCO_3^--CO_3^{2-}-Cl^--CO_2-H_2O, H^+-HSO_4^--SO_4^{2-}-H_2O, and H^+-K^+-$H_2PO_4^-$-H_3PO_4-H_2O, over a wide range of concentration and temperature (Peiper and Pitzer, 1982; Pitzer *et al.*, 1977; Pitzer and Silvester, 1976).

I.3 Chelating Agents

I.3.1 Literature Review

Equilibrium constants and enthalpies for the stepwise ionization of DTPA, tartaric acid, and the formation of their metal complexes at 298.15 K and 0.1 MPa have been widely studied (Anderegg and Malik, 1976; Letkeman and Martell, 1979; Chaberek *et al.*, 1958; Wright *et al.*, 1965, etc.). Several sources of critically compiled data are available (Martell and Smith, 1982, 1997; Pettit and Powell, 1997). To ensure self consistency wherever possible, we have adopted data from Martell and Smith (1982,1997). The data cited and corresponding literature sources are listed in Tables I.1 and I.2. The only study

on temperature-dependent thermodynamic functions for the stepwise ionization of DTPA acid in aqueous solution over the range 283 to 313 K, and ionic strength, 0.1 m has been done by Milyukov and Polenova (1981), and these results were used to calculate the high temperature values of log K and ΔH°. A similar study on the dissociation constants of tartaric acid from temperature 273 to 323 K by Bates and Canham (1951) was also used in the related calculations presented in Chapter V.

No studies have been found on the C_p° and V° of aqueous DTPA species and metal complexes at any temperatures. Before the current research, the only reported studies on partial molar heat capacities and volumes of aminopolycarboxylic chelating agents and metal complexes were those on EDTA species and their metal complexes at 298.15 K (Hovey and Tremaine, 1985; Hovey *et al.*, 1988); on Na_2H_2EDTA (aq) and $Na_2CuEDTA$(aq) from 283 to 328 K (Wang, 1998); and on NTA aqueous species and the Cu(II) complex from 283 to 328 K (Wang, 1998), which all are from work done in our lab. For hydroxycarboxylic acid chelating agents, such as tartaric acid, citric acid, etc., apparent and partial molar heat capacities and volumes have been determined at 298.15 K (Høiland and Vikingstad, 1975; Manzurola and Apelblat, 1984; Apelblat and Manzurola, 1990; Sijpkes *et al.*, 1989), but no C_p° and V° data at temperatures above 333 K have ever been reported in the literature.

There are many studies on the structures of DTPA and metal complexes in the solid state and in aqueous solutions. For example, Martell *et al.* (1962) determined the structures of the predominant DTPA species in solution at various pH values by infrared

spectroscopy. The structure of the $NiDTPA^{3-}$ complex in aqueous solution was determined over a wide pH range from PMR studies (Trzebiatowska et al., 1977; Grazynski and Trzebiatowska, 1980). NMR studies on rare-earth DTPA complexes were also reported (Peters, 1988). The crystal structure for $CuH_3DTPA{\cdot}H_2O$ was reported by Seccombe *et al.* (1975), and the structure of Cu_2DTPA^- (aq) was proposed by Siever and Bailar (1962), based on an interpretation of its infrared spectrum. The structures of $[FeH_2DTPA]_2{\cdot}2H_2O$ and $Na_2FeDTPA{\cdot}2H_2O$ complexes were determined by Finnen *et al.* (1991) using X-ray crystallography. Several infrared and Raman studies have been done on solid and aqueous tartaric acid and its metal complexes (Kaneko *et al.*, 1984; Barron *et al.*, 1992; Bhattacharjee *et al.*, 1989), and information about the vibrational modes of tartaric acid and metal complexes has been obtained.

I.3.2 Current Work: Objectives and Significance

Chelating agents are widely used as sequestrants in a number of industrial applications and in many medicinal applications (Yaeger, 1983; Boscolo *et al.*, 1983; Wedeen *et al.*, 1983). Most of these applications focus on the complexation of metal ions with the ligands. Stability constants for the equilibria of most metal ions of interest have been determined at or near 298.15 K, but many of the applications involve temperatures considerably higher than 298.15 K where there are no data available. Values in the range 273 to 310 K are very useful for environmental and medical applications, while data in the range 373 to 573 K are required to model the use of chelating agents in boilers in

conventional and nuclear power systems. The desired stability constants for high temperature solutions can be calculated by combining the known stability constants and enthalpies at 298.15 K with the experimentally determined partial molar heat capacities and volumes of the reactant and product species.

Among the "big three" chelating agents, EDTA, DTPA, and NTA, the DTPA system is the most complicated one. Eight ionized forms of DTPA acid exist in aqueous solution at various pH values. These are discussed in detail in Chapter III. Because neutral or alkaline solutions are used in many industrial and medical applications, and also because of the complexity of the speciation of DTPA acid at low pH range, we chose H_2DTPA^{3-}(aq), $HDTPA^{4-}$(aq), and $DTPA^{5-}$(aq), which are the predominant species at pH > 6.0. In this study, the first objective was to determine the apparent and partial molar heat capacities and volumes of H_2DTPA^{3-}(aq) and $DTPA^{5-}$(aq) from 283 to 328 K, then to estimate the properties of $HDTPA^{4-}$ (aq) by interpolation.

Because it is a multi-dentate ligand, DTPA shows strong ability to form chelates with trivalent cations and either one or two divalent cations. As a transition metal ion, copper(II) has many industrial applications, and it was chosen as a model system in this study. From the available literature studies, the different metal-DTPA complexes are thought to have similar structures which indicates that the partial molar properties of these complexes may show regular behaviour, which raises the possibility of developing predictive models to calculate the partial molar properties of different metal ions at various conditions. As a result, the second objective of this project was to obtain the

apparent and partial molar heat capacities and volumes of $CuDTPA^{3-}$ (aq), Cu_2DTPA^- (aq), $NiDTPA^{3-}$ (aq), $FeDTPA^{2-}$ (aq) and $FeHDTPA^-$(aq) from 283 to 328 K, and develop predictive methods from the experimental results for estimating "missing" values of C_p^o and V^o for complexes with other metal ions.

The hydroxy acid chelating agent, tartaric acid was also of interest in this study, because of its many commercial applications. It is also of fundamental interest because of its simplicity as a small molecule, which shows strong hydrogen-bonding and a different type of complexation behaviour than the aminopolycarboxylic acid ligands. As the stability constants of metal tartrate are much less than those of DTPA complexes, high temperature volumetric data could be determined with the Memorial University platinum vibrating-tube densitometer (Xiao and Tremaine, 1997), which gave insights into the effect of ionization and hydrogen-bonding functional groups on partial molar volumes at elevated temperatures. In the current study, we measured the apparent and partial molar heat capacities and volumes of H_2Tar (aq), NaHTar (aq), and Na_2Tar from 283 to 328 K, and apparent and partial molar volumes of H_2Tar (aq) and Na_2Tar (aq) from 283 to 523 K, pressures up to 10 MPa.

The significance of this study lies in the complexity of the systems chosen for study. This is the first reported C_p^o and V^o study on the DTPA species and their metal complexes, and also the first study on a electrolyte with such a large negative charge, as $DTPA^{5-}$(aq). Data are now available for calculating the properties of free DTPA species using the HKF equation of state. Widely applicable predictive equations were developed

in this study, which make it possible to estimate the standard partial molar properties of DTPA-metal complexes at elevated temperatures. These are expected to be very useful in modelling chemical processes at high temperatures and pressures. This study also first reports the partial molar volume V° data for tartaric acid and sodium tartrate at temperatures above 373 K. The neutral tartaric acid species was found to display unusual behaviour at temperatures above 473 K.

Table I.1. Thermodynamic Constants for the Ionization of $H_5DTPA(aq)$ and Complexation of $DTPA^{5-}(aq)$ with Copper(II), Nickel(II) and Iron(III) at 298.15 K and 0.1m Ionic Strength.[a]

n	log K	ΔH^o	ΔS^o	ΔC_p^o [b]	ΔV^o
	$H_{5-n}DTPA^{n-}(aq) \rightleftharpoons H_{4-n}DTPA^{(n-1)-}(aq) + H^+(aq)$				
0	-2.0±0.2	-2.09	-45.1	-69.7	-
1	-2.70±0.1	1.26	-47.6	-86.5	-
2	-4.28±0.04	6.28	-61.1	-181.2	-
3	-8.60±0.05	17.99	-104.6	-51.6	-
4	-10.50±0.07	33.47	-88.7	-62.8	-
	$Cu^{2+}(aq) + H_2DTPA^{3-}(aq) \rightleftharpoons CuDTPA^{3-}(aq) + 2H^+(aq)$				
	2.1±0.18	-5.44	24.3	-	-
	$Cu^{2+}(aq) + DTPA^{5-}(aq) \rightleftharpoons CuDTPA^{3-}(aq)$				
	21.2±0.3	-56.90	217.6	-	-
	$H^+(aq) + CuDTPA^{3-}(aq) \rightleftharpoons CuHDTPA^{2-}(aq)$				
	4.80±0.1	-	-	-	-
	$H^+(aq) + CuHDTPA^{2-}(aq) \rightleftharpoons CuH_2DTPA^-(aq)$				
	2.96±0.08	-	-	-	-
	$Cu^{2+}(aq) + CuDTPA^{3-}(aq) \rightleftharpoons Cu_2DTPA^-(aq)$				
	6.79±0.0	-	-	-	-

Table I.1. Continued.

n	log K	ΔH°	ΔS°	ΔC_p°	ΔV°
		$Ni^{2+}(aq) + DTPA^{5-}(aq) \rightleftharpoons NiDTPA^{3-}(aq)$			
	20.1±0.1	-46.8	227.6	-	-
		$H^+(aq) + NiDTPA^{3-}(aq) \rightleftharpoons NiHDTPA^{2-}(aq)$			
	5.64±0.04	-	-	-	-
		$Ni^{2+}(aq) + NiDTPA^{3-}(aq) \rightleftharpoons Ni_2DTPA^-(aq)$			
	5.59	-	-	-	-
		$Fe^{3+}(aq) + DTPA^{5-}(aq) \rightleftharpoons FeDTPA^{2-}(aq)$			
	28.0±0.4	-	-	-	-
		$H^+(aq) + DTPA^{5-}(aq) \rightleftharpoons FeHDTPA^-(aq)$			
	3.56	-	-	-	-
		$H^+(aq) + Fe(OH)DTPA^-(aq) \rightleftharpoons FeDTPA^{2-}(aq) + H_2O(l)$			
	9.66	-	-	-	-

[a] log K, ΔH° and ΔS° values are selected from NIST Standard Reference Database 46 Version 4.0, (Smith and Martell, 1997); [b] ΔC_p values are calculated from $d\Delta H/dT$ (Milyukov and Polenova, 1981). Unit: ΔH°, kJ mol^{-1}; ΔS°, J K^{-1} mol^{-1}; ΔC_p°, J K^{-1} mol^{-1}; ΔV°, cm^3 mol^{-1}.

Table I.2. Thermodynamic Constants for the Ionization of Aqueous L-Tartaric Acid (H_2Tar, aq) at 298.15 K and Infinite Dilution.[a]

Reaction	log K	ΔH°	ΔS°
$H_2Tar\ (aq) = H^+\ (aq) + HTar^-\ (aq)$	-3.036	0.75	-81.1
$HTar^-\ (aq) = H^+\ (aq) + Tar^{2-}\ (aq)$	-4.366	2.9	-48.5

[a] log K, ΔH° and ΔS° values are selected from NIST Standard Reference Database 46 Version 4.0, (Smith and Martell, 1997).

Chapter II. Experimental Methods

II. 1 Picker Flow Calorimeter

The heat capacity measurements in this work were performed with a Picker flow micro-calorimeter (Sodev model CP-C), which is described schematically in Figure II.1. The construction and principles of operation have been described in detail previously by Picker *et al.* (1971), Desnoyers *et al.* (1976), Smith-Magowan and Wood (1981), and White and Wood (1982). The calorimeter consists of two symmetrical cells (sample cell and reference cell) that were made of platinum tube to which are connected heaters (Zener diodes) in the up-stream area of each tube and two sensitive temperature sensors in the down-stream area. As the reference fluid (water) flows through the cell, electrical power heats the liquid in each cell so that the temperature rise ΔT is the same. The power applied to the Zener diode of the sample cell W_o can be monitored as a water baseline. When the water in the cell is replaced by a solution to be measured, the power in the sample cell heater can be adjusted by an amount ΔW so that the temperature rise ΔT remains the same. The ratio of power applied to the heaters is proportional to the ratio of heat capacity fluxes through the cell:

$$\frac{c_{p,s}}{c_{p,l}^{\bullet}} = \left(1 + \frac{f\Delta W}{W_o}\right)\left(\frac{\rho_l^{\bullet}}{\rho_s}\right) \qquad \text{(II.1)}$$

where W_o, ΔW, c_p, and ρ are power in the heaters, change of the heating power of the sample cell, massic heat capacity, and density, respectively. The subscript s refers to the solution and $c^*_{p,l}$ and ρ^*_l refer to the pure water. The heat-loss correction factor f may be determined by a calibration based on the specific heat capacities and densities of NaCl(aq) solutions as in the expression (Desnoyers *et al.*, 1976):

$$f = \frac{(c_p\rho)_{std} - c^*_{p,l}\rho^*_l}{(c_p\rho)_{exp} - c^*_{p,l}\rho^*_l} \qquad \text{(II.2)}$$

where $(c_p\rho)_{exp}$ and $(c_p\rho)_{std}$ are the products of the specific heat capacity and density for the standard NaCl(aq) solution measured in the calibration experiments and those calculated from literature data (Archer, 1991), respectively.

In this study, the calorimeter was connected to a Sodev thermal detection unit (model DT-C) that was used for tuning and calibrating the calorimeter and for detecting the output of the differential calorimetric signal. The temperature of the calorimeter was controlled to ±0.01 K by a Sodev high flow, high stability circulating fluid pump (model PC-B) and a temperature control unit (model CT-L). The thermistor (Omega, 44107) used to measure the temperature of densitometer was calibrated with a Hewlett-Packard 2804A quartz-crystal thermometer traceable to NBS standards. The differential output V, voltages across the two heaters V_1 and V_2, the heating current I_o, and the resistance of the thermistor were measured by a Hewlett-Packard (HP 3457A) multichannel digital multi-

meter and were recorded by a computer.

The detection limit of the relative specific heat capacity ($c_{p,s}$ - $c^{\bullet}_{p,l}$) is about 7×10^{-5} $J\cdot K^{-1}\cdot g^{-1}$ if ΔT is set to be 1.6 K. The statistical uncertainty of the relative specific heat capacity has been estimated to be 0.5 per cent (Picker *et al.*, 1971, Desnoyers *et al.*, 1976).

II.2 Vibrating Tube Densitometer

A commercial Sodev 03D vibrating-tube flow densitometer described in detail previously by Picker *et al.* (1974) was used to measure differences between solution and pure water at 298.15 K and 0.1 MPa. High temperature (T > 373 K) and pressure (p > 0.1 MPa) density measurements were performed in a vibrating-tube densitometer (see Figure II.2), constructed according to the design of Albert and Wood (1984), as modified by Corti *et al.* (1990). More completed experimental details are presented elsewhere (Xiao *et al.*, 1997). The densitometer measures the natural period of oscillation of a vibrating tube filled with fluid. At the beginning of an experiment, the reference fluid (water) with density $\rho^{\bullet}_{l}$ was flowed through the vibrating unit at a constant mass flow rate, and the period of oscillation τ_o (water baseline) was monitored. Then a solution of density ρ was introduced into the vibrating tube and the new oscillation period τ (sample plateau) was established and monitored. The density of the solution relative to water was calculated from τ and τ_o by the expression:

$$\Delta\rho = \rho - \rho_o = K(\tau^2 - \tau_o^2) \qquad \text{(II.3)}$$

where K is a calibration constant. The calibration constant was obtained by measuring the period of oscillation for water and another fluid of known density. A standard NaCl(aq) solution was used for daily calibration (m = 1.0 mol·kg^{-1} below T = 328 K; m = 3.0 mol·kg^{-1} below T = 530 K). The reference values of the densities of water and the NaCl(aq) solution were calculated from the equation of state of water reported by Hill (1992) and the equation of state of NaCl(aq) reported by Archer (1992). The reproducibility of the calibration constants over a four day interval was about ± 0.04%.

The temperature of the Sodev 03D vibrating-tube densitometer was controlled to ±0.01 K by a Sodev CT-L circulating bath. The thermistor was calibrated by the same procedure as that for the calorimeter. The temperature of the high-temperature vibrating-tube densitometer was controlled to ±0.02 K by a well-insulated brass oven, with a large thermal mass that surrounded the densitometer tube. The pressure of the flow system was maintained by a nitrogen cylinder and a back-pressure regulator (Tescom model 26-1700) connected to the pressurized reservoir at the exit of the densitometer tube. The system pressure was measured by means of an Omega PX951 pressure transducer traceable to NIST standards and an Omega DP41-E process indicator. The accuracy of the pressure measurement was confirmed to be within the manufacturer's specified error limit by determining the bubble point of water at 573 K (Xiao *et al.*, 1997). The error $\Delta\rho$ in

density due to the uncertainty in measured $\Delta\tau^2$ ranged from $\approx 2\times10^{-6}$ g·cm^{-3} at T = 328 K to $\approx 2\times10^{-4}$ g·cm^{-3} at T = 530 K.

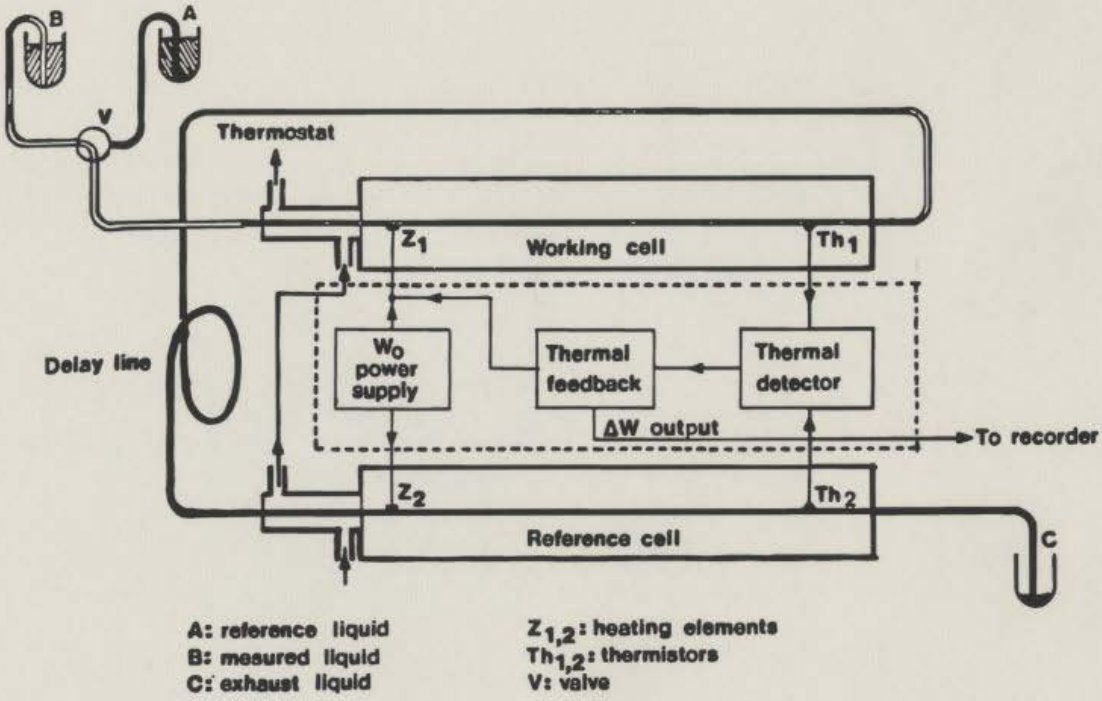

Figure II.1. Schematic diagram of the Picker flow micro-calorimeter.

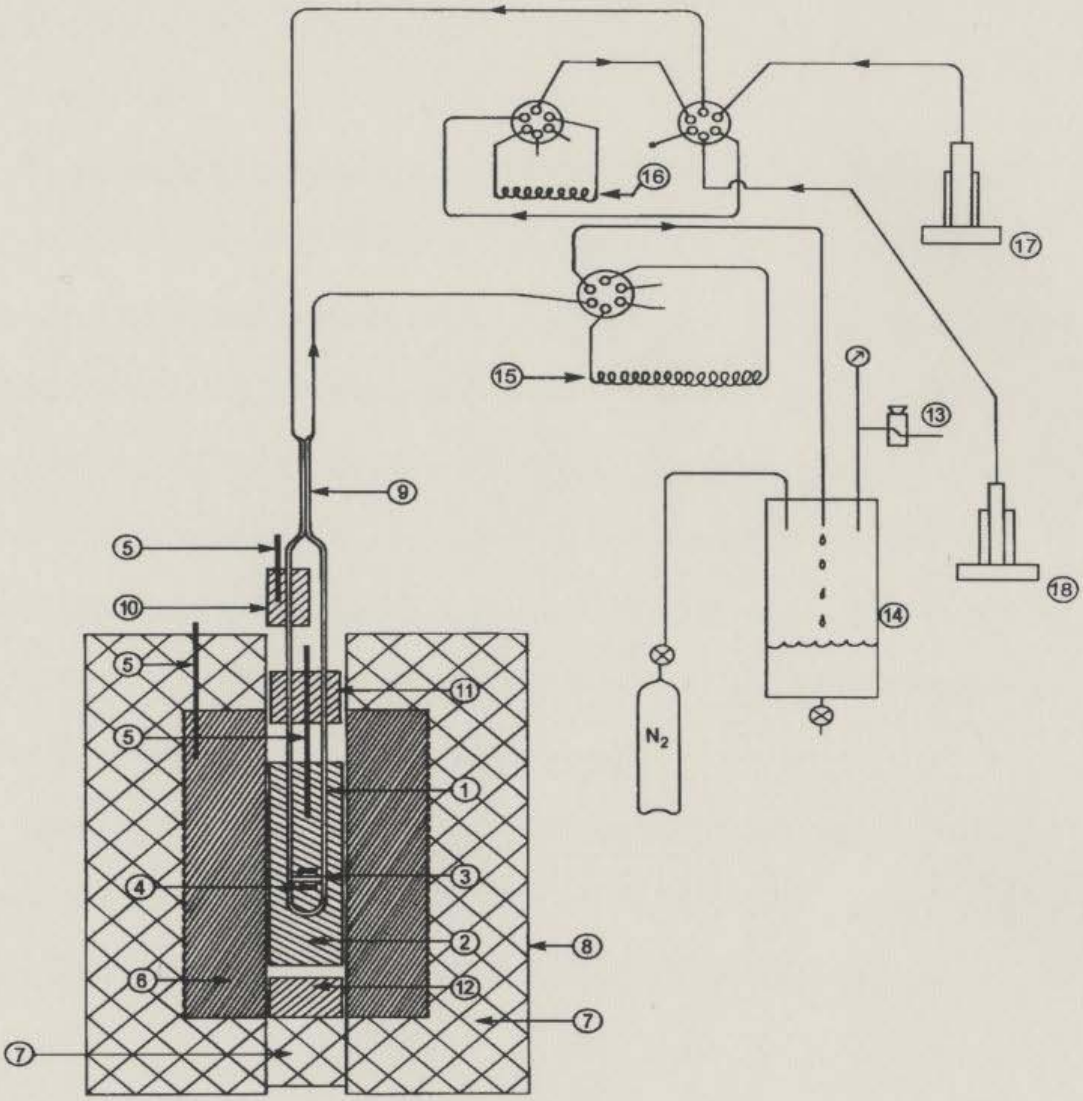

Figure II.2. Schematic diagram of the densitometer. 1, platinum U-shaped vibrating tube; 2, densitometer cell body; 3, Inconel rods for sensing and driver current; 4, permanent magnet; 5, RTD; 6, brass oven; 7, thermal insulation; 8, stainless steel container; 9, heat exchanger; 10, aluminum preheater; 11, aluminum heat shield; 12, brass heat shield; 13, back-pressure regulator; 14, stainless steel reservoir; 15, sampling loop; 16, injection loop; 17, pump; 18, pre-pressurizing pump.

II.3 Calculations

II.3.1 Young's rule

The speciation of most aqueous chelating agents in solution is very complex, because several equilibria exist. To control the speciation, a small excess of acid or base is often added to the solution, usually standardized HCl and NaOH. For example, in some of our measurements high pH values are desirable to maintain nearly all of the dissolved DTPA in the form of $DTPA^{5-}$ (aq). Because these high pH solutions contain two anion species, $DTPA^{5-}$ (aq) and OH^- (aq), it is necessary to use some method to subtract the effect of the additional electrolyte, OH^-(aq), from the experimental excess thermodynamic properties of the mixed electrolyte solutions to permit extraction of the desired properties of $DTPA^{5-}$ (aq). One of the methods often used is based on Young's rule.

Young's rule expresses the apparent molar properties of a mixture of electrolytes in terms of properties (at an ionic strength equal to the total ionic strength of the solution) of the solute components of the mixture. Young's rule can be expressed as:

$$Y_\phi = \sum\left(\frac{m_i}{\sum m_i}\right)Y_{\phi,i} + \delta \qquad \text{(II.4)}$$

where m_i is the molality of the *i*th solute, $Y_{\phi,i}$ is the corresponding apparent molar property, and δ is an excess mixing term. For solutions containing two solutes whose

molalities are denoted by m_2 and m_3, δ has the form:

$$\delta = k_{23}\left[\frac{m_2 m_3}{(m_2 + m_3)^2}\right]I = k_{23}F_2F_3I \qquad \text{(II.5)}$$

in which k_{23} is a binary interaction coefficient, $F_i = m_i / \Sigma m_i$, and I is the total ionic strength. δ is usually ignored in calculating the properties of the major components where there is a common cation or anion. Equation (II.4) can also be applied to systems in which one of the solutes dissociates or complexes to form other species.

II.3.2 Dissociation and Relaxation Corrections

The ionic species of strong electrolytes and weak electrolytes in aqueous solutions may dissociate or hydrolyse to an appreciable extent at the experimental conditions, and the contributions of the resulting "unwanted" ions to the measured heat capacities can be subtracted by Young's rule. Another contribution to the experimental values comes from the so-called "chemical relaxation" effect which is caused by a shift in the degree of dissociation due to the temperature increment associated with the measurement of the heat capacity.

The most comprehensive descriptions of the contributions from "chemical relaxation" effects were derived by Hepler and co-workers (Woolley and Hepler, 1977; Mains *et al.*, 1984). According to Woolley and Hepler (1977), for a simple acid ionization

reaction:

$$HA\ (aq) \rightleftharpoons H^{+}\ (aq) + A^{-}\ (aq) \tag{II.6}$$

the apparent molar heat capacity for the above reaction is expressed by:

$$\begin{aligned} C_{p,\phi}^{exp} &= C_{p,\phi}^{sp} + C_{p}^{rel} \\ &= (1-\alpha)C_{p,\phi}(HA) + \alpha[C_{p,\phi}(H^{+}) + C_{p,\phi}(A^{-})] + \Delta_{rxn}H(\partial\alpha / \partial T)_{p} \end{aligned} \tag{II.7}$$

where $C_{p,\phi}^{sp}$ is the sum of the heat capacities of all *species*, and C_{p}^{rel} is the chemical relaxation contribution expressed as:

$$C_{p}^{rel} = \Delta_{rxn}H\left(\frac{\partial\alpha}{\partial T}\right)_{p} \tag{II.8}$$

in which $\Delta_{rxn}H$ is the reaction enthalpy, and α is the degree of the dissociation. In very dilute solutions, where the solute is only slightly dissociated, $(\partial\alpha/\partial T)_{p}$ could be calculated by:

$$\left(\frac{\partial\alpha}{\partial T}\right)_{p} = \frac{\alpha}{2RT^{2}}\Delta_{rxn}H^{o} \tag{II.9}$$

In the current study, hydrolysis or dissociation and chemical relaxation effects for aqueous DTPA species and metal complexes, tartaric acid and its sodium salts must be considered, and detailed calculations are described in Chapter III and Chapter V of this thesis.

II.3.3 Uncertainty Estimation

The primary purpose of this study is to determine the standard partial molar heat capacity, C_p^o and volume V^o of aqueous species, and along with excess properties within the temperature range of the data. The determination of C_p^o and V^o requires the extrapolation of experimental data to infinite dilution, and consequently, their values are known with an accuracy which is limited by experimental uncertainty and also by the reliability of the extrapolation procedure. Uncertainties in C_p^o and V^o consist of statistical uncertainty, which was assigned as twice the standard deviation from isothermal fits, and systematic uncertainty, which was also assigned as twice of the estimated uncertainty from the experimental measurements of $C_{p,\phi}$ and V_ϕ.

In the apparent molar heat capacity measurements, the specific heat capacity ratio of the sample solution $c_{p,s}$ to that of pure water $c_{p,l}^*$ was calculated by the equation:

$$\frac{c_{p,s}}{c_{p,l}^*} = \left\{1 - \frac{f(W_s - W_w)}{W_w}\right\} \cdot \frac{\rho_l^*}{\rho_s} \qquad \text{(II.10)}$$

where f is the correction factor for the heat losses, W_s is the electric power when the sample solution was in the cell, W_w is the power when water was in the cell, and ρ_s and ρ_l^* are the densities of the solution and water, respectively. For the experimental apparent molar heat capacities, the error estimates were calculated from the sensitivity limit in determining the ratio of powers, which was approximately $\pm 2.0\times10^{-4}$, and the accuracy of the calibration factor, ± 0.5 percent. Estimated uncertainties in $C_{p,\phi}^{exp}$ are less than 1 J K^{-1} mol^{-1} for molality < 0.1 mol kg^{-1}, and T > 313.15 K.

The errors associated with the density measurements in the high temperature and pressure vibrating-tube densitometer come from the random errors associated with the calibration constant, the periods of frequencies measured for water and the solution, and the fluctuations of temperature and pressure. The error limits in density measurement may be estimated through the expression (Xiao and Tremaine, 1997):

$$\delta\rho = \{(\rho-\rho_l^*)^2(\delta K/K)^2 + 8[K\tau(\delta\tau)]^2 + [\beta_l^*\rho_l^*(\delta p)]^2 + [\alpha_l^*\rho_l^*(\delta T)]^2\}^{1/2} \qquad \text{(II.11)}$$

where $\delta\rho$ is the statistical uncertainty of density, δK and $\delta\tau$ denote the standard deviation of calibration constant and vibrational periods, respectively; α_l^* and β_l^* are the thermal expansivity coefficient and the isothermal compressibility of water, respectively. For the measurements on tartaric acid at temperatures below 573 K, and pressures up to 20 MPa, $\delta T < 0.02$ K, $\delta p < 0.01$ MPa, and $\delta K/K \approx 0.002$. The standard deviation of $\delta\tau$ was based

on the average of 20 values (Xiao and Tremaine, 1997). The error limits of densities $\delta\rho$ at all temperatures were $\pm$ 0.1 kg m^{-3} for 0.1 m solutions, and $\pm$ 0.2 kg m^{-3} for 1.0 m solutions; the corresponding uncertainties associated with V_ϕ were 1.5 cm^3 mol^{-1} and 0.3 cm^3 mol^{-1} , respectively.

Because larger experimental uncertainty occurs at high temperatures and very low concentrations, (see Figure III.2), weighted least squares curve fitting techniques have been used to fit the experimental data at different temperatures and molalities. It has been found that the random errors in $C_{p,\phi}$ and V_ϕ are inversely proportional to the molality of solution (Xiao and Tremaine, 1997), and thus weighting factors proportional to the molalities of the solutions were used in the curve fitting for this work.

Chapter III. Thermodynamics of Aqueous Diethylenetriaminepentaacetic Acid (DTPA) Systems: Apparent and Partial Molar Heat Capacities and Volumes of Aqueous H_2DTPA^{3-}, $DTPA^{5-}$, $CuDTPA^{3-}$, and Cu_2DTPA^- from 283 to 328 K

III.1 Introduction

Chelating agents are used widely in many industrial applications including environmental cleanup of heavy metals, boiler water treatment, nuclear reactor decontamination and oilwell treatments. Chemical and geochemical equilibrium models of these processes require stability constant data over a range of temperatures and pressures. Although a large database of stability constants and enthalpies has been developed for 298.15 K, there are few data at other temperatures and pressures. Standard partial molar heat capacities C_p° and volumes V° are important in this context because they define the temperature- and pressure-dependence of the stability constants, respectively. Standard partial molar heat capacities and volumes are also of considerable interest in the development of semi-empirical models and simulations of ionic solvation, because both are sensitive indicators of hydration effects.

Diethylenetriaminepentaacetic acid (DTPA), the second member of the series of polycarboxylic acids derived from the polyethylenepolyamines, has become an important industrial chelating agent. Because the $DTPA^{5-}$ anion has a large negative charge, and is capable of acting as an octadentate ligand, its interactions with metal ions are also of fundamental interest. Eight ionized forms of the acid exist, and it can form chelates with

either one or two divalent cations. No measurements of C_p^o and V^o for any DTPA species or complex have been reported in the literature.

In this chapter, we report apparent and partial molar heat capacities and volumes for aqueous H_2DTPA^{3-}, $DTPA^{5-}$ and the 1:1 and 2:1 copper(II)-DTPA complexes, $CuDTPA^{3-}$ and Cu_2DTPA^-, over a range of temperatures between 283 and 328 K, all as the sodium salts. Because the equilibria are so complex, care must be taken to control speciation of DTPA by adjusting the pH and metal/DTPA ratio to optimize the contribution of the species of interest. Plots of the distribution of species as a function of pH and copper molality, calculated from formation constants tabulated by Martell and Smith (1982) and Chaberek *et al.*(1959), are shown in Figure III.1.

III.2 Experimental

Diethylenetriaminepentaactic acid (H_5DTPA) (Alfa) was recrystallized from hot water twice and dried at 353 K for several hours (Mehdi and Budesinsky, 1974). The purity was found to be >99.9 percent by titration against standard NaOH solution. Aqueous solutions of NaOH (50 weight percent) were prepared from carbonate-free 50% solution (Fisher "Certified" ACS) and standardized by titration against potassium hydrogen phthalate (Baker, "99.97 percent"). A stock solution of Na_3H_2DTPA was prepared by adding the stoichiometric mass of H_5DTPA to a known mass of the standard

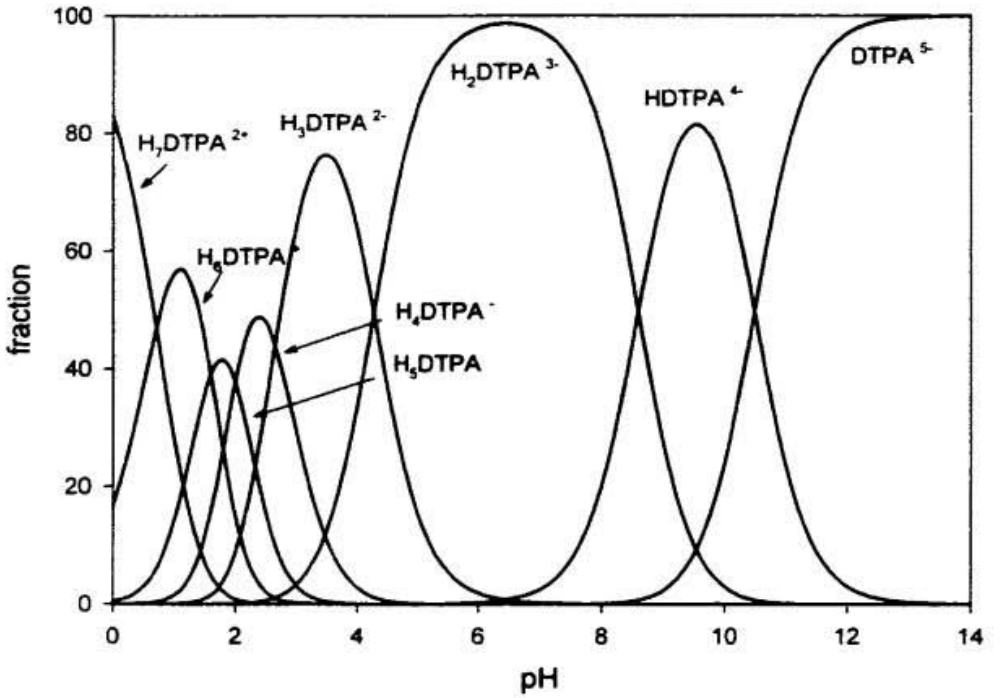

Figure III.1 Speciation of aqueous DTPA at 298.15 K and I = 0.1 m: (a), H_5DTPA.

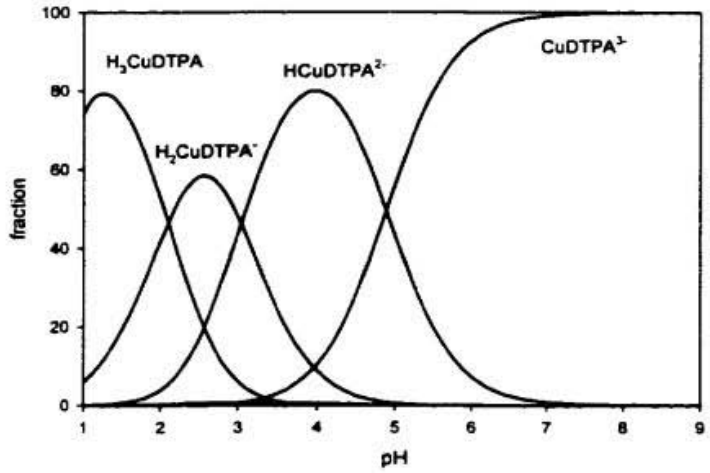

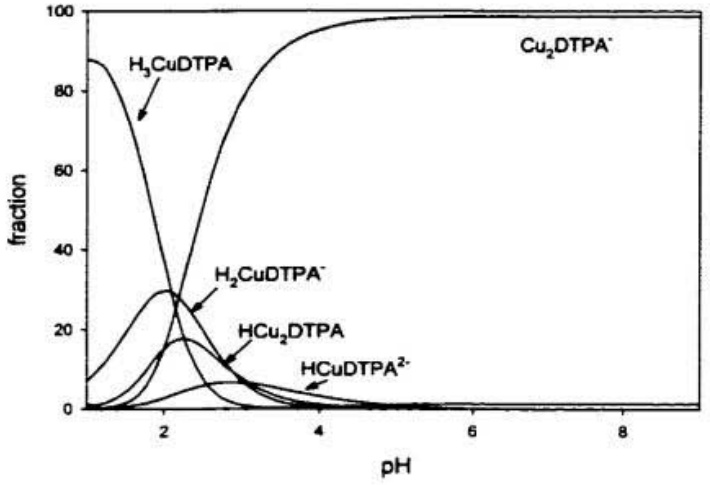

Figure III.1 (Continued). Speciation of aqueous DTPA at 298.15 K and I = 0.1 m: (b), Cu(II)/DTPA = 1: 1; and (c), Cu(II)/DTPA = 2:1.

NaOH solution, then buffered with methenamine and standardized by titration against lead nitrate using xylenol orange as the indicator (Jeffery *et al.*, 1989). The pH of the standard Na_3H_2DTPA solution was about 6.5. A standard solution of Na_5DTPA was also prepared by mass, by adding the standardized Na_3H_2DTPA solution to a weighed amount of standard NaOH solution, followed by adjustment to pH= 12.0 with 0.001*m* NaOH. More dilute solutions were prepared by mass, by adding 0.001*m* NaOH to aliquots of the standard solutions.

Solutions of $H_3CuDTPA$ and HCu_2DTPA were prepared by adding a stoichiometric quantity of freshly prepared copper (II) hydroxide (Weiser *et al.*, 1942) to 19.65g (0.05 mole) to dried H_5DTPA, then dissolving the solid mixture in an appropriate amount of water. Because copper (II) hydroxide may occur in non-stoichiometric forms, the molar mass of our freshly prepared material was determined by potentiometric titration against a standardized solution of ethylenedinitrilotetraacetic acid ($Na_2H_2EDTA{\cdot}2H_2O$), and was found to be 97.78 $g{\cdot}mol^{-1}$, corresponding to $Cu(OH)_2{\cdot}0.0122H_2O$. Solutions of $Na_3CuDTPA$ and $NaCu_2DTPA$ were prepared by mass, by adding the stoichiometric amounts of standard hydroxide solution to the $H_3CuDTPA$ and HCu_2DTPA solutions, followed by adjustment to pH= 8.0 and pH = 6.0 with 0.001*m* NaOH solution, respectively. The concentrations of the protonated copper complexes of DTPA in the stock solutions were also determined by titration against our standard NaOH solution. The molalities of the solutions prepared by mass agreed with those determined by titration to within 0.5 percent. Further solutions were prepared by

dilution by mass with water. Spectrophotometric studies on the Cu(II)-DTPA stock solutions at pH ≈ 6 revealed an absorption band with a maximum at 660 nm for a solution in which the metal/ligand ratio was equal to 1.00, whereas the maximum shifted to 740 nm, when the ratio was 2. These results were consistent with those of Chaberek *et al.*(1959) for the species $CuDTPA^{3-}$(aq) and Cu_2DTPA^-(aq), respectively.

Nanopure water (resistivity > 8 MΩ·cm) was used to prepare all solutions. Solutions of NaCl (Aldrich "99.99 percent") for calibrating the densimeter and calorimeter were prepared by mass after drying the salt at 383 K for 24 hours. The standard solution of Na_2H_2EDTA (Aldrich) was prepared by the method of Vogel (Jeffery *et al.*, 1989).

A Sodev CP-C flow microcalorimeter (Picker *et al.*, 1971) and a Sodev 03D vibrating flow densitometer (Picker *et al.*, 1974) equipped with platinum cells were employed in this work. The temperatures of the calorimeter and densitometer were independently controlled to ±0.01 K by two Sodev CT-L circulating baths. The thermistor (Omega, 44107) used to measure the temperatures of calorimeter and densitometer were calibrated with a Hewlett-Packard 2804A quartz-crystal thermometer traceable to NBS standards. The densitometer was calibrated daily with pure water and standard 1 $mol \cdot kg^{-1}$ NaCl(aq). The experimental values of $\{c_p \cdot \rho / (c^*_{p,1} \cdot \rho^*_1) - 1\}$ for the standard NaCl(aq) were compared with literature values compiled by Archer (1992) to correct for a small heat-leak effect, according to the method of Desnoyers *et al.* (1976). Here, c_p, $c^*_{p,1}$, ρ and ρ^*_1 are the massic heat capacities and densities of the solution and

$H_2O(l)$, respectively. Measurements on $Na_3H_2DTPA(aq)$ and $Na_3CuDTPA(aq)$ at 298.15 K were carried out on two independently prepared standard solutions to confirm that systematic errors associated with the preparation of the solutions is small.

III.3 Results

III.3.1 Apparent Molar Properties

The experimental values for the relative densities (ρ - ρ_1^*) and heat capacity ratios $\{c_p \cdot \rho / (c_{p,1}^* \cdot \rho_1^*) - 1\}$ of the solutions are listed in Tables A.III.1 to A.III.7. The tables also tabulate the experimental apparent molar volumes V_ϕ and heat capacities $C_{p,\phi}$, which were calculated from these results using densities and specific heat capacities of pure water taken from Hill's (1990) equation of state. By definition:

$$Y_\phi = \{ Y(sln) - n_1 Y_1^* \} / (n_2 + n_3) \qquad \text{(III.1)}$$

where Y(sln) is the heat capacity or volume of solution; Y_1^* is the molar heat capacity or volume of pure $H_2O(l)$, and n_1, n_2 and n_3 are the number of moles of water, the DTPA salt and sodium hydroxide, respectively. The effect of the small amount of excess NaOH used to control the speciation in the Na_5DTPA, $Na_3CuDTPA$, and $NaCu_2DTPA$ solutions was subtracted by means of the procedure used by Hovey *et al.* (1986, 1988). Briefly, the contribution of each solute can be described by Young's rule (Young and Smith, 1954; Reilly and Wood, 1969):

$$Y_\phi = F_2 Y_{\phi,2} + F_3 Y_{\phi,3} + \delta \qquad \text{(III.2)}$$

where $F_2 = \{m_2 / (m_2 + m_3)\}$ and $F_3 = \{m_3 / (m_2 + m_3)\}$. Here, $Y_{\phi,2}$ and $Y_{\phi,3}$ are the values for the hypothetical solution of the individual species at an ionic strength identical to the mixture; m_2 and m_3 are the molality of the salt and sodium hydroxide, respectively; and δ is an excess mixing term, which usually may be ignored in calculating the properties of the major components where there is a common cation or anion. Both $C_{p,\phi,3}$ and $V_{\phi,3}$ were calculated as functions of ionic strength at $283 \leq T \leq 328$ K from the equations for NaOH reported by Hovey *et al.* (1986, 1988). The resulting values of $C_{p,\phi,2}$ and $V_{\phi,2}$ for $Na_5DTPA(aq)$, $Na_3CuDTPA(aq)$, and $NaCu_2DTPA(aq)$ are tabulated in Tables A.III.2 to A.III.7.

III.3.2 Partial Dissociation of $Na_3H_2DTPA(aq)$ and $Na_5DTPA(aq)$

The interpretation of the apparent molar properties of $Na_3H_2DTPA(aq)$ and $Na_5DTPA(aq)$ is further complicated by small equilibrium concentrations of $HDTPA^{4-}(aq)$ and $H_2DTPA^{3-}(aq)$. The principle equilibria in solutions containing $H_2DTPA^{3-}(aq)$ as the major anion are:

$$\begin{array}{ccccc} H_2DTPA^{3-}(aq) & \rightleftharpoons & H^-(aq) & + & HDTPA^{4-}(aq) \\ (1-\alpha-\beta)m_2 & & (\alpha-\beta)m_2 & & \alpha m_2 \end{array} \qquad \text{(III.3)}$$

and

$$H_2DTPA^{3-}(aq) + H^+(aq) \rightleftharpoons H_3DTPA^{2-}(aq) \qquad \text{(III.4)}$$

$$(1 - \alpha - \beta)m_2 \quad (\alpha - \beta)m_2 \qquad \beta m_2$$

whereas in solutions containing $DTPA^{5-}(aq)$, only one equilibrium is important:

$$DTPA^{5-}(aq) + H_2O(l) \rightleftharpoons HDTPA^{4-}(aq) + OH^-(aq) \qquad \text{(III.5)}$$

$$(1 - \alpha)m_2 \qquad \alpha m_2 \qquad \alpha m_2 + m_3$$

Here α and β are the degrees of dissociation to form $HDTPA^{4-}(aq)$ and $H_3DTPA^{2-}(aq)$, respectively. The "experimental" apparent molar volumes $V_{\phi,2}^{exp}$ of $Na_3H_2DTPA(aq)$ and $Na_5DTPA(aq)$ are considered to result from the sum of the contribution of each species in solution according to Young's rule (equation III.2). The "experimental" apparent molar heat capacities $C_{p,\phi,2}^{exp}$ of $Na_3H_2DTPA(aq)$ and $Na_5DTPA(aq)$ contain an additional term to correct the shift in the dissociation caused by the temperature increment in the heat capacity measurement, the so-called chemical relaxation effect (Woolley and Hepler, 1977; Barbero *et al.*, 1983; Mains *et al.*, 1984). The expressions for $C_{p,\phi,2}^{exp}$ are:

$$\begin{aligned} C_{p,\phi,2}^{exp}(Na_3H_2DTPA,aq) = {} & (1 - \alpha - \beta)C_{p,\phi,2}(H_2DTPA^{3-},aq) + \alpha C_{p,\phi,2}((HDTPA^{4-},aq) \\ & + \beta C_{p,\phi,2}(H_3DTPA^{2-},aq) + (\alpha - \beta)C_{p,\phi,2}(H^-,aq) \\ & + 3C_{p,\phi,2}(Na^+,aq) + C_{p,\phi,\alpha}^{rel} + C_{p,\phi,\beta}^{rel} \end{aligned} \qquad \text{(III.6)}$$

and $$C^{exp}_{p,\phi,2}(Na_5DTPA,aq) = F_2\,[\,(1-\alpha)C_{p,\phi,2}(DTPA^{5-},aq) + \alpha C_{p,\phi,2}(HDTPA^{4-},aq) + \alpha C_{p,\phi,2}(OH^-,aq) + 5C_{p,\phi,2}(Na^+,aq) - \alpha C^{o}_{p}(H_2O,l)\,] + F_3\,C_{p,\phi,2}(Na^+,aq) + C^{rel}_{p,\phi} \quad \text{(III.7)}$$

The chemical relaxation contributions are given by:

$$C^{rel}_{p,\phi,\alpha} = \Delta H[\text{Eq. (3)}](\partial\alpha/\partial T)_m \quad \text{(III.8)}$$

$$C^{rel}_{p,\phi,\beta} = \Delta H[\text{Eq. (4)}](\partial\beta/\partial T)_m \quad \text{(III.9)}$$

$$C^{rel}_{p,\phi} = \{m_2 / (m_2 + m_3)\}\ \Delta H[\text{Eq. (5)}](\partial\alpha/\partial T)_m \quad \text{(III.10)}$$

Further, in dilute solutions that are only slightly dissociated (Woolley and Hepler, 1977):

$$(\partial\alpha/\partial T)_m = \alpha\Delta H^{o}[\text{Eq. (3)}]/2RT^2 \quad \text{(III.11)}$$

$$(\partial\beta/\partial T)_m = \beta\Delta H^{o}[\text{Eq. (4)}]/RT^2 \quad \text{(III.12)}$$

$$(\partial\alpha/\partial T)_m = \{m_2 / (m_2 + m_3)\}\ K(1-\alpha)\ \{\Delta H^{o}[\text{Eq. (5)}]\}^2 / \{RT^2(2\alpha m_2 + m_3 + K)\} \quad \text{(III.13)}$$

The terms α and β were calculated from compiled values of log K at ionic strength 0.1M (Martell and Smith, 1982). These values of α and β were used with enthalpy and heat capacity data for reactions (III.3-III.5) from Milyukov and Polenova (1981) to calculate $C^{rel}_{p,\phi,\alpha}$, $C^{rel}_{p,\phi,\beta}$ and $C^{rel}_{p,\phi}$. The results are summarized in Tables A.III.8 and A.III.9, along with the final values of $C_{p,\phi,2}(3Na^+ + H_2DTPA^{3-},aq)$ and $C_{p,\phi,2}(5Na^+ + DTPA^{5-},aq)$. The effect of partial dissociation on V_ϕ is much less pronounced, in part because there is no contribution from chemical relaxation. Our analysis indicates that the correction would be insignificant, less than 0.1 $cm^3 \cdot mol^{-1}$. The effect of sodium complexation with H_2DTPA^{3-}(aq) and $DTPA^{5-}$(aq) is also negligible (Martell and Smith, 1982). No chemical relaxation correction to the experimental heat capacities of $Na_3CuDTPA$(aq) and $NaCu_2DTPA$(aq) was necessary because the formation constants of $HCuDTPA^{2-}$(aq) from $CuDTPA^{3-}$(aq), and Cu^{2+}(aq) from $HCuDTPA^{2-}$(aq) are too small to affect $C^{exp}_{p,\phi,2}$ [At 25°C, log K = -9.25 and -16.04, respectively.]

III.3.3 Partial Molar Properties

The molality dependence of the apparent molar heat capacities $C_{p,\phi,2}$ and volumes $V_{\phi,2}$ is well represented by the Guggenheim form of the extended Debye-Hückel equation (Millero, 1979; Pitzer *et al.*, 1961):

$$C_{p,\phi,2} = C^{o}_{p,2} + 1.5\omega A_C [I - 2I^{1/2} + 2\ln(1 + I^{1/2})]/I + B_C I + C_C I^{3/2} \qquad \text{(III.14)}$$

$$V_{\phi,2} = V_2^o + 1.5\omega A_V [I - 2I^{1/2} + 2\ln(1 + I^{1/2})]/I + B_V I + C_V I^{3/2} \qquad \text{(III.15)}$$

where $I = \omega\, m = \frac{1}{2}\sum m_i z_i^2$. A_C in equation (III.14), and A_V in equation (III.15) are the Debye-Hückel limiting slopes for the heat capacity and volume, respectively, whose values were taken from the compilation by Archer and Wang (1990). It was found that the temperature dependence of the B_Y and C_Y parameters could be described adequately by the following equations:

$$B_C = c_4 + c_5 T \qquad \text{(III.16a)}$$

$$C_C = c_6 + c_7 T + c_8 T^2 \qquad \text{(III.16b)}$$

and

$$B_V = v_4 + v_5 T \qquad \text{(III.17a)}$$

$$C_V = v_6 + v_7 T + v_8 T^2 \qquad \text{(III.17b)}$$

where the c_i and v_i terms are fitting coefficients and T is temperature in Kelvins. By definition, $C_{p,2}^o$ and V_2^o are the standard partial molar heat capacity and standard partial molar volume, respectively. Their temperature dependencies were modelled by equations of the form (Xiao and Tremaine, 1996):

$$C_{p,2}^o = c_1 + c_2 / (T - \Theta)^2 + c_3 T \qquad \text{(III.18)}$$

$$V_2^o = v_1 + v_2 / (T - \Theta) + v_3 T \qquad \text{(III.19)}$$

Here, the terms c_i and v_i are species-dependent fitting coefficients, and $\Theta = 228$ K is a solvent-dependent parameter associated with the anomalous behaviour of super-cooled water (Angell, 1982).

Equations (III.14) and (III.15) were fitted to the experimental results at each temperature by the Marquardt-Levenberg non-linear least-squares algorithm within the commercial software package SigmaPlot.© Values below $I \leq 0.1$ mol·kg^{-1} at T = 328.15 K were considered to be unreliable and were not used in the fit. The fitted values for the standard partial molar properties are listed in Table III.1 and plotted in Figures III.10 and III.11. The entire array of values at all temperatures and all molalities was then used to optimize the parameters in equations (III.14-III.19) by the least squares curve-fitting program. The results are listed in Tables III.2 and III.3, and are compared with the experimental data in Figures III.2 to III.9.

The overall standard deviations of $C_{p,\phi,2}$ for Na_3H_2DTPA(aq), Na_5DTPA(aq), $Na_3CuDTPA$(aq) and $NaCu_2DTPA$(aq) are 2.8, 5.7, 3.5 and 2.1 J·K^{-1}·mol^{-1}, respectively. The standard deviations of $V_{\phi,2}$ for these four species are all ~0.2 cm^3·mol^{-1}. We estimate that the combined statistical and systematic errors lead to an uncertainty of ±1.0 cm^3·mol^{-1} in V_2^o, ±12 J·K^{-1}·mol^{-1} in $C_{p,2}^o$ (Na_3H_2DTPA, aq), and ±20 J·K^{-1}·mol^{-1} or less in $C_{p,2}^o$ for Na_5DTPA(aq), $Na_3CuDTPA$(aq) and $NaCu_2DTPA$(aq).

Table III.1. Partial Molar Volumes and Heat Capacities for DTPA Species at Infinite Dilution and at I = 0.1m from 283 to 328 K from Least Squares Fits to Isothermal Data.[a]

T	V_2^o	$V_2(I = 0.1m)$	$C_{p,2}^o$	$C_{p,2}(I = 0.1m)$
		$Na_3H_2DTPA(aq)$		
283.15	204.38(0.22)	208.81	-9.73(6.7)	72.95
298.15	213.98(0.18)	218.51	169.50(1.9)	254.75
313.15	220.54(0.18)	225.48	271.32(1.9)	359.49
328.15	224.04(0.45)	230.04	316.86(2.0)	415.71
		$Na_5DTPA(aq)$		
283.15	189.59(0.85)	198.74	-141.41(19.7)	3.41
298.15	196.47(0.17)	206.69	58.63(5.4)	233.29
313.15	198.40(0.29)	210.05	144.74(6.4)	341.59
328.15	197.41(0.61)	210.94	135.96(15.9)	359.89
		$Na_3CuDTPA(aq)$		
283.15	208.39(0.35)	212.49	-32.28(2.0)	42.94
298.15	215.32(0.12)	219.81	156.95(0.8)	236.25
313.15	218.87(0.19)	223.92	257.61(0.8)	343.26
328.15	220.45(0.31)	226.00	300.74(2.2)	394.85
		$NaCu_2DTPA(aq)$		
283.15	237.74(0.34)	242.49	316.00(2.8)	436.85
298.15	243.74(0.21)	247.51	470.78(1.9)	550.24
313.15	247.54(0.20)	250.80	572.71(1.5)	631.25
328.15	250.07(0.45)	253.18	637.86(4.9)	698.68

[a] Values in parenthesis are standard deviations from fitting equations (III.14) and (III.15). Units: $cm^3 \cdot mol^{-1}$ and $J \cdot K^{-1} \cdot mol^{-1}$.

Table III.2. Fitting Parameters for Equations (III.14), (III.16), and (III.18) for the Apparent Molar Heat Capacities.

Parameter	Na_3H_2DTPA	Na_5DTPA	$Na_3CuDTPA$	$NaCu_2DTPA$
c_1	-6.825×10^{2}	5.537×10^{2}	2.314×10^{3}	1.103×10^{3}
c_2	-8.106×10^{5}	-1.339×10^{6}	-6.388×10^{4}	-4.060×10^{4}
c_3	3.392×10^{0}	-7.816×10^{-1}	-4.183×10^{0}	-1.776×10^{-1}
c_4	9.769×10^{2}	5.015×10^{2}	4.627×10^{3}	2.301×10^{4}
c_5	-2.956×10^{0}	-1.613×10^{0}	-2.805×10^{1}	-1.413×10^{2}
c_6	5.886×10^{2}	4.625×10^{2}	4.267×10^{-2}	2.191×10^{-1}
c_7	-4.720×10^{0}	-3.251×10^{0}		
c_8	8.996×10^{-3}	5.706×10^{-3}		

Units: c_1, $J\cdot K^{-1}\cdot mol^{-1}$; c_2, $J\cdot K\cdot mol^{-1}$; c_3, $J\cdot K^{-2}\cdot mol^{-1}$; c_4; $J\cdot kg\cdot K^{-1}\cdot mol^{-2}$; c_5, $J\cdot kg\cdot K^{-2}\cdot mol^{-2}$; c_6, $J\cdot kg^{3/2}\cdot K^{-1}\cdot mol^{-5/2}$; c_7, $J\cdot kg^{3/2}\cdot K^{-2}\cdot mol^{-5/2}$; c_8, $J\cdot kg^{3/2}\cdot K^{-3}\cdot mol^{-5/2}$. [a] The equations for $Na_3CuDTPA(aq)$ and $NaCu_2DTPA(aq)$ are: $C^{o}_{p,2} = c_1 + \{ c_2 / (T - \Theta) \} + c_3T$, $B_C = c_4 + c_5T + c_6T^2$.

Table III.3. Fitting Parameters for the Equations (III.15), (III.17), and (III.19) for the Apparent Molar Volumes.

Parameter	Na_3H_2DTPA	Na_5DTPA	$Na_3CuDTPA$	$NaCu_2DTPA$
v_1	1.873×10^{2}	3.867×10^{2}	2.925×10^{2}	2.723×10^{2}
v_2	-1.586×10^{3}	-3.514×10^{3}	-2.305×10^{3}	-1.616×10^{3}
v_3	1.648×10^{-1}	-4.696×10^{-1}	-1.491×10^{-1}	-1.850×10^{-2}
v_4	2.073×10^{1}	1.461×10^{1}	-1.511×10^{2}	4.500×10^{2}
v_5	-5.868×10^{-2}	-4.390×10^{-2}	1.055×10^{0}	-2.637×10^{0}
v_6	3.492×10^{1}	-1.349×10^{-1}	-1.806×10^{-3}	3.961×10^{-3}
v_7	-2.439×10^{-1}	-6.089×10^{-3}		
v_8	4.191×10^{-4}	2.132×10^{-5}		

Units: v_1, $cm^3\cdot mol^{-1}$; v_2, $cm^3\cdot K\cdot mol^{-1}$; v_3, $cm^3\cdot K^{-1}\cdot mol^{-1}$; v_4, $cm^3\cdot kg\cdot mol^{-2}$; v_5, $cm^3\cdot kg\cdot K^{-1}\cdot mol^{-2}$; v_6, $cm^3\cdot kg^{3/2}\cdot mol^{-5/2}$; v_7, $cm^3\cdot kg^{3/2}\cdot K^{-1}\cdot mol^{-5/2}$; v_8, $cm^3\cdot kg^{3/2}\cdot K^{-2}\cdot mol^{-5/2}$. [a] The equations for $Na_3CuDTPA(aq)$ and $NaCu_2DTPA(aq)$ are: $V_2^o = v_1 + \{ v_2 / (T - \Theta) \} + v_3T$. $B_V = v_4 + v_5T + v_6T^2$.

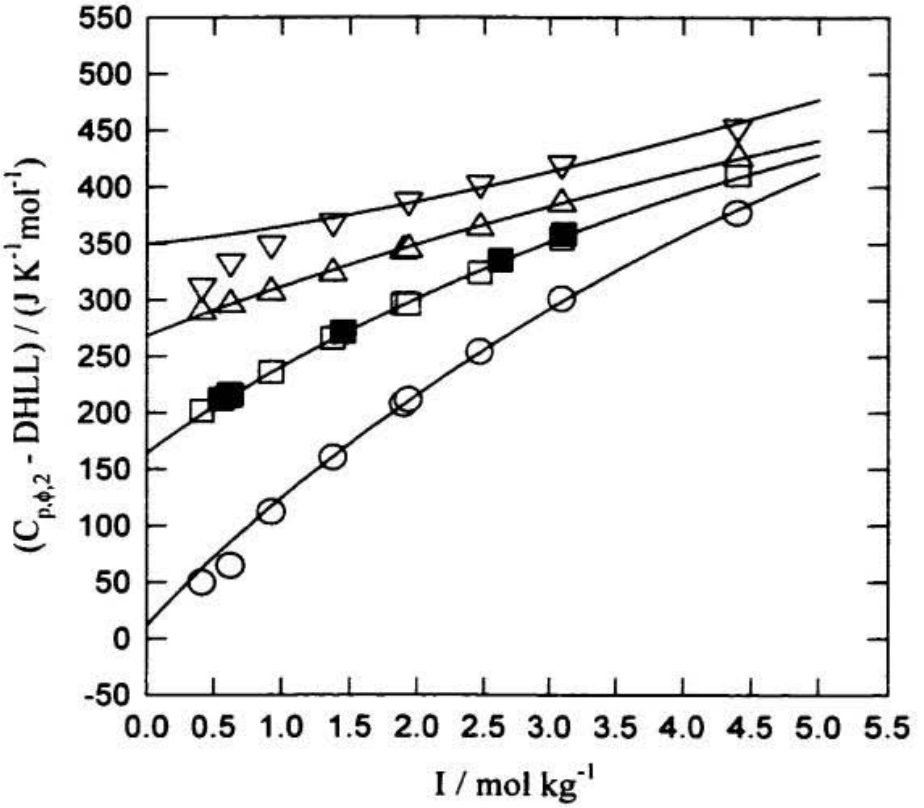

Figure III.2. Apparent molar heat capacities of $Na_3H_2DTPA(aq)$ plotted as a function of ionic strength I after subtracting the Debye-Hückel limiting law (DHLL) term according to equation (III.14): ○, T = 283.15 K □, T = 298.15 K; ■, T = 298.15 K (Solution 2); △, T = 313.15 K; ▽, T = 328.15 K. Symbols are experimental results and lines represent the global least-squares fits to equation (III.14).

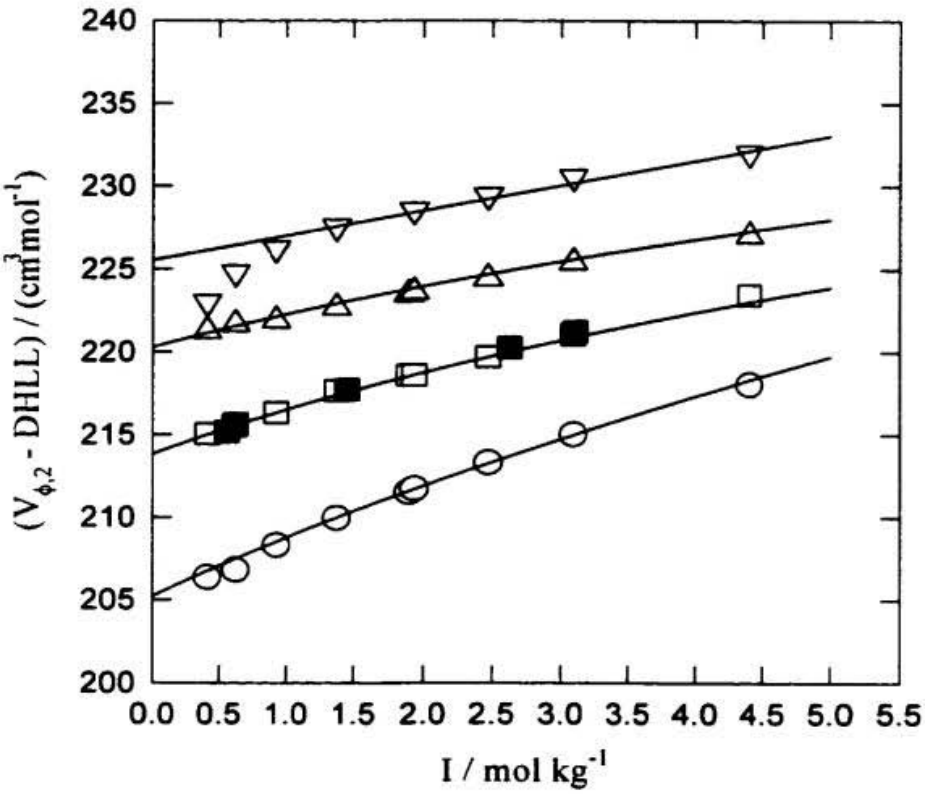

Figure III.3. Apparent molar volumes of $Na_3H_2DTPA(aq)$ plotted as a function of ionic strength I after subtracting the Debye-Hückel limiting law (DHLL) term according to equation (III.15): ○, T = 283.15 K □, T = 298.15 K; ■, T = 298.15 K (Solution 2); △, T = 313.15 K; ▽, T = 328.15 K. Symbols are experimental results and lines represent the global least-squares fits to equation (III.15).

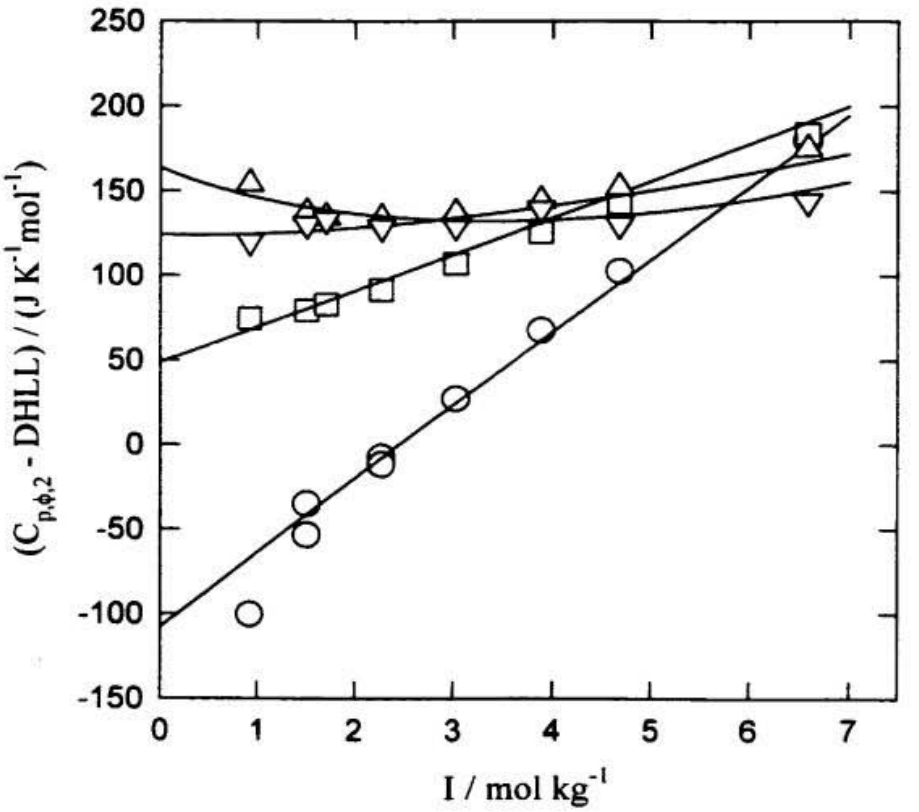

Figure III.4. Apparent molar heat capacities of $Na_5DTPA(aq)$ plotted as a function of ionic strength I after subtracting the Debye-Hückel limiting law (DHLL) term according to equation (III.14): ○, T = 283.15 K; □, T = 298.15 K; △, T = 313.15 K; ▽, T = 328.15 K. Symbols are experimental results and lines represent the global least-squares fits to equation (III.14).

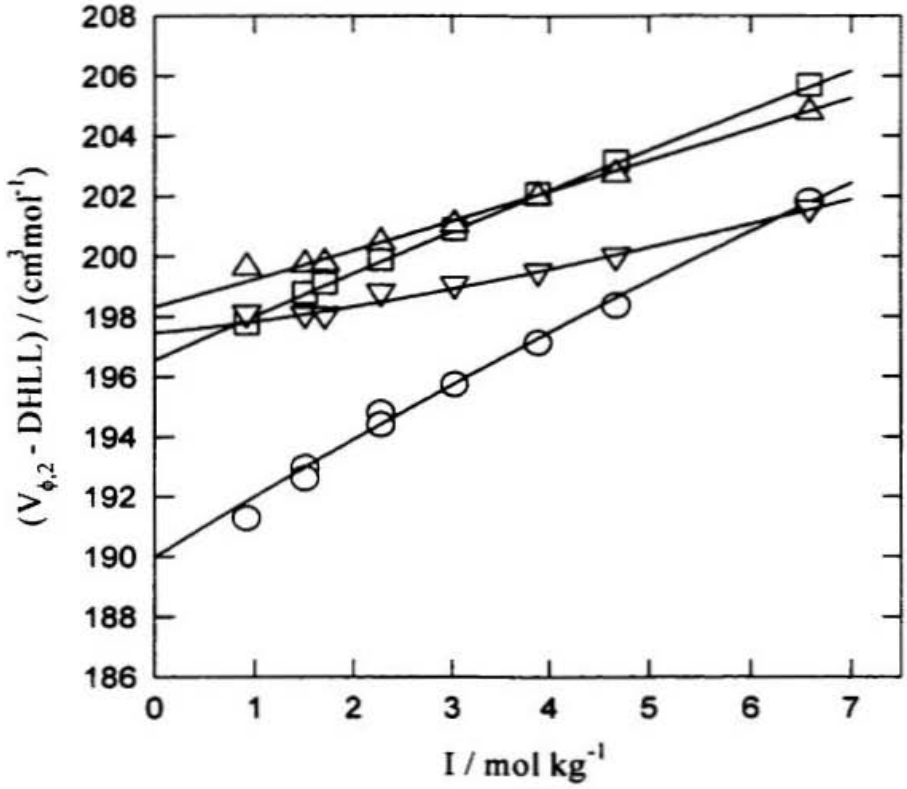

Figure III.5. Apparent molar volumes of $Na_5DTPA(aq)$ plotted as a function of ionic strength I after subtracting the Debye-Hückel limiting law (DHLL) term according to equation (III.15): ○, T = 283.15 K; □, T = 298.15 K; △, T = 313.15 K; ▽, T = 328.15 K. Symbols are experimental results and lines represent the global least-squares fits to equation (III.15).

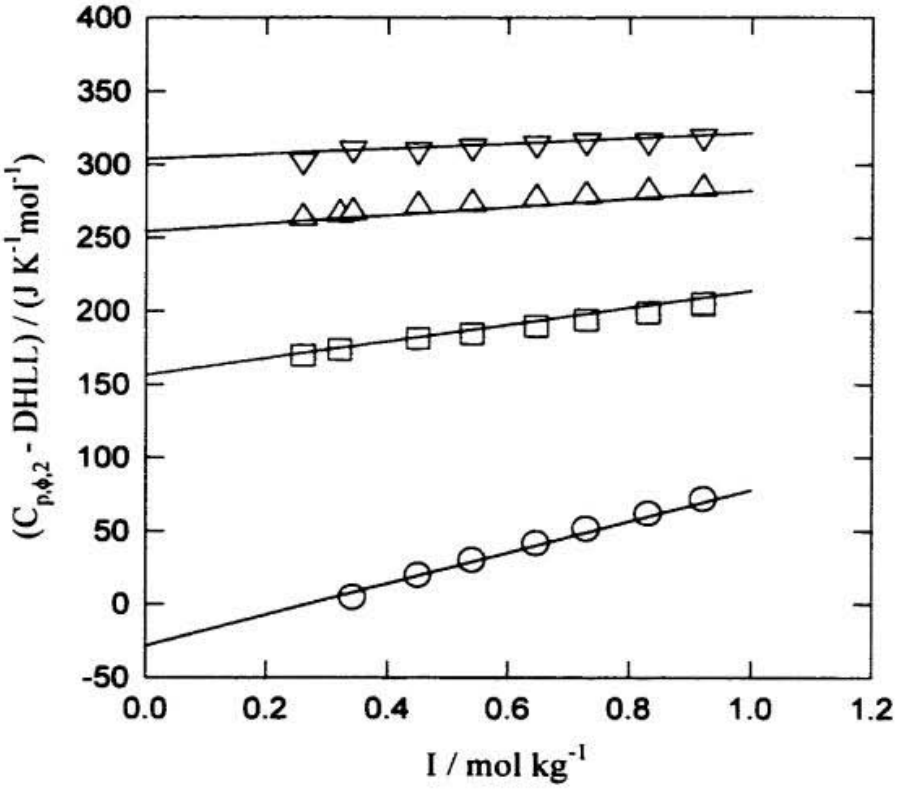

Figure III.6. Apparent molar heat capacities of $Na_3CuDTPA(aq)$ plotted as a function of ionic strength I after subtracting the Debye-Hückel limiting law (DHLL) term according to equation (III.14): ○, T = 283.15 K; □, T = 298.15 K; △, T = 313.15 K; ▽, T = 328.15 K. Symbols are experimental results and lines represent the global least-squares fits to equation (III.14).

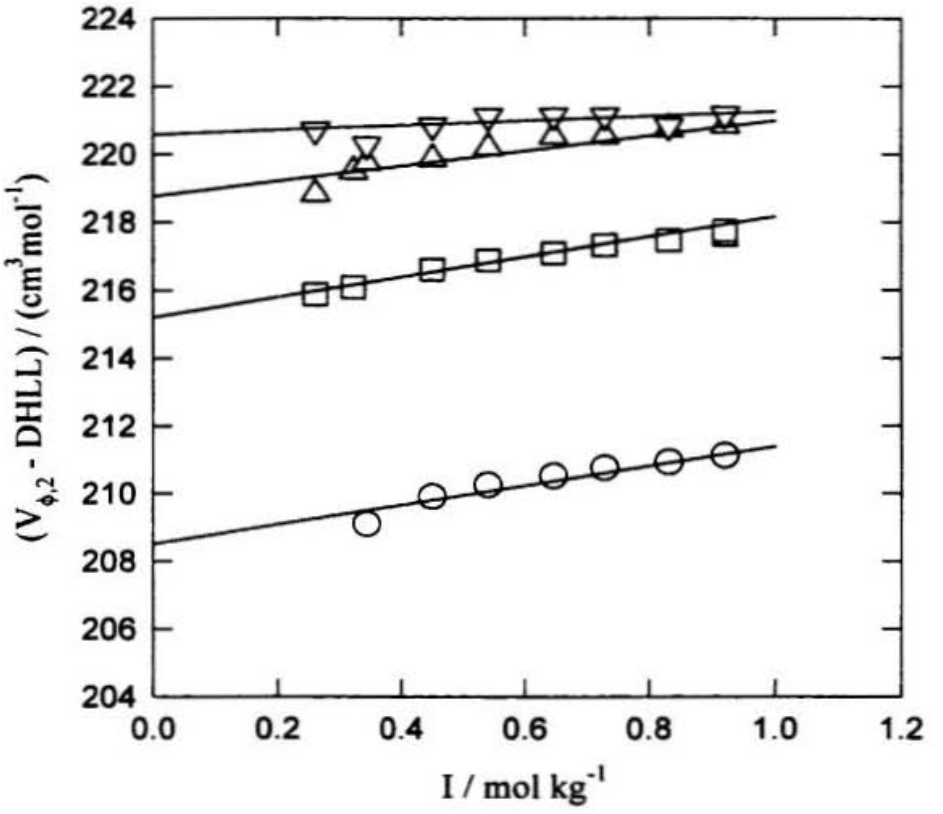

Figure III.7. Apparent molar volumes of $Na_3CuDTPA(aq)$ plotted as a function of ionic strength I after subtracting the Debye-Hückel limiting law (DHLL) term according to equation (III.15): ○, T = 283.15 K; □, T = 298.15 K; △, T = 313.15 K; ▽, T = 328.15 K. Symbols are experimental results and lines represent the global least-squares fits to equation (III.15).

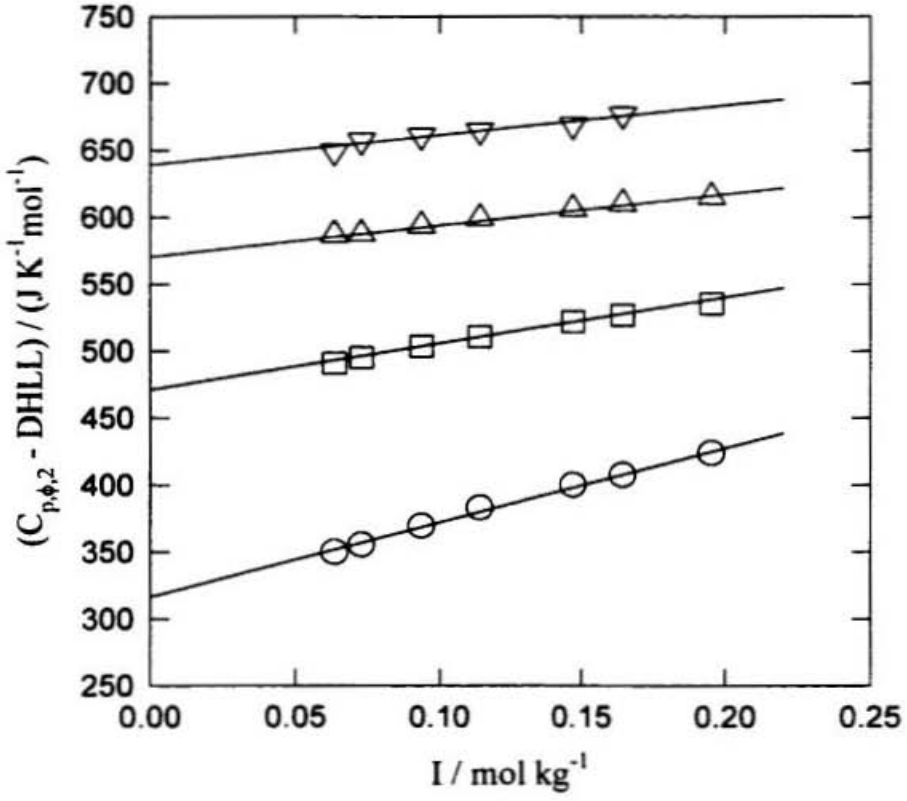

Figure III.8. Apparent molar heat capacities of $NaCu_2DTPA(aq)$ plotted as a function of ionic strength I after subtracting the Debye-Hückel limiting law (DHLL) term according to equation (III.14): ○, T = 283.15 K; □, T = 298.15 K; △, T = 313.15 K; ▽, T = 328.15 K. Symbols are experimental results and lines represent the global least-squares fits to equation (III.14).

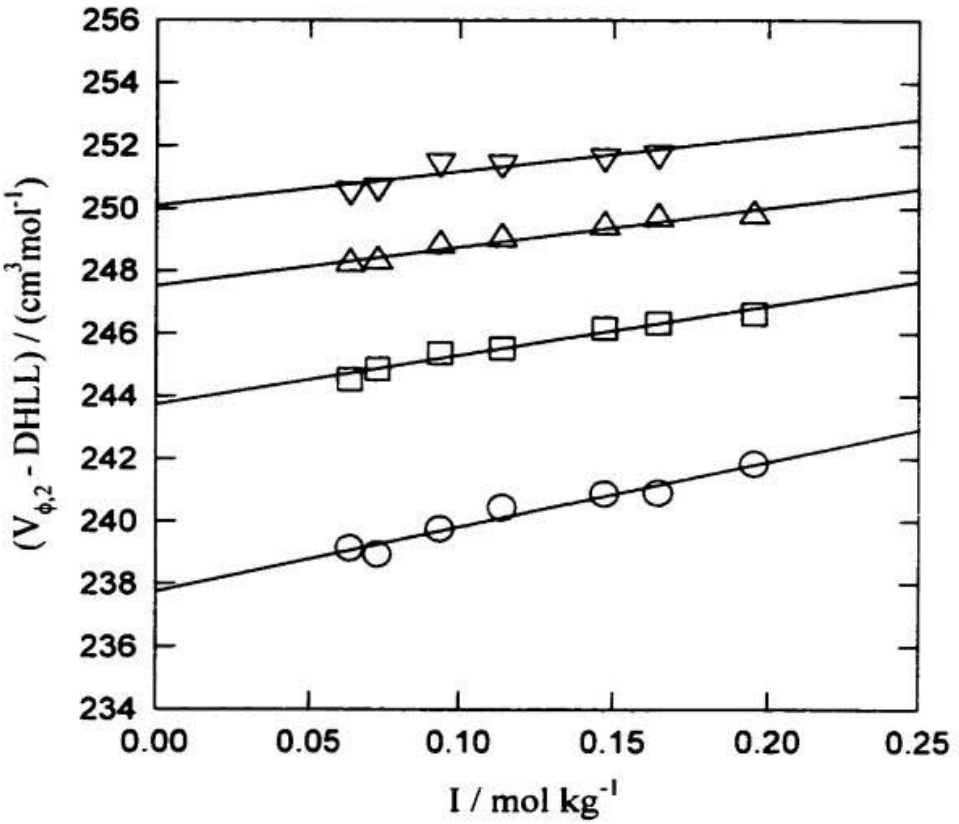

Figure III.9. Apparent molar volumes of $NaCu_2DTPA(aq)$ plotted as a function of ionic strength I after subtracting the Debye-Hückel limiting law (DHLL) term according to equation (III.15): ○, T = 283.15 K; □, T = 298.15 K; △, T = 313.15 K; ▽, T = 328.15 K. Symbols are experimental results and lines represent the global least-squares fits to equation (III.15).

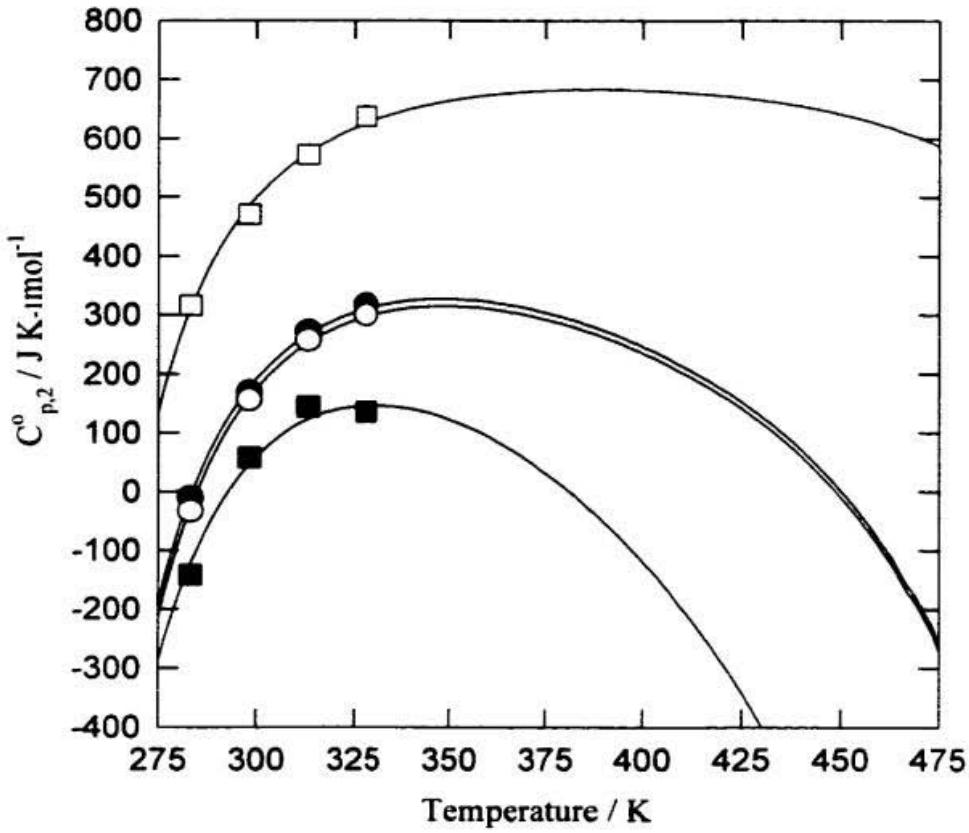

Figure III.10. Standard partial molar heat capacities $C^o_{p,2}$ of aqueous DTPA species obtained from fitting equation (III.14) to the experimental results at each temperature (shown as symbols), and the extrapolation to elevated temperatures by fitting the HKF equation (shown as solid lines). ●, $Na_2H_3DTPA(aq)$; ■, $Na_5DTPA(aq)$; ○, $Na_3CuDTPA(aq)$; and □, $NaCu_2DTPA(aq)$.

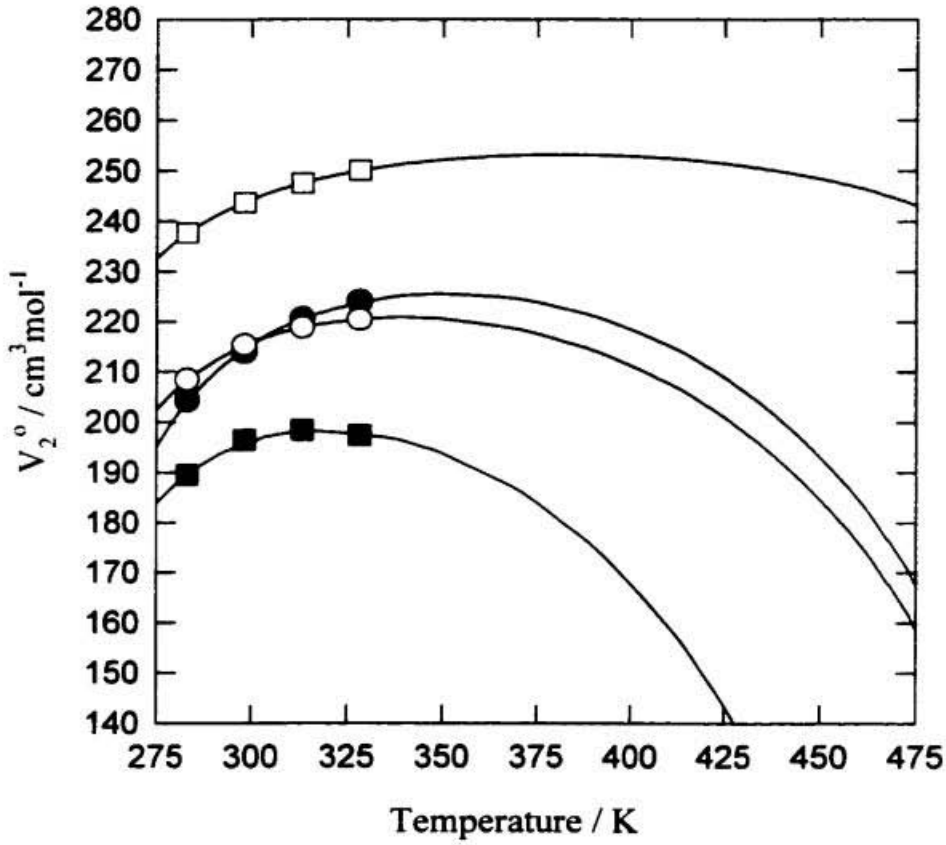

Figure III.11. Standard partial molar volumes V_2^o of aqueous DTPA species obtained from fitting equation (III.15) to the experimental results at each temperature (shown as symbols), and the extrapolation to elevated temperatures by fitting the HKF equation (shown as solid lines). ●, $Na_2H_3DTPA(aq)$; ■, $Na_5DTPA(aq)$; ○, $Na_3CuDTPA(aq)$; and □, $NaCu_2DTPA(aq)$.

To ensure that the results calculated from the Young's rule model were not significantly affected by our choice of the Guggenheim form of the extended Debye-Hückel equation, we have also chosen to treat our data with the Pitzer ion-interaction model (Pitzer, 1973, 1974, 1986 and 1991). The ion interaction model has been used with success to represent the properties of both single- and multi-component electrolyte solutions to very high ionic strengths. The application of the Pitzer model to the apparent molar properties of a single electrolyte $M_{\nu M}X_{\nu X}$ leads to the expressions:

$$C_{p,\phi,2} = C^{o}_{p,2} + \nu \mid z_M z_X \mid (A_C/2b) \ln(1 + bI^{1/2}) - 2\nu_M \nu_X RT^2[mB^C - m^2(\nu_M z_M)C^C] \quad \text{(III.20)}$$

$$V_{\phi,2} = V^{o}_{2} + \nu \mid z_M z_X \mid (A_V/2b) \ln(1 + bI^{1/2}) + 2\nu_M \nu_X RT[mB^V + m^2(\nu_M z_M)C^C] \quad \text{(III.21)}$$

in which $\nu = \nu_M + \nu_X$, $b = 1.2$. C^Y is an adjustable parameter, and B^Y is a function of ionic strength that has the form:

$$B^Y = \beta^{(0)Y} + 2\beta^{(1)Y}[1 - (1 + \alpha I^{1/2}) \exp(-\alpha I^{1/2})]/\alpha^2 I \quad \text{(III.22)}$$

here $\beta^{(0)Y}$ and $\beta^{(1)Y}$ are adjustable parameters and $\alpha = 2$.

For solutions of two electrolytes, the equations for the experimental apparent

molar properties can be represented in a form analogous to Young's rule:

$$Y_\phi \approx \{m_2 / (m_2 + m_3)\} Y_{\phi,2} + \{m_3 / (m_2 + m_3)\} Y_{\phi,3} + \delta \qquad \text{(III.2)}$$

The single-component terms, $Y_{\phi,2}$ and $Y_{\phi,3}$, are described by equations (III.20, III.21). When the two salts share a common cation, the binary interaction cross-terms and higher order terms, which we represent by δ, are small relative to the contibution of the major component $Y_{\phi,2}$. Pitzer parameters for $Y_{\phi,3}$(NaOH,aq) have been reported by Hovey *et al.*(1988) through fitting equations (III.20, III.21) to the data from Roux *et al.*(1984) These parameters, Y_3^o, $\beta_3^{(0)Y}$, $\beta_3^{(1)Y}$and C_3^Y, were then used in fitting equations (III.2, III.20-III.22) to our experimental data at each temperature. The fitted values for the standard partial molar properties of Na_3H_2DTPA(aq) and Na_5DTPA(aq) are listed in Table III.4. As is usually the case, values for $C_{p,2}^o$ and V_2^o from the Pitzer treatment differ slightly from those obtained with the Young's rule. The differences in V_2^o for both species are less than 1.0 $cm^3 \cdot mol^{-1}$ at 298.15 K, and no more than 2.5 $cm^3 \cdot mol^{-1}$ at 328.15 K. Differences in $C_{p,2}^o$ of up to 20 $J \cdot K^{-1} \cdot mol^{-1}$ and 40 $J \cdot K^{-1} \cdot mol^{-1}$, were observed for Na_3H_2DTPA(aq) and Na_5DTPA(aq), respectively. Because the standard deviations were smaller, the standard partial molar properties derived from the Guggenheim equations were used in the following calculations.

Partial molar properties at the standard ionic strength I = 0.1 $mol \cdot kg^{-1}$ are useful in relating heat capacities and volumes to other published thermodynamic constants. These

were obtained from the fitted parameters using the relationship:

$$\overline{Y_2} = Y_\phi + I(\partial Y_\phi/\partial I) \qquad \text{(III.23)}$$

where $\overline{Y_2}$ refers to the partial molar properties at ionic strength I. The results of these calculations are also given in Table III.1.

For some thermodynamic calculations, it is more convenient to tabulate the partial molar heat capacities and volumes of individual ions on the conventional scale, $Y_2^\circ(H^+, aq) \equiv 0$, and $\overline{Y_2}\ (H^+, I) \equiv 0$. These results are listed in Table III.5.

Table III.4. Standard Partial Molar Volumes and Heat Capacities for $Na_3H_2DTPA(aq)$ and $Na_5DTPA(aq)$ from 283 to 328 K from the Pitzer Ion Interaction Model.

T	V_2^o	$C_{p,2}^o$
	$Na_3H_2DTPA(aq)$	
283.15	202.99(0.52)	-68.66(15.5)
298.15	213.60(0.23)	153.39(3.8)
313.15	220.65(0.25)	271.02(3.1)
328.15	222.11(0.99)	298.34(2.7)
	$Na_5DTPA(aq)$	
283.15	188.64(1.66)	-187.25(38.0)
298.15	197.22(0.46)	97.26(2.2)
313.15	200.83(0.73)	238.32(4.0)
328.15	199.83(1.56)	188.74(35.9)

Units: $cm^3 \cdot mol^{-1}$ and $J \cdot K^{-1} \cdot mol^{-1}$.

III.4 Discussion

III.4.1 Comparison with Other Workers

Although no other measurements of $C_{p,\phi,2}$ and $V_{\phi,2}$ have been reported for these species, Milyukov and Polenova (1981) have determined temperature-dependent thermodynamic functions for the stepwise ionization of diethylenetriaminepentaacetic acid in aqueous solution over the range 283 - 313 K. Their results for the enthalpy of ionization of $HDTPA^{4-}$(aq) and H_2DTPA^{3-}(aq) at ionic strength 0.1m were expressed as: $\Delta_{ion}H(HDTPA^{4-}, I=0.1)/(J\cdot mol^{-1}) = 52340 - 62.8\ T$, and $\Delta_{ion}H(H_2DTPA^{3-}, I=0.1)/(J\cdot mol^{-1}) = 33850 - 51.6\ T$, respectively. From these we obtain the values $\Delta_{ion}C_p\ (H_2DTPA^{3-}, I=0.1) = -51.6\ J\cdot K^{-1}\cdot mol^{-1}$ = and $\Delta_{ion}C_p = (HDTPA^{4-}, I=0.1) = -62.8\ J\cdot K^{-1}\cdot mol^{-1}$ from the thermodynamic relationship $\Delta_{ion}C_p = (\partial\Delta_{ion}H/\partial T)_p$. The resulting value for the ionization of H_2DTPA^{3-}(aq) to $DTPA^{5-}$(aq), $\Delta_{ion}C_p\ (I=0.1) = -114.4\ J\cdot K^{-1}\cdot mol^{-1}$, is in excellent agreement with our value of $-113.9\ J\cdot K^{-1}\cdot mol^{-1}$, calculated from the data in Table III.5. Combining Polenova's experimental values of $\Delta_{ion}C_p$ with the values of $C_p\ (DTPA^{5-}, I=0.1)$ and $C_p\ (H_2DTPA^{3-}, I=0.1)$ listed in Table III.5, yields values for $C_p(HDTPA^{4-}, I=0.1)$ at I = 0.1 m and 298.15 K. The results, $C_p(HDTPA^{4-}, I=0.1) = 65.1\ J\cdot K^{-1}\cdot mol^{-1}$ from the ionization reaction of $HDTPA^{4-}$(aq), and $C_p(HDTPA^{4-}, I=0.1) = 64.6\ J\cdot K^{-1}\cdot mol^{-1}$ from the ionization reaction of H_2DTPA^{3-}(aq), agree well with each other and we have entered the value $64.9\pm4.0\ J\cdot K^{-1}\cdot mol^{-1}$ in Table III.5. We note that the proton dependance of $C_p(I=0.1)$ for H_2DTPA^{3-}(aq), $HDTPA^{4-}$(aq) and $DTPA^{5-}$(aq) is approximately linear.

Table III.5. Partial Molar Volumes and Heat Capacities for Individual Ions on the Conventional Scale at 298.15[a].

Scale	Conventional Scale			Absolute Scale		
ion	V_2^o	V_2 (I = 0.1m)	$C_{p,2}^o$	$C_{p,2}$ (I = 0.1m)	V_2^{oabs}	$C_{p,2}^{oabs}$
H^+	0	0	0	0	-6.4	-71
Na^+	-1.21	-1.08	42.8	46.2	-7.6	-28
Cu^{2+}	-25.3	-25.0	-18.2	-17.0		
H_2DTPA^{3-}	217.61	221.75	41.1	116.2	237	254
$HDTPA^{4-}$			(-57.2)	64.9		227
$DTPA^{5-}$	202.52	212.09	-155.4	2.3	234	200
$CuDTPA^{3-}$	218.95	223.05	28.6	97.7	238	242
Cu_2DTPA^-	244.95	248.72	428.0	504.0	251	499

[a] Values for DTPA complexes are from isothermal fits in this work, while those for other ions are from Hovey *et al.*(1988). Units: $cm^3 \cdot mol^{-1}$ and $J \cdot K^{-1} \cdot mol^{-1}$.

This is consistent with the structures proposed by Nakamoto *et al.*(1963), shown in Figure III.12, in which the protons are attached to the terminal amine groups of the central chain and all five carboxylic groups are ionized.

As no measurements were performed to determine the apparent molar properties of $HDTPA^{4-}$(aq), it is impossible to convert the calculated value of C_p($HDTPA^{4-}$, I = 0.1m) to $C^o_{p,2}$. Based on the trend observed for the heat capacities of $DTPA^{5-}$(aq), $HDTPA^{4-}$(aq) and H_2DTPA^{3-}(aq) at ionic strength I = 0.1m, we have used linear interpolation to obtain the value $C^o_{p,2}$ ($HDTPA^{4-}$,aq) ≈ -57 $J \cdot K^{-1} \cdot mol^{-1}$. We estimate the uncertainty to be no more than ±6 $J \cdot K^{-1} \cdot mol^{-1}$.

III.4.2 Low Temperature Structural and Hydration Effects

No crystal structures for the sodium copper complexes of DTPA have been reported, and aqueous copper complexes are not amenable to study by NMR. Nevertheless, some information about the structures of $CuDTPA^{3-}$ and Cu_2DTPA^- at pH = 7.4 may be inferred from spectroscopic data by several authors (Sievers and Bailar, 1962; Trzebiatowska *et al.*, 1977; Choppin *et al.*, 1979; Finnen *et al.*, 1991) Plausible structures are are shown in Figure III.12. The structure shown for $CuDTPA^{3-}$ is that of the corresponding nickel complex, with three bound amine groups and three of the four terminal carboxylate groups forming labile ligands to the central metal (Sievers and Bailar, 1962; Trzebiatowska *et al.*, 1977). The infrared spectrum of $CuDTPA^{3-}$ contains fine features which suggest a more complicated structure than the nickel analogue

(Sievers and Bailar, 1962). An alternative sexadentate structure, observed for the alkaline earth complexes (Choppin *et al.*, 1979) would have only the two terminal amine groups and four carboxylate groups coordinated to the metal. The structure of the $Cu_2DTPA^-(aq)$ complex shown in Figure III.12, was proposed by Sievers and Bailar (1962), based on an interpretation of its infrared spectrum. Their structure has two very distinct sites for the Cu(II) ions, each with a coordination number of four.

The structure of the $FeDTPA^{2-}$ complex at low and high pH has been determined by Finnen *et al.* (1991) using X-ray crystallography. At low pH, the iron is in a six-coordinate, roughly octahedral site, bonded to two nitrogen and three oxygen atoms from the ligand and one oxygen atom from water (Finnen *et al.*, 1991; Kennard, 1967), while, at high pH, an additional ligand carboxyl was found to join the coordination sphere, making the iron seven-coordinate and roughly pentagonal bipyramidal (Finnen *et al.*, 1991; Kennard, 1967; Lopez-Alcala *et al.*, 1984). The high-pH complex is similar to that suggested for $CuDTPA^{3-}$ in Figure III.12, except that the fourth terminal carboxlate group is also coordinated. In the following section we have used the interatomic distances from $FeDTPA^{2-}$ to estimate the ionic radius $CuDTPA^{3-}$, since both complexes reflect the most efficient wrapping of the charged ligand groups around the metal ion and do not contain coordinated water.

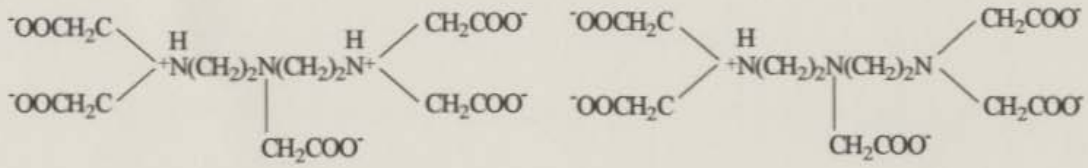

H_2DTPA^{3-}(aq)

$HDTPA^{4-}$ (aq)

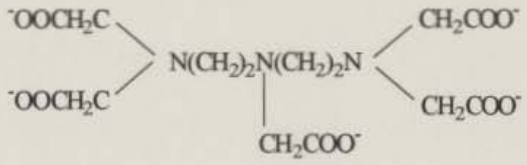

$DTPA^{5-}$ (aq)

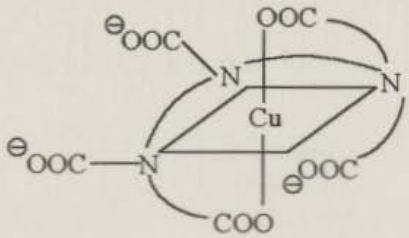

$CuDTPA^{3-}$ (?)

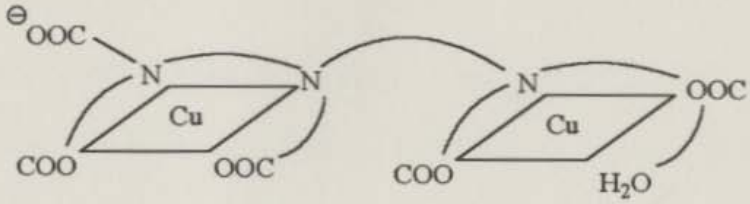

Cu_2DTPA^- (?)

Figure III.12. Structural formulas for H_2DTPA^{3-}(aq), $HDTPA^{4-}$(aq) and $DTPA^{5-}$(aq); the mono-copper (II) complex, $CuDTPA^{3-}$(aq); and the di-copper (II) complex, Cu_2DTPA^-(aq).

The experimental values for $C^{o}_{p,2}$ and V^{o}_{2} in Figures III.10 and III.11 all show a steep temperature dependance, and there are major differences in the values obtained for the salts of DTPA species with different charges. All of these data include significant contributions from Na^{+}(aq). In order to compare the partial molar properties of the DTPA species themselves, we have subtracted the contributions of the sodium ions using the approximate scale of "absolute" single ion properties developed by Marcus and co-workers (1985, 1986) form the tetraphenylarsonium/tetraphenylborate ion approximation. The estimated contributions of the individual species at 298.15 K are listed as $C^{o}_{p,2}{}^{abs}$ and V^{oabs}_{2} in Table III.5. As might be expected from their structures, H_2DTPA^{3-}(aq), $HDTPA^{4-}$ (aq) and $DTPA^{5-}$(aq) have similar single-ion volumes while the single-ion heat capacities show a systematic change with the degree of ionization. Standard partial molar volumes reflect the intrinsic volume and primary hydration sphere effects, while heat capacities are more sensitive to secondary solvation effects. As is evident from Figure III.12, ion-solvent hydrogen-bonding effects must be large for these molecules, so that significant differences in secondary solvation would be expected.

It is intriguing that the values of $C^{o}_{p,2}$ and V^{o}_{2} for Na_3H_2DTPA and $Na_3CuDTPA$ in Table III.5 and Figures III.10 and III.11 are approximately the same, suggesting that the two species have the same hydration behaviour in high pH aqueous solutions despite significant differences in their structures and charge distribution. The standard partial molar heat capacity and volume functions of EDTA complexes show similar behaviour if they process the same charge (Hovey and Tremaine, 1985; Hovey *et al.*, 1986, 1988),

however DTPA is a more complex molecule and its behaviour might have been expected to be less regular. The single-ion properties of $Cu_2DTPA^-(aq)$ are very different from those of $CuDTPA^{3-}(aq)$, suggesting that there are major differences in hydration between the two species, as is consistent with the structures in Figure III.12.

III.4.3 Extrapolation to Elevated Temperatures

One of the purposes of the present work is to obtain the equilibrium constants for the ionization reactions of aqueous H_5DTPA, and the stability constants of the Cu(II)-DTPA complexes at elevated temperatures.

Helgeson and coworkers (1981, 1988 and 1992) have developed a semi-empirical equation of state to describe the standard partial molar properties of aqueous electrolytes. This treatment is based on the assumption that the contribution of long-range solvent polarization to the standard partial molar properties can be described by the simple Born equation for a charged sphere in a dielectric continuum. The HKF equation of state has been used with some success to extrapolate the standard partial properties of aqueous electrolytes to temperatures as high as 573 K by Tremaine *et al.*(1986) and Conti *et al.*(1992). When pressure effects are ignored, the revised HKF equations (Tanger and Helgeson,1988; Shock *et al.*, 1992) for the standard partial molar heat capacity and volume can be written as:

$$C^{o}_{p,2} = a_1 + a_2 / (T - \Theta)^2 + \omega_{Born} TX \qquad \text{(III.24)}$$

$$V_2^o = b_1 + b_2 / (T - \Theta) + \omega_{Born} Q \qquad \text{(III.25)}$$

Here, the terms a_1, a_2, b_1, and b_2 are species-dependent fitting parameters, and $\Theta = 228$ K is a solvent-dependent parameter. The terms $\omega_{Born} TX$ and $\omega_{Born} Q$ are the electrostatic contributions to the standard partial molar heat capacity and volume according to the Born equation. X, Q and ω_{Born} are given by:

$$Q = \varepsilon^{-1} (\partial \ln \varepsilon / \partial p)_T \qquad \text{(III.26)}$$

$$X = \varepsilon^{-1} \{ (\partial^2 \ln \varepsilon / \partial T^2)_p - (\partial \ln \varepsilon / \partial T)_p^2 \qquad \text{(III.27)}$$

and

$$\omega_{Born} = Z^2 \eta / r_e \qquad \text{(III.28)}$$

where ε is the static dielectric constant of water, $\eta = 6.9466 \times 10^{-5}$ J-m^{-1}-mol^{-1}, Z is ionic charge, and r_e is an effective electrostatic radius of the ion: $r_e = r_{cryst} + 0.94$ Z for cations; $r_e = r_{cryst}$ for anions (Helgeson *et al.*, 1981). Values for X and Q were taken from Tanger and Helgeson (1988).

For our HKF calculations, the effective radius of $CuDTPA^{3-}$ was estimated by calculating the distance between the iron and the outer-sphere oxygen atoms of the Fe(III)-DTPA complex from the crystallographic data of Finnen *et al.* (1991). The

effective radius of $CuDTPA^{3-}$ was assumed to be the average value, 4.82 Å, plus the van der Waals radius of oxygen, 1.20 Å, from which the coefficients r_{eff} and ω_{Born} could be calculated. In the absence of any crystallographic data, the values of r_{eff} for $Cu_2DTPA^-(aq)$ and the aqueous DTPA species were assumed to be identical to those for $CuDTPA^{3-}(aq)$. The structure of these species is is quite different from $CuDTPA^{3-}(aq)$, and the estimated values for r_{eff} are certainly less accurate.

The standard partial molar properties $C^o_{p,2}$ and V^o_2 were extrapolated up to 473 K by fitting equations (III.24) and (III.25) to the values from the isothermal curve fits in Table III.1. The results are plotted in Figures III.10 and III.11. The parameters for the HKF equation are listed in Table III.6.

High temperature equilibrium constants can be calculated from the tabulated values at 298.15 K, from the following expression:

$$\ln K_T = \ln K_{298} + (\Delta H^o_{298}/R)[(1/298.15) - (1/T)] + (1/R)\int_{298}^{T} \Delta C^o_p \, dT$$
$$- [1/(RT)]\int_{298}^{T} \Delta C^o_p/T \, dT - [1/(RT)]\int_{1}^{P} \Delta V^o dT \qquad \text{(III.29)}$$

using literature values for $\ln K_{298}$ and ΔH^o_{298} (Martell and Smith, 1982), which are tabulated in Table III.7, and the HKF expressions for the temperature-dependent standard partial molar heat capacities and volumes of $Na_3H_2DTPA(aq)$, $Na_5DTPA(aq)$, $Na_3CuDTPA(aq)$, and $NaCu_2DTPA(aq)$ from Table III.6. These calculations were conveniently carried out with the software package *SUPCRT92* (Johnson *et al.*, 1992).

Temperature-dependant formation constants were calculated for the following equilibria:

$$H_2DTPA^{3-}(aq) \rightleftharpoons 2H^+(aq) + DTPA^{5-}(aq) \qquad \text{(III.30)}$$

$$H_2DTPA^{3-}(aq) \rightleftharpoons H^+(aq) + HDTPA^{4-}(aq) \qquad \text{(III.31)}$$

$$Cu^{2+}(aq) + H_2DTPA^{3-}(aq) \rightleftharpoons CuDTPA^{3-}(aq) + 2H^+(aq) \qquad \text{(III.32)}$$

and

$$Cu^{2+}(aq) + DTPA^{5-}(aq) \rightleftharpoons CuDTPA^{3-}(aq) \qquad \text{(III.33)}$$

The calculated values of log K for reactions (III.30) to (III.33) are tabulated in Table III.8 and plotted as a function of temperature in Figure III.13. By way of comparison, we have also plotted values of log K extrapolated, according to the expression:

$$\ln K_T = \ln K_{298} + \Delta H_{298}^\circ[(1/298.15) - (1/T)]/R + \Delta C_p^\circ [\ln(T/298.15) - 1 + (298.15/T)]/R \qquad \text{(III.34)}$$

which assumes that the values of $\Delta C^\circ_{p,298}$ for these isocoulombic reactions are independent of temperature. The term for ΔV has been neglected, as the effect of pressure on $\ln K_T$ is quite small below 573 K.

The uncertainty of the equilibrium constants listed in Table III.8 includes the

statistical and systematic uncertainties of ln K_{298}, ΔH^{o}_{298} and ΔC^{o}_{p}. The uncertainties caused by ΔV^{o} are negligible at steam saturation pressures. (An error of ±50 $cm^{3}\cdot mol^{-1}$ in ΔV^{o} would lead to an error of less than 0.05 in log K at 573 K.) The following approximate expression was used to calculate the uncertainties in the values calculated from the HKF parameters through equation (III.29):

$$\begin{aligned}\sigma^{2}_{\ln KT} = \sigma^{2}_{\ln K298} &+ \sigma^{2}_{\Delta H298^{o}}\{[(1/298.15) - (1/T)]/R\}^{2} \\ &+ \sigma^{2}_{\Delta C^{o}p298}\{[\ln(T/298.15) - 1 + (298.15/T)]/R\}^{2} \\ &+ \sigma^{2}_{\Delta G^{o}BORN,T,p}/(RT)^{2} \qquad \text{(III.35)}\end{aligned}$$

Here we assume that the error in the low temperature HKF parameters can be approximated by the uncertainty of $\Delta C^{o}_{p,298}$. The effect of uncertainties in estimating the effective radius of the DTPA species on the Born term was calculated by assuming an error of ±10 percent in r_{e}. The error limits for the formation constants of the complexation of copper(II) with DTPA are listed in Table III.8.

Table III.6. HKF Parameters for $Na_3H_2DTPA(aq)$, $Na_5DTPA(aq)$, $Na_3CuDTPA(aq)$, and $NaCu_2DTPA(aq)$.

	$C^o_{p,2}$		V^o_2	
solute	a_1	a_2	b_1	b_2
Na_3H_2DTPA	701.11±12.13	$-(1.59\pm0.058)\cdot10^6$	268.36±1.02	$-(2.90\pm0.074)\cdot10^3$
Na_5DTPA	821.08±15.73	$-(1.63\pm0.074)\cdot10^6$	252.54±1.30	$-(2.02\pm0.094)\cdot10^3$
$Na_3CuDTPA$	691.04±7.73	$-(1.62\pm0.037)\cdot10^6$	255.68±0.24	$-(1.96\pm0.020)\cdot10^3$
$NaCu_2DTPA$	820.44±18.31	$-(1.43\pm0.087)\cdot10^6$	269.70±0.14	$-(1.62\pm0.010)\cdot10^3$

Units: a_1, $J\cdot K^{-1}\cdot mol^{-1}$; a_2, $J\cdot K\cdot mol^{-1}$; b_1, $cm^3\cdot mol^{-1}$; b_2, $cm^3\cdot K\cdot mol^{-1}$.

Table III.7. Thermodynamic Constants for the Ionization of $H_5DTPA(aq)$ and Complexation of $DTPA^{5-}(aq)$ with Copper(II) at 298.15 K and 0.1m Ionic Strength.

n	log K	ΔH^o	ΔS^o	ΔC_p^o [a]	ΔV^o
		$H_{5-n}DTPA^{n-}(aq) \rightleftharpoons H_{4-n}DTPA^{(n+1)-}(aq) + H^+(aq)$			
0	-2.0±0.2	-2.09	-45.1	-69.7	
1	-2.70±0.1	1.26	-47.6	-86.5	
2	-4.28±0.04	6.28	-62.8	-181.2	
3	-8.60±0.05	17.99	-104.6	-51.6	
4	-10.50±0.07	33.47	-87.9	-62.8	
		$Cu^{2+}(aq) + H_2DTPA^{3-}(aq) \rightleftharpoons CuDTPA^{3-}(aq) + 2H^+(aq)$			
	2.1±0.18	-5.44	24.3	-1.5	26.3
		$Cu^{2+}(aq) + DTPA^{5-}(aq) \rightleftharpoons CuDTPA^{3-}(aq)$			
	21.2±0.3	-56.90	217.6	112.4	35.96

[a] ΔC_p values calculated from $d\Delta H/dT$. Units: ΔH^o, $kJ \cdot mol^{-1}$; ΔS^o, $J \cdot K^{-1} \cdot mol^{-1}$; ΔC_p, $J \cdot K^{-1} \cdot mol^{-1}$, ΔV^o, $cm^3 \cdot mol^{-1}$.

Table III.8. Ionization Constants and Formation Constants for the Complexation of Copper(II) with DTPA According to Reactions (III.30) to (III.33), Calculated Using the HKF Model .

	log K_T [a]			
T	reaction(III.30)	reaction(III.31)	reaction(III.32)	reaction(III.33)
273	-19.95±0.12	-8.90±0.05	2.40±0.18	22.34±0.30
298	-19.09±0.12	-8.60±0.05	2.31±0.18	21.40±0.30
323	-18.41±0.12	-8.37±0.05	2.23±0.18	20.65±0.30
348	-17.88±0.12	-8.19±0.05	2.17±0.18	20.03±0.30
373	-17.46±0.13	-8.06±0.06	2.11±0.19	19.55±0.31
398	-17.14±0.13	-7.97±0.07	2.07±0.20	19.18±0.31
423	-16.93±0.14	-7.93±0.08	2.03±0.22	18.91±0.33
448	-16.82±0.15	-7.93±0.10	2.01±0.24	18.75±0.34
473	-16.81±0.16	-7.97±0.11	2.00±0.27	18.75±0.34
498	-16.93±0.19	-8.07±0.13	2.01±0.30	18.79±0.39
523	-17.19±0.20	-8.25±0.15	2.04±0.34	19.04±0.41
548	-17.66±0.20	-8.52±0.16	2.10±0.38	19.50±0.45
573	-18.44±0.21	-8.94±0.18	2.22±0.41	20.28±0.48

[a] Calculated from equation (III.29) using data in Tables III.6 and III.7, assuming $\log K_{298} \approx \log K_{298}(I = 0.1\ m)$, $\Delta H^{o}_{298} \approx \Delta H_{298}(I = 0.1\ m)$.

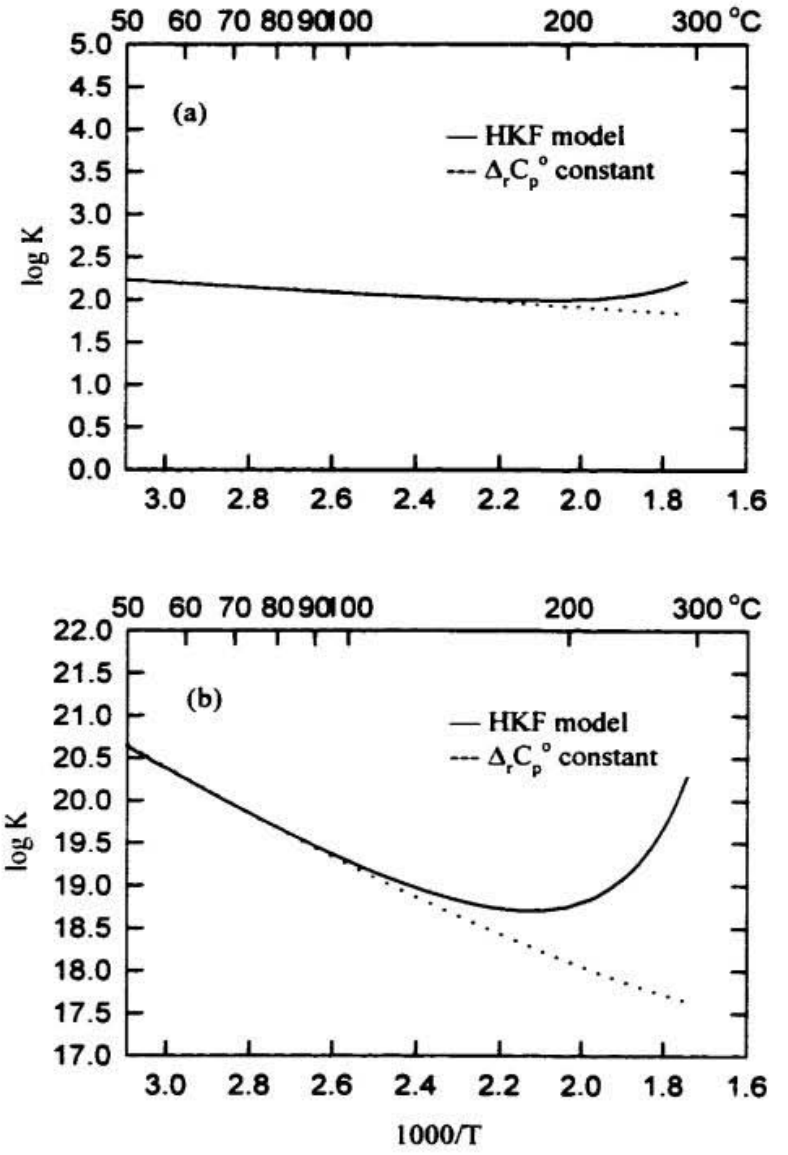

Figure III.13. Stability constants for (a), reactions (III.32); and (b), reaction (III.33). Solid line, HKF extrapolation; dashed line, isocoulombic extrapolation, equation (III.34).

In Figure III.13, we also plotted the values of log K for reactions (III.32) and (III.33) as a function of reciprocal temperature, so the effect of ΔC_p^o is apparent as curvature in the plots. The magnitude of $\Delta C_{p,298}^o$ for both reactions is quite small because the values of $C_{p,298}^o$ for $CuDTPA^{3-}(aq)$, $H_2DTPA^{3-}(aq)$ and $DTPA^{5-}(aq)$ are very similar (Table III.5). As a result, the agreement of log K obtained from equation (III.34) is in acceptable agreement with that of the HKF extrapolation until about 398 K, where the Born term becomes significant. The Born term becomes very large at high temperature, especially for $DTPA^{5-}(aq)$. The effect of the Born term is greatest for reaction (III.33) which is electrically unsymmetric, whereas reaction (III.32) is almost iso-coulombic.

The data in Table III.8 should be used with caution because aqueous DTPA species and their copper complexes are expected to undergo thermal decomposition at high temperatures. Although no experiments to determine the decomposition kinetics of aqueous H_5DTPA and the copper(II)-DTPA complexes have been reported, Martell *et al.*(1975) and Motekaitis *et al.* (1979) have studied the thermal decomposition of EDTA and NTA under hydrothermal conditions. Their results indicate that at 473 K, $EDTA^{4-}$ decomposed stepwise through the sequential loss of acetate groups, and NTA did not cleave below 533 K, but decomposed at about 663 K. Some cations are known to stabilize EDTA complexes relative to the free EDTA while others are destabilizing.

Chapter IV. Thermodynamics of the Complexes of Aqueous Nickel (II) and Iron (III) Cations with Diethylenetriaminepentaacetic Acid (DTPA)

IV.1 Introduction

In the previous chapter, we reported measurements of the apparent and partial molar volumes and heat capacities for aqueous H_2DTPA^{3-}, $DTPA^{5-}$ and the 1:1 and 2:1 copper(II)-DTPA complexes, $CuDTPA^{3-}$ and Cu_2DTPA^-, over a temperature range between 283 and 328 K. The low temperature hydration behaviour of Cu(II)-DTPA complexes could be better understood if the structures of these complexes were known in aqueous solution. Unfortunately, no crystal structures for the sodium copper complexes of DTPA have been reported, and aqueous copper complexes are not amenable to study by NMR.

As discussed in Chapter III, DTPA was selected in this study because the $DTPA^{5-}$ anion has a large negative charge, and is capable of acting as an octadentate ligand. Its interactions with metal ions are also of fundamental interest. Earlier calorimetric studies of aqueous EDTA systems showed that simple relationships for the partial molar properties of the EDTA metal complexes can be derived by considering the charge and size of the metal ion (Hovey et al., 1986,1988; Hovey and Tremaine, 1985). To apply these models to the partial molar properties of DTPA complexes, it is necessary to examine the effect of other charge-type metal ions.

We extended our calorimetric study to nickel(II) and iron(III) DTPA complexes.

These metals were chosen because the aqueous Ni(II)-DTPA complex had been determined by NMR (Trzebiatowska *et al.*, 1977; Grazynski and Trzebiatowska, 1980) under a wide variety of conditions, and because crystal structures of $[FeH_2DTPA]_2 \cdot 2H_2O$ and $Na_2FeDTPA \cdot 2H_2O$ are known from X-ray diffraction (Finnen *et al.*, 1991). In this chapter, we report apparent and partial molar volumes and heat capacities for aqueous $NiDTPA^{3-}$, $FeDTPA^{2-}$ and $FeHDTPA^{-}$ at 298.15 K, all as the sodium salts, and compare the contributions of the non-Born term to the partial molar properties of DTPA metal complexes. A general correlation was obtained for the calculation of partial molar properties of metal DTPA complexes at various conditions. We also report preliminary measurements of the structure of Cu(II)-DTPA by XRD.

IV.2 Experimental

IV.2.1 Chemical Syntheses

Diethylenetriaminepentaactic acid (H_5DTPA) (Alfa) was recrystallized from hot water twice and dried at 80°C for several hours (Mehdi and Budesinsky, 1974). The purity was found to be >99.9 percent by titration against standard NaOH solution. Aqueous solutions of NaOH (50 weight percent) were prepared from carbonate-free 50% solution (Fisher "Certified" ACS) and standardized by titration against potassium hydrogen phthalate (Baker, "99.97 percent"). $NiCO_3$ (Baker) and $Fe(NO_3)_2 \cdot 9H_2O$ (Fisher) were used as supplied without further purification. The Ni(II), Fe(III) and Cu(II)-DTPA complexes were prepared by the procedure of Sievers and Bailer (1962) as outlined

below.

$NiH_3DTPA \cdot 2.68H_2O$

Powered nickel(II) carbonate (5.93 g, 0.05 mol) was added to a solution of H_5DTPA (19.65 g, 0.05 mol) in deionized H_2O (100 ml), after the evolution of CO_2 subsided, the blue-green solution was heated to 373 K. Absolute ethanol (15 ml) was added when the heating was discontinued, the solution was cooled in an ice-bath and blue-green crystal formed. The solid was collected, dried, and recrystallized by slow evaporation from H_2O. The product was dried at 383 K for five days, and the concentration of the protonated nickel complexes of DTPA in stock solutions was determined by titration against standard NaOH solution, which gave the stoichiometry, $NiH_3DTPA \cdot 2.84H_2O$. Solutions of $Na_3NiDTPA$ were prepared by mass, by adding the stoichiometric amounts of standard hydroxide solution to the NiH_3DTPA solution, followed by adjustment to pH $\approx$8.0 with 0.001 m NaOH.

FeH_2DTPA

An aqueous solution (100 ml) containing equivalent amounts of $Fe(NO_3)_2 \cdot 9H_2O$ (20.2 g, 0.05 mol) and solid H_5DTPA (19.65 g, 0.05 mol) was heated to 343 K. The clear orange solution turned bright yellow and turbid during the heating process. Absolute ethanol (15 ml) was added, the solution was allowed to cool slowly, and bright yellow crystals formed. The solid was dried at 383 K for five days, anhydrous product was

confirmed by differential scanning calorimeter (DSC) and potentiometric titration with standard NaOH solution. Solutions of NaFeHDTPA and $Na_2FeDTPA$ were prepared by adding stoichiometric amounts of standard NaOH solution to the FeH_2DTPA solution.

$CuH_3DTPA{\cdot}H_2O$

To a warm solution (20 ml) of H_5DTPA (0.39 g, 1 mmol), an equimolar quantity of freshly prepared copper(II) hydroxide (Weiser *et al.*, 1942) was added. The clear blue solution was allowed to cool slowly while well defined blue crystals were formed. The blue crystals are suitable for X-ray crystallography.

IV.2.2 Calorimetry Measurements

Nanopure water (resistivity > 8 MΩ·cm) was used to prepare all solutions. Solutions of NaCl (Aldrich "99.99 percent") for calibrating the densimeter and calorimeter were prepared by mass after drying the salt at 383 K for 24 hours.

A Sodev CP-C flow microcalorimeter (Picker *et al.*, 1971) and a Sodev 03D vibrating flow densitometer (Picker *et al.*, 1974) equipped with platinum cells were employed in this work. The temperatures of the calorimeter and densitometer were independently controlled to ±0.01 K by two Sodev CT-L circulating baths. The thermistor (Omega, 44107) used to measure the temperatures of calorimeter and densitometer were calibrated with a Hewlett-Packard 2804A quartz-crystal thermometer traceable to NBS standards. The densitometer was calibrated daily with pure water and

standard 1 mol·kg^{-1} NaCl(aq). The experimental values of $\{c_p \cdot \rho / (c^*_{p,1} \cdot \rho^*_1) - 1\}$ for the standard NaCl(aq) were compared with literature values complied by Archer and Wang (1992) to correct for a small heat-leak effect, according to the method of Desnoyers *et al.* (1976). Here, c_p, $c^*_{p,1}$, ρ and ρ^*_1 are the massic heat capacities and densities of the solution and $H_2O(l)$, respectively.

IV.2.3 Structure Determination

Crystals for X-ray measurements were mounted on a glass fibre. All measurements were made on a Rigaku AFC6S diffractometer with graphite monochromated Mo-Kα radiation. The intensity data were collected at a temperature of 26±1 °C using the ω-2θ scan technique to maximum 2θ values of 55.1°. Of the 4608 reflections which were collected, 4346 were unique, the final cycle of full-matrix least-squares refinement was based on 3536 observed reflections ($I > 2.00\sigma(I)$) and 331 variable parameters. The structure was solved by the direct method and refined by the Fourier technique. The function minimized was $\Sigma\omega(|F_o| - |F_c|)^2$ with $\omega = |\sigma^2(F_o)|$. The non-hydrogen atoms were refined anisotropically and hydrogen atoms were included but not refined. Neutral atom scattering factors were taken from Cromer and Waber (1974). Anomalous dispersion effects were included in F_c (Ibers and Hamilton, 1964), the values for $\Delta f'$ and $\Delta f''$ were those of Creagh and McAuley (1992). The values for the mass attenuation coefficient are those of Creagh and Hubbell (1992). All calculations were performed using the teXsan crystallography software package of Molecular Structure

Corporation. Detailed information about the structure determination is given in Appendix C.

IV.3 Results

IV.3.1 Apparent Molar Properties

The experimental values for the relative densities (ρ - ρ_1^*) and heat capacity ratios $\{c_p \cdot \rho / (c_{p,1}^* \cdot \rho_1^*) - 1\}$ of the solutions are listed in Tables A.IV.1, A.IV.2 and A.IV.3. The tables also tabulate the experimental apparent molar volumes V_ϕ and heat capacities $C_{p,\phi}$ which were calculated from these results using the procedure described in Chapter III. The effect of the small amount of excess NaOH used to control the speciation in the Na_3NiDTPA(aq) solution was subtracted by means of Young's rule (Young and Smith, 1954; Reilly and Wood, 1969), which was also described in Chapter III. The resulting values of $V_{\phi,2}$ and $C_{p,\phi,2}$ for Na_3NiDTPA(aq) are tabulated in Tables A.IV.1 and A.IV.2.

No excess NaOH was added to the solution of Na_2FeDTPA(aq), because a cloudy precipitate was observed to form at high pH. The hydrolysis of Na_2FeDTPA(aq) in aqueous solution is very small and therefore the contribution to the experimental values from the chemical relaxation effect was neglected. Because there are no literature values of stability constant and enthalpy data for NaFeHDTPA(aq), no corrections were made to the experimental values, and the derived standard partial molar properties of NaFeHDTPA(aq) should therefore be used cautiously. The speciation of Fe(III)-DTPA complex as a function of pH is plotted in Figure IV.1.

IV.3.2 Partial Molar Properties

The molality dependence of the apparent molar volumes $V_{\phi,2}$ and heat capacities $C_{p,\phi,2}$ were adequately represented by the simple Debye-Hückel equation (Hovey and Tremaine, 1986) instead of the more complex Guggenheim form of the extended Debye-Hückel equation (Millero, 1979; Pitzer *et al.*, 1961) required in Chapter III:

$$V_{\phi,2} = V_2^o + \omega A_V I^{1/2} + B_V I \qquad \text{(IV.1)}$$

$$C_{p,\phi,2} = C_{p,2}^o + \omega A_C I^{1/2} + B_C I \qquad \text{(IV.2)}$$

Here $I = \omega m = \frac{1}{2}\sum m_i z_i^2$. The terms A_V in equation (IV.1), and A_C in equation (IV.2) are the Debye-Hückel limiting slopes for the volume and heat capacity, respectively, whose values were taken from the compilation by Archer and Wang (1992). By definition, V_2^o and $C_{p,2}^o$ are the standard partial molar volume and heat capacity, respectively. Equations (IV.1) and (IV.2) were fitted to the experimental results by the Marquardt-Levenberg non-linear least-squares algorithm within the commercial software package SigmaPlot.© The fitted values for the standard partial molar properties are listed in Table IV.1 and plotted in Figure IV.2 and IV.3.

Partial molar properties at the standard ionic strength $I = 0.1$ mol-kg^{-1} are useful in relating volumes and heat capacities to other published thermodynamic constants. These were obtained from the fitted parameters using the relationship:

$$\overline{Y_2} = Y_\phi + I(\partial Y_\phi / \partial I) \qquad \text{(IV.3)}$$

where $\overline{Y_2}$ refers to the partial molar properties at ionic strength I. The results of these calculations are also given in Table IV.1. For some thermodynamic calculations, it is more convenient to tabulate the partial molar volumes and heat capacities of individual ions on the conventional scale, Y_2^o (H^+, aq) ≡ 0, and $\overline{Y_2}$ (H^+, I) ≡ 0. These results are listed in Table IV.2.

Table IV.1. Partial Molar Volumes and Heat Capacities for $Na_3NiDTPA(aq)$, $Na_2FeDTPA(aq)$ and $NaFeHDTPA(aq)$at Infinite Dilution and at I = 0.1m and T = 298.15 K from Least Squares Fits.[a]

salt	V_2^o	B_V	V_2	$C_{p,2}^o$	B_C	$C_{p,2}$
$Na_3NiDTPA$	215.81(0.24)	1.66(0.44)	221.48	163.05(5.63)	31.12(10.22)	262.58
$Na_2FeDTPA$	233.37(0.14)	5.44(0.94)	237.13	290.76(5.14)	18.77(34.10)	341.17
NaFeHDTPA	243.49(0.51)	16.45(10.81)	247.67	397.39(9.05)	129.59(190.6)	438.86

[a] Values in parenthesis are standard deviations from fitting equations (IV.3.1) and (IV.3.2). Units: $cm^3 \cdot mol^{-1}$ and $J \cdot K^{-1} \cdot mol^{-1}$.

Table IV.2. Partial Molar Volumes and Heat Capacities for Individual Ions on the Conventional Scale at T = 298.15 K[a].

Scale	Conventional Scale			Absolute Scale		
ion	V_2^o	V_2 (I=0.1m)	$C_{p,2}^o$	$C_{p,2}$ (I=0.1m)	V_2^{oabs}	$C_{p,2}^{oabs}$
H^+	0	0	0	0	-6.4	-71
Na^+	-1.21	-1.08	42.8	46.2	-7.6	-28
Cu^{2+}	-25.3	-25.0	-18.2	-17.0	-38.1	-162
Ni^{2+}	-28.6	-28.0	-38.9	-38.7	-41.4	-184
$CuDTPA^{3-}$	218.95	223.05	28.6	97.7	238	242
$NiDTPA^{3-}$	219.44	224.72	34.7	124.0	239	247
$FEDTPA^{2-}$	235.79	239.29	205.2	248.8	249	347
$HFeDTPA^-$	244.70	248.75	354.6	392.7	251	425
Cu_2DTPA^-	244.95	248.72	428.0	504.0	251	499

[a] Values for DTPA complexes are from isothermal fits in this work, while those for other ions are from Hovey *et al.*(1988). Units: $cm^3 \cdot mol^{-1}$ and $J \cdot K^{-1} \cdot mol^{-1}$.

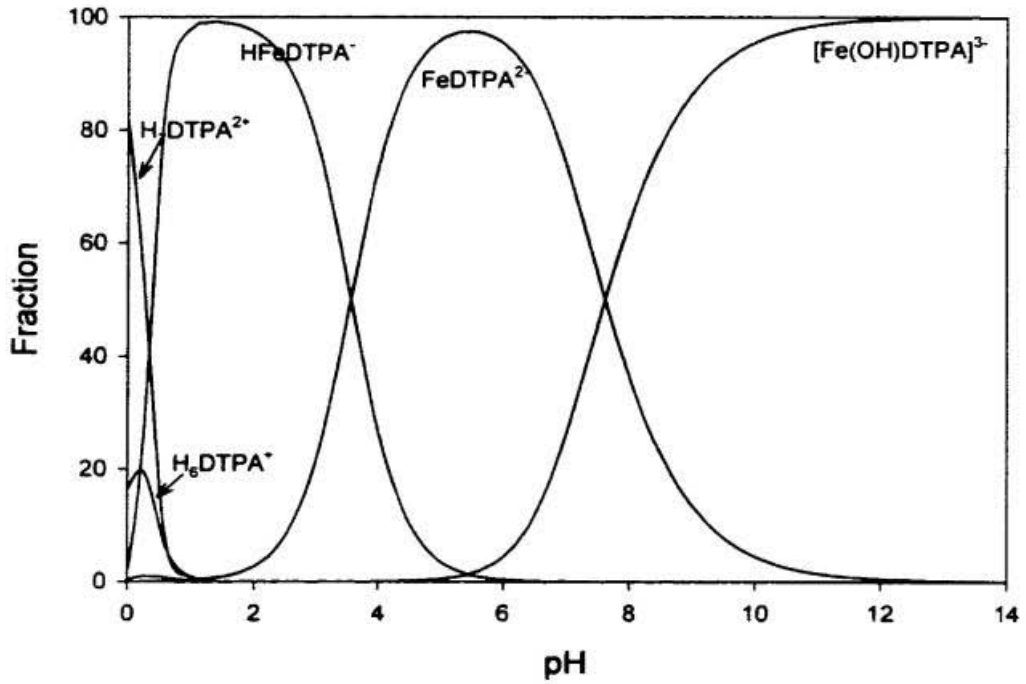

Figure IV.1. Speciation of aqueous Fe/DTPA = 1:1 at 298.15 K and I = 0.1 molar.

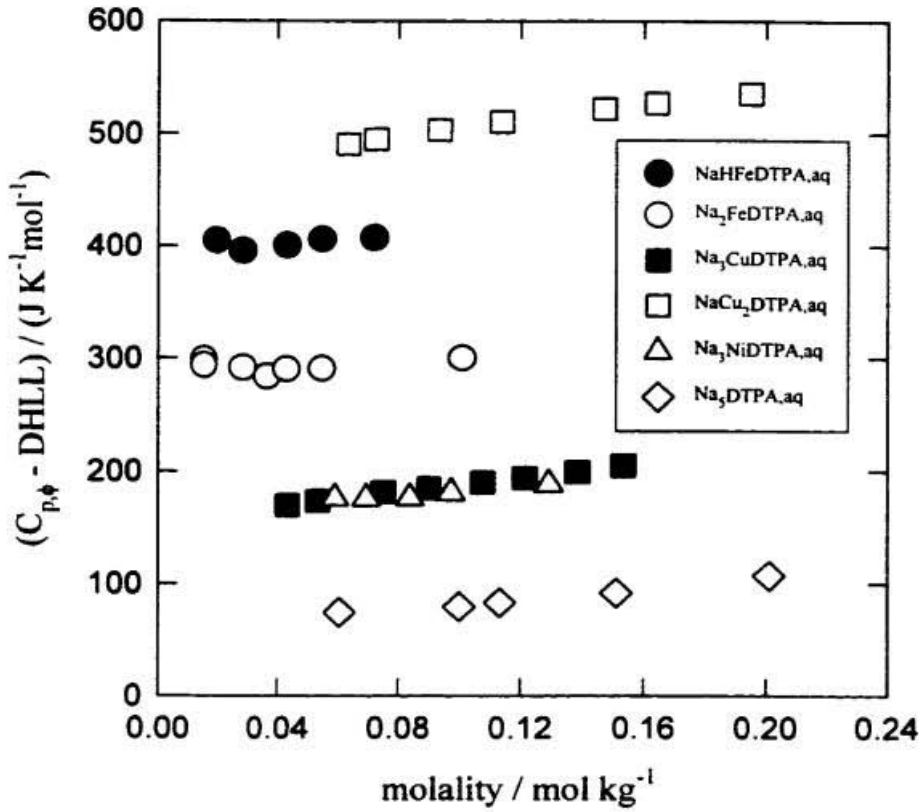

Figure IV.2. Apparent molar volumes of aqueous DTPA species and complexes plotted as a function of ionic strength I after subtracting the Debye-Hückel limiting law (DHLL) term according to equation (IV.3).

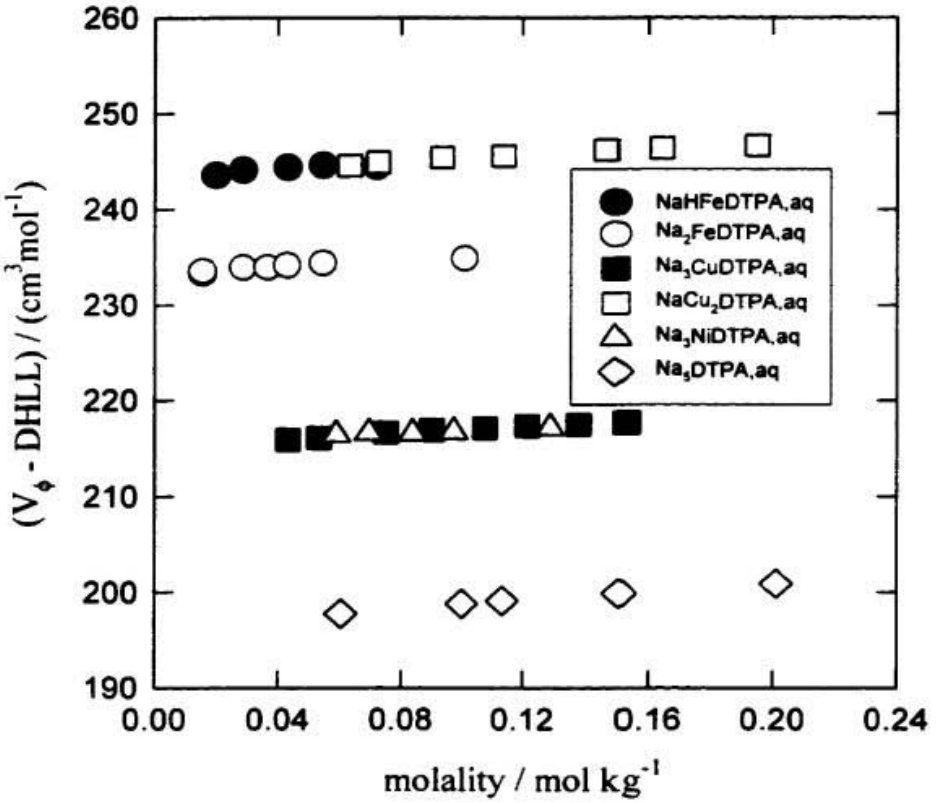

Figure IV.3. Apparent molar heat capacities of aqueous DTPA species and complexes plotted as a function of ionic strength I after subtracting the Debye-Hückel limiting law (DHLL) term according to equation (IV.4).

IV.4 Discussion

IV.4.1 Non-Born Term Contribution

The positive values of the conventional standard partial molar properties of DTPA complexes with Ni^{2+}, Cu^{2+} and Fe^{3+} are typical of large organic ions having a central charge surrounded by bulky polar groups (French and Criss, 1982). In order to compare the partial molar properties of the DTPA complexes themselves, the conventional partial molar properties in Table IV.2 must be converted to "absolute" values, by subtracting the effects of the H^+(aq) cation. We used $V^{abs}(H^+,aq) = -6.4\ cm^3\ mol^{-1}$ and $C_p^{abs}(H^+,aq) = -71\ J\ K^{-1}\ mol^{-1}$. These are based on the assumption that $C_p^o(Ph_4As^-,aq) = C_p^o(Ph_4B^-,aq)$ by Marcus and co-workers (Marcus, 1985; Abraham and Marcus,1986). The results are listed in Table IV.2.

The standard partial molar properties of ions are usually assumed to contain contributions from both "electrostatic" and "non-electrostatic" terms. Electrostatic contributions result from the formation of a tightly bound primary solvation sphere about small cations and long-range solvent polarization due to charge-dipole interactions, while non-electrostatic contributions include the intrinsic values for the ion as it might exist in the gas phase, the formation of a cavity in bulk water, the contribution from perturbations in the hydrogen-bonded structure of water caused by the presence of the solute through dispersion forces and geometric effects. The magnitude of the electrostatic contribution to both volume and heat capacity can be calculated by the Born equation:

$$V^{abs}_{2,Born} = -69.466 \times 10^5 (z^2 / r)(1 / \varepsilon)(\partial \ln\varepsilon / \partial p)_T \quad \text{(IV.5)}$$

$$C^{abs}_{p,2,Born} = 6.9466 \times 10^5 (z^2 / r)(T / \varepsilon)[(\partial^2 \ln\varepsilon / \partial T^2)_p - (\partial \ln\varepsilon / \partial T)_p^2] \quad \text{(IV.6)}$$

where ε is the dielectric constant of water, z is the charge of the DTPA complex ion. The terms $(\partial \ln\varepsilon / \partial p)_T$, $(\partial^2 \ln\varepsilon / \partial T^2)_p$ and $(\partial \ln\varepsilon / \partial T)_p$ were calculated from the compilation reported by Archer and Wang (1990). We assume the value r = 4.60 Å for the radius of the complex ion, based on the mean values of V_2^{abs}, calculated from Table IV.1. After subtracting the contribution of the Born term from the volume and heat capacity, we could obtain the non-electrostatic or "non-Born" contributions for the DTPA complex anions:

$$V^{abs}_{2,non\text{-}Born} = V^o_2 - 6.4z + 0.90z^2 \quad \text{(IV.7)}$$

$$C^{abs}_{p,2,non\text{-}Born} = C^o_{p,2} - 71z + 12.5z^2 \quad \text{(IV.8)}$$

The non-Born volumes and heat capacities of DTPA complexes and aqueous species from the equations above are illustrated in Figure IV.4. It is interesting to see that the volumes and heat capacities of $CuDTPA^{3-}$(aq), $NiDTPA^{3-}$(aq) and $FeDTPA^{2-}$(aq) are very close to one and another. The partial molar volume data for the DTPA complexes are

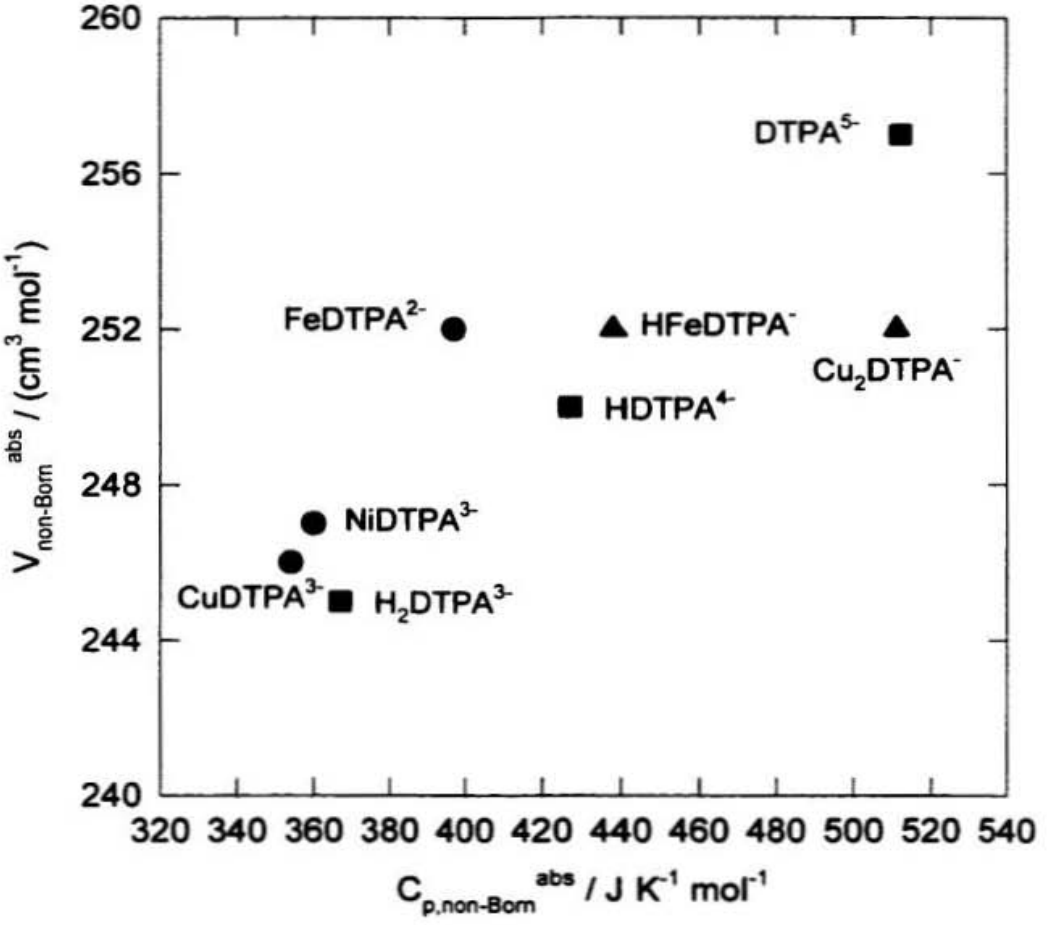

Figure IV.4. Partial molar volumes and heat capacities of aqueous DTPA species and metal complexes on the absolute ionic scale after subtraction of the Born contribution.

tightly grouped in the range 245 to 255 $cm^3 \cdot mol^{-1}$, and the heat capacity values for mono-nuclear complexes are in the range 350 to 400 $J \cdot K^{-1} \cdot mol^{-1}$. Much larger positive values are obtained for the di-nuclear and protonated DTPA complexes. The error limits for the calculated values of the non-Born contributions to the standard partial molar volumes and heat capacities of DTPA complexes are ± 5 cm^3 mol^{-1} and ± 36 J K^{-1} mol^{-1}, respectively. These come from the uncertainties in $C^{o}_{p,2}$ and V^{o}_{2}, uncertainties in the estimation of absolute values of partial molar properties of H^{+}(aq), and the effect of uncertainties in the effective radius of the DTPA complexes on the Born term, for which an error of ± 10 percent in r was assumed.

IV.4.2 Stuctures of DTPA Complexes

The crystal structure we obtained for $CuH_3DTPA \cdot H_2O$ is exactly the same as that reported by Seccombe *et al.* (1975). The complex is six-coordinated species, with three amine groups and three of the four terminal carboxylate groups bound to the central metal. Two nitrogen atoms, one from the central and the other from a terminal amine group, and two oxygen atoms of the carboxylate groups lie roughly at the corners of the a square. The remaining two ligands are much more weakly bound. From PMR studies (Trzebiatowska *et al.*, 1977; Grazynski and Trzebiatowska, 1980), the structure of $NiDTPA^{3-}$ complex in aqueous solution at pH > 7 was found to have three bound amine groups and three of the four terminal carboxylate groups coordinated to the central metal, while at pH < 7, one nitrogen was released from its coordination sphere and protonated,

and one water molecule entered the first coordination sphere. The crystal structure of $CuH_3DTPA{\cdot}H_2O$ is consistent with the high pH structure, and it is reasonable to expect that in high pH solution, the structure of Cu(II)-DTPA will be similar with that of Ni(II)-DTPA. The structure of the $Na_2FeDTPA{\cdot}2H_2O$ complex has been determined by Finnen *et al.* (1991) using X-ray crystallography. The iron is seven-coordinated and the complex is roughly pentagonal bipyramidal. The two axial atoms are oxygens, and the equatorial plane has a cis arrangement of oxygen atoms.

Although the structure of the complex in solution may not be the same as its structure in the solid, it is commonly believed that the crystal structure will persist in the solution to some extent. For EDTA complexes, the spectroscopic evidence (Oakes and Smith, 1983; Higginson and Samuel, 1970) suggests that the crystal structures of the Ca(II)-EDTA, Mg(II)-EDTA, Mn(II)-EDTA and Fe(III)-EDTA are preserved in aqueous solutions. From the analysis of the Cu(II), Ni(II) and Fe(III)-DTPA complexes, it can be inferred that the structures of these complexes are similar with each other in high pH solution, since all the complexes reflect the most efficient wrapping of the charged ligand groups around the metal ion and do not contain coordinated water. The coordination of DTPA in these complexes is not complete, because only the Nd(III)-DTPA complex (Stezowski and Hoard, 1984) has been observed to coordinate the middle carboxylate group, and the similarity of the non-Born terms needs to be verified for each structure-type.

The structure of the $Cu_2DTPA^-(aq)$ complex was proposed by Sievers and Bailer

(1962), based on an interpretation of its infrared spectrum. Their structure has two very distinct sites for the Cu(II) ions, each with a coordination number of four. The difference in the volumes and heat capacities between mono-nuclear and di-nuclear DTPA complexes suggests that hydration is different between these complexes.

IV.4.3 General Correlation

One of the purposes of the current study is to develop a predictive method for estimating the "missing" C_p^o and V^o for complexes with other metals.

The earlier calorimetric studies of the complexes of various divalent and trivalent metal ions with EDTA (Hovey and Tremaine, 1985), and the results for the Cu(II), Ni(II) and Fe(III)-DTPA complexes presented above are quite independent of the central metal ion, which indicates that the solvation effects at ambient temperature are very similar despite rather complicated structures of the complexes. The similarity in the values of $V^{abs}_{2,\text{non-Born}}$ and $C^{abs}_{p,2,\text{non-Born}}$ implies that a mean value could be used to represent the "non-Born" contributions to the partial molar properties of each chelate. If the temperature-dependence of these "non-Born" terms could be obtained, the partial molar heat capacities and volumes of different metal-chelates could be calculated at any temperature. The copper-chelates with EDTA, DTPA and NTA were chosen as model systems, because the temperature-dependent partial molar heat capacities and volumes from 283 to 328 K of these copper-chelates are known from the experimental measurements, and the HKF parameters for the "non-Born" contributions have been derived.

Our correlation is based on the assumption that the 'non-Born" contributions for the other metal chelates could be represented by the "non-Born" terms of the copper-chelates. Because the HKF equation is based on the conventional scale, so the conventional "non-Born" terms in Table III.6 must be converted to "absolute" values to subtract the effects Na^+(aq). The non-Born contribution of $Na_3CuDTPA$ (aq) could be expressed as:

$$Y^{o}_{non\text{-}Born}(Na_3CuDTPA, aq) = 3Y^{abs}_{non\text{-}Born}(Na^+, aq) + Y^{abs}_{non\text{-}Born}(CuDTPA^{3-}, aq) \quad (IV.9)$$

By assuming that $Y^{abs}_{non\text{-}Born}(MDTPA^{5-n}, aq) = Y^{abs}_{non\text{-}Born}(CuDTPA^{3-}, aq)$, the non-Born terms for the metal DTPA complexes $Y^{o}_{non\text{-}Born}(MDTPA^{5-n}, aq)$ can be derived from equation (I.14) as:

$$\begin{aligned} Y^{o}_{non\text{-}Born}(MDTPA^{5-n}, aq) &= Y^{abs}_{non\text{-}Born}(CuDTPA^{3-}, aq) + nY^{abs}_{non\text{-}Born}(H^+, aq) \\ &= Y^{o}_{non\text{-}Born}(Na_3CuDTPA, aq) - 3Y^{abs}_{non\text{-}Born}(Na^+, aq) \\ &\quad + nY^{abs}_{non\text{-}Born}(H^+, aq) \end{aligned} \quad (IV.10)$$

For EDTA and NTA metal complexes, similar assumptions are used to represent the "non-Born" contributions to the partial molar properties, and a general predictive

equation can be developed:

$$Y^{o}_{non\text{-}Born}(MX^{Z\text{-}n}, aq) = Y^{o}_{non\text{-}Born}(Na_{Z\text{-}2}CuX, aq) - (Z\text{-}2)Y^{abs}_{non\text{-}Born}(Na^{+}, aq) + nY^{abs}_{non\text{-}Born}(H^{+}, aq) \quad (IV.11)$$

Here, n and Z are the charges of the metal ion (M^{n+}) and chelate (X^{Z-}), respectively. The adjustable parameters from HKF equations to calculate the values of $Y^{o}_{non\text{-}Born}(Na_{Z\text{-}2}CuX, aq)$ are listed in Table IV.3, and the absolute values of $Y^{abs}_{non\text{-}Born}(H^{+}, aq)$ and $Y^{abs}_{non\text{-}Born}(Na^{+}, aq)$ are assumed to be temperature independent. Subtracting Shock and Helgeson's (1988) values for $V^{abs}_{Born}(H^{+}, aq) = -1.5\ cm^3\ mol^{-1}$, $C^{abs}_{p,\ Born}(H^{+}, aq) = -20.5\ J\ K^{-1}\ mol^{-1}$, $V^{abs}_{Born}(Na^{+}, aq) = -0.9\ cm^3\ mol^{-1}$, and $C^{abs}_{p,\ Born}(Na^{+}, aq) = -12.6\ J\ K^{-1}\ mol^{-1}$ from the absolute values in Table IV.2 yields practical equations that can be used to calculate the non-Born contributions to the partial molar heat capacities and volumes of different metal chelates:

$$C^{o}_{p,non\text{-}Born}(MX^{Z\text{-}n}, aq) = c_1 + c_2 / (T - \Theta)^2 + 15(Z\text{-}2) - 51n \quad (IV.12)$$

$$V^{o}_{non\text{-}Born}(MX^{Z\text{-}n}, aq) = v_1 + v_2 / (T - \Theta) + 6.7(Z\text{-}2) - 4.9n \quad (IV.13)$$

Here, c_1, c_2, v_1 and v_2 are the adjustable parameters, and $\Theta = 228$ K.

It should be pointed that the predictive equations for the NTA system are approximate, because further experimental results for other metal complexes are needed

to verify the regular behaviour of the NTA metal complexes. Also the temperature-dependence of the "absolute" partial molar heat capacities and volumes of $H^+(aq)$ and $Na^+(aq)$, which are not well known, should be included to make the calculations more accurate.

Table IV.3. Parameters for Predictive Equations Based on Non-Born term for Cu(II) Complexes.

Chelating agents	C_p^o (Non-Born)		V^o (Non-Born)	
	c_1	c_2	v_1	v_2
EDTA(aq)	505.52	-1.07×10^6	199.03	-1.63×10^3
DTPA(aq)	691.04	-1.62×10^6	255.68	-1.96×10^3
NTA(aq)	268.97	-7.48×10^6	114.94	-1.08×10^3

Chapter V. Apparent and Partial Molar Heat Capacities and Volumes of Aqueous L-Tartaric Acid and Its Sodium Salts at Elevated Temperature and Pressure

V.1 Introduction

The properties of aqueous electrolytes and non-electrolytes at elevated temperatures and pressures have long been the object of many studies, both because of their great importance in modelling geological fluids and many industrial processes, and because an understanding of the effects of widely varying water properties yields fundamental insights into hydration phenomena. The increasingly negative values of the standard partial molar volumes and heat capacities of simple electrolytes at elevated temperatures are now understood to arise from the high degree of long range solvent polarization when the critical point of water is approached. The behaviour of aqueous non-electrolytes is less well understood. Recently, Wood and coworkers (Criss and Wood, 1996; Inglese *et al.*, 1996; Inglese and Wood, 1996) reported a series of studies on the apparent molar heat capacities and volumes of non-polar gases and organic compounds in aqueous solutions at high temperatures and pressures. In contrast to electrolytes, the standard partial molar heat capacities and volumes of these non-electrolyte solutions become more and more positive as the temperatures were increased. The resulting values of C_p^o and V^o at temperatures from 373 to 523 K were successfully decomposed into functional group contributions, and were used to predict the properties of solutes composed of these functional groups in this temperature range. Even so,

compared with the studies on electrolytes, the work on the properties of non-electrolytes at high temperatures and pressures is far from complete.

Recently our laboratory has undertaken a series of calorimetric and volumetric studies on chelating agents and hydrogen bonding solutes (Hovey and Tremaine, 1985; Xie and Tremaine, 1998). L-Tartaric acid (HOOC-CH(OH)-CH(OH)-COOH) is of interest in this context, first because it is a small molecule with extreme hydrogen-bonding, due to its two -OH groups and two -COOH groups on a chain of only two alkyl carbons. Second, in comparison with the "big three", EDTA, DTPA and NTA, it is a different kind of chelating agent that acts as a bidentate ligand, with many applications in industry. Many potentiometric and spectroscopic studies have been done on tartaric acid at ambient temperatures (Blomqvist and Still, 1984; Kaneko *et al.*, 1983; Bhattacharjee *et al.*, 1989). Low temperature data for the apparent molar volumes and heat capacities of tartaric acid and its salts have been determined at 298.15 K by Apelblat and Manzurola (1985, 1990), Sijpkes *et al.* (1989) and authors (1998), and from 298.15 to 308.15 K by Høiland and Vikingstad (1975). No studies above 323.15 K on its partial molar properties have been reported in the literature.

In this chapter we report the apparent molar volumes of L-tartaric acid and sodium tartrate at temperatures up to 530 K, as a means of examining the effect of ionization and hydrogen-bonding functional groups on partial molar volumes at elevated temperatures. Apparent molar heat capacities of L-tartaric acid and its sodium salts at temperatures from 283.15 to 328.15 K are also reported.

V.2 Experimental

L-Tartaric acid (Aldrich reagent grade) was used as received. Sodium hydroxide solution was prepared from 50 percent carbonate-free solutions (Fisher) by dilution and titrated against a standard solution of potassium hydrogen phthalate. A titration of triplicate ~ 2 g samples of the tartaric acid with 0.1 molar standard NaOH solution agreed with the calculated values to within 0.1 %. Buffer solutions were prepared by mass by mixing the appropriate amount of the solid L-tartaric acid with standard solutions of sodium hydroxide to give the desired molar ratios. The molar ratios between sodium ion and the acid were 0.4999, and 1.5001 for the buffer solutions. The accuracy in the molar ratios was 0.2 percent or better.

L-Tartaric acid, disodium salt dihydrate (Aldrich, 99+ percent) was recrystallized from water-ethanol mixtures and dried at 393 K for several days. Weight loss after dehydration at T = 393 K confirmed the hydration number to be 2.00 H_2O. Stock solutions were prepared by mass. Nanopure water (resistivity > 8 MΩ·cm) was used to prepare all solutions. Standard solutions of NaCl were prepared by mass after drying the salt at 393 K for 24 hours.

Low temperature heat capacity and density measurements were performed with a Sodev CP-C flow microcalorimeter (Picker *et al.*, 1971) and a Sodev 03D vibrating flow densitometer (Picker *et al.*, 1974) equipped with platinum cells. The densitometer was calibrated daily with pure water and standard 1 mol·kg^{-1} NaCl (aq). The experimental values of $\{c_p \cdot \rho / (c^*_{p,1} \cdot \rho^*_1) - 1\}$ for the standard solution of NaCl (aq) were compared with

literature values compiled by Archer and Wang (1990) to correct for a small heat-leak effect, according to the method of Desnoyers *et al.* (1976). The heat loss factor f = 1.008 ± 0.002 was obtained daily. Here, $c_p \cdot \rho$ and $c^*_{p,1} \cdot \rho^*_1$ are the products of massic heat capacity and density of the solution and H_2O (l), respectively.

High temperature volumetric measurements were made in a vibrating-tube densitometer, constructed according to the design of Albert and Wood (1984), as modified by Corti *et al.* (1990). A detailed description of the densitometer and the experimental procedures have been given by Xiao *et al.* (1997) with some modifications due to Clarke and Tremaine (1999). The densitometer was also calibrated daily with pure water and standard solution of 3.2351 mol kg^{-1} NaCl (aq), using the reference values compiled by Hill (1990) and Archer (1990), respectively. The combined uncertainty in the measured relative densities, ($\rho - \rho^*_1$), due to the sensitivity limits of the instrument itself and the accuracy of the reference data is estimated to be ± 0.0002 g cm^{-3}. The precision is ± 0.00002 g cm^{-3}.

At high temperatures, it was expected that aqueous solutions of L-tartaric acid and sodium tartrate may decompose. Two 5 ml samples which had passed through the densitometer at T = 529.15 K were removed from the sample loop in the exit stream and analysed for decomposition products. ^{13}C NMR indicated no decomposition products. A potentio-metric titration with standard NaOH (aq) solution of a sample that included a small amount of water from the sampling lines, agreed with the calculated value to within ± 4 percent. We estimate the degree of decomposition to be less than 1 %.

V.3 Results

The density of solutions in the vibrating-tube densitometer was determined from the expression:

$$\rho = \rho_1^* + K(\tau^2 - \tau_o^2) \qquad (V.1)$$

where ρ and ρ_1^* are the densities of the solution and the water, respectively; τ and τ_o are the resonance periods of the solution and water, respectively; and K is a characteristic constant determined by calibration with the solvent water and the standard NaCl solution.

The apparent molar properties were calculated through the expression:

$$Y_\phi = \{ Y(sln) - n_1 Y_1^* \}/n_2 \qquad (V.2)$$

where Y(sln) is the heat capacity or volume of solution; Y_1^* is the molar heat capacity or volume of pure $H_2O(l)$, and n_1, and n_2 are the number of moles of water and salt. The equations that relate the apparent molar volumes V_ϕ and apparent molar heat capacities $C_{p,\phi}$ to the densities, specific heat capacities and total molality are:

$$V_\phi = 1000(\rho_1^* - \rho)/(m\rho\rho_1^*) + M/\rho \qquad (V.3)$$

$$C_{p,\phi} = 1000(c_p - c_{p,1}^*)/m + Mc_p \qquad (V.4)$$

where $c^*_{p,l}$, ρ^*_l, c_p and ρ are the specific heat capacities and densities of pure water and solution, respectively. M is the molar mass of solute, for the buffer solutions, the mean molar mass M^* is defined by:

$$M^* = FM(Na^-) + (2-F)M(H^-) + M(A^{2-}) \qquad (V.5)$$

where M(X) is the molar mass of species X. The errors associated with the density measurements in a vibrating-tube densimeter have been discussed by Majer *et al.* (1991) and Oakes *et al.* (1995). A detailed calculation of statistical uncertainties for densities and the resulting statistical errors for apparent molar volumes is described by Xiao (1997). Estimated uncertainties in V_ϕ were within $\pm 10^{-2} \cdot V_\phi$ or less at the temperatures below 529 K, where the uncertainty in molality is the main contributor. The experimentally determined relative densities (ρ - ρ^*_l) and apparent molar volumes are listed in Table A.V.1 for aqueous L-tartaric acid; two buffer solutions of $H_2Tar(aq)/NaHTar(aq)$ and $NaHTar(aq)/Na_2Tar(aq)$; and disodium tartrate, $Na_2Tar(aq)$. The experimental values of $\{c_p \cdot \rho / (c^*_{p,l} \cdot \rho^*_l) - 1\}$ and apparent molar heat capacities of the above systems are also listed in Table A.V.1. The experimental values of densities (ρ - ρ^*_l) and apparent molar volumes for $H_2Tar(aq)$ and NaTar(aq) at T > 373 K are listed in Table A.V.2.

It is known that the neutral species and sodium salts of L-tartaric acid undergo hydrolysis or dissociation in aqueous solution to some degree, and the dissociation products therefore may contribute to the apparent molar properties. Another contribution

to the experimental values for the apparent molar heat capacity comes from the so-called " chemical relaxation" effect, which should also be taken into consideration. It was found that the two buffer solutions and sodium tartrate, $Na_2Tar(aq)$, undergo less than 0.5 percent hydrolysis and the chemical relaxation contributions to the heat capacities are negligible. The corrections to the heat capacities and volumes of aqueous L-tartaric acid because of hydrolysis involved a rather complex set of calculations, and the details are given in Appendix B.

The ionic strength dependence of the apparent molar volumes $V_{\phi,2}$ and heat capacities $C_{p,\phi,2}$ are well represented by the extended Debye-Hückel equation (Hovey and Tremaine, 1986):

$$V_{\phi,2} = V_2^{\circ} + 1.5\omega A_V[I - 2I^{1/2} + 2\ln(1 + I^{1/2})]/I + B_V I \qquad (V.6)$$

$$C_{p,\phi,2} = C_{p,2}^{\circ} + 1.5\omega A_C[I - 2I^{1/2} + 2\ln(1 + I^{1/2})]/I + B_C I \qquad (V.7)$$

where $I = \omega m = \frac{1}{2}\sum m_i z_i^2$, m_i is the molality of a particular solute species, and m is the total molality. A_V in equation (V.6), and A_C in equation (V.7) are the Debye-Hückel limiting slopes for the volume and heat capacity, respectively, whose values were taken from the compilation by Archer and Wang (1990). By definition, V_2° and $C_{p,2}^{\circ}$ are the standard partial molar volume and heat capacity, respectively.

Equations (V.6) and (V.7) were fitted to the apparent molar volumes and heat

capacities of the buffer solutions of $H_2Tar(aq)/NaHTar(aq)$ and $NaHTar(aq)/Na_2Tar(aq)$, and the solution of sodium tartrate, $Na_2Tar(aq)$ at each temperature by the method of least-squares. The resulting values of V_2^o, B_V, $C_{p,2}^o$, and B_C for the buffer solutions are presented in Table V.1 and those of the sodium tartrate solution are listed in Table V.2. The calculated values for $V_{\phi,2}$ and $C_{p,\phi,2}$ after subtracting the Debye-Hückel limiting law (DHLL) term are shown in Figures V.1, V.2 and V.3.

For the neutral species L-tartaric acid, the following equations were fitted to the experimental results to obtain values of the partial molar volumes and heat capacities at infinite dilution:

$$V_{\phi,2} = V_2^o + B_V\, m \tag{V.8}$$

$$C_{p,\phi,2} = C_{p,2}^o + B_C\, m \tag{V.9}$$

The resulting values of V_2^o, B_V, $C_{p,2}^o$ and B_C are listed in Table V.2, and illustrated in Figure V.4.

Tanger and Helgeson (1992) pointed out that for many electrolytes, the steep increase in V_2^o as the temperature increases from 273 to 373 K can be described by a function of the form $\{v_1 + v_2/(T - 228)\}$ with two adjustable parameters v_1 and v_2. It has been demonstrated by Anderson *et al.* (1991), Simonson *et al.* (1994) and Tremaine *et al.* (1997) that the compressibility coefficient of the solvent water $\beta_1^* = -(1/V)(\partial V/\partial p)_T$ is a

good independent variable to formulate simple empirical equations to represent the behaviour of V_2^o at elevated temperatures. At temperatures between 283 and 373 K, a linear relationship was found between the values for V_2^o (Na_2Tar, aq), which was obtained by fitting equation (V.3.6), and that of 1/(T-228), which clearly indicated that a two parameter term of the form $\{v_1 + v_2/(T - 228)\}$ could represent the behaviour of V_2^o well within the experimental uncertainty. At temperatures above 373 K, a linear relationship was also found between V_2^o and $T\beta_1^*$. As a result, the following equation was used to represent the temperature and pressure dependent of V_2^o using values of β_1^* calculated from the equation of state of Hill (1990):

$$V_2^o = v_1 + v_2 /(T - 228) + v_3T + v_4R\beta_1^* - v_5R\beta_1^* T \qquad (V.10)$$

It can be seen from equation (V.10) that the solvent density terms dominate at elevated temperatures.

As no apparent molar heat capacities were measured at temperatures higher than 328.15 K, the temperature dependence of $C_{p,2}^o$ was modelled by a simple equation (Tremaine *et al.*, 1997):

$$C_{p,2}^o = c_1 + c_2 /(T - 228)^2 + c_3 / T^3 \qquad (V.11)$$

where c_1, c_2 and c_3 are the adjustable parameters. It was found that the temperature

dependence of the B_V and B_C parameters could be described adequately by the following equation:

$$B_Y = b_1 + b_2T + b_3T^2 \qquad (V.12)$$

where B_Y represents B_V or B_C, the b_i terms are the adjustable constants and T is the temperature in Kelvins.

The entire array of values for the apparent molar heat capacities $C_{p,\phi,2}$ of $H_2Tar(aq)/NaHTar(aq)$, $NaHTar(aq)/Na_2Tar(aq)$, $Na_2Tar(aq)$ and $H_2Tar(aq)$ at all temperatures and all molalities were used to optimize the parameters in equations (V.7), (V.9), (V.11) and (V.12) in order to obtain a global fit to the data. The fitted parameters are listed in Table V.3. Plots of the fitted results for ($C_{p,\phi,2}$ - DHLL) against molality are compared with the experimental data in Figures V.1, V.2 and V.3. The entire array of values of apparent molar volumes V_ϕ of $H_2Tar(aq)/NaHTar(aq)$, $NaHTar(aq)/Na_2Tar(aq)$ and $Na_2Tar(aq)$ at all temperatures and molalities were used to fit equations (V.6), (V.10) and (V.12), and the results are listed in Table V.4. The molality dependence of the apparent molar volumes was found to be well represented by the above treatment. Plots of the fitted results for ($V_{\phi,2}$ - DHLL) against molality are compared with the experimental data in Figure V.1, V.2 and V.3. The deviations between the calculated and the observed values of $V_{\phi,2}$ for $Na_2Tar(aq)$ are shown in Figure V.5.

Table V.1. Values of Parameters from the Extended Debye-Hückel Equation for the Aqueous $H_2Tar(aq)/NaHTar(aq)$ and $NaHTar(aq)/Na_2Tar(aq)$ Systems at Temperatures from 283.15 to 328.15 K and Pressure 0.1 MPa.

T	C_p^o	B_C	V^o	B_V
K	$J \cdot K^{-1} \cdot mol^{-1}$	$J \cdot kg \cdot K^{-1} \cdot mol^{-2}$	$cm^3 \cdot mol^{-1}$	$cm^3 \cdot kg \cdot mol^{-2}$
		$H_2Tar(aq)/NaHTar(aq)$, F = 0.500		
283.15	142.62(1.87)	161.36(13.06)	74.24(0.08)	7.86(0.59)
298.15	196.01(1.96)	121.53(13.72)	78.24(0.15)	6.11(1.06)
313.15	234.58(1.81)	65.32(12.65)	81.18(0.22)	4.37(1.55)
328.15	257.53(1.04)	33.19(7.59)	83.70(0.07)	3.61(0.51)
		$NaHTar(aq)/Na_2Tar(aq)$, F = 1.500		
283.15	-43.25(5.17)	145.57(10.85)	59.10(0.10)	4.20(0.21)
298.15	61.70(0.90)	75.68(1.92)	64.58(0.07)	3.09(0.15)
313.15	114.33(0.61)	44.41(1.30)	68.07(0.06)	2.06(0.12)
328.15	140.77(1.93)	26.72(4.27)	70.90(0.10)	1.51(0.22)

Table V.2. Values of Parameters from Equations (V.6 - V.9) for the Aqueous $H_2Tar(aq)$ and $Na_2Tar(aq)$ Systems at Temperatures from 283.15 to 529.15 K and Pressures from 0.1 to10 MPa.

T	p	C_p^o	B_C	V^o	B_V
K	MPa	$J \cdot K^{-1} \cdot mol^{-1}$	$J \cdot kg \cdot K^{-1} \cdot mol^{-2}$	$cm^3 \cdot mol^{-1}$	$cm^3 \cdot kg \cdot mol^{-2}$
			$H_2Tar(aq)$		
298.15	0.1	249.63(0.46)	15.95(1.19)	84.32(0.05)	0.77(0.12)
313.15	0.1	270.74(1.24)	14.93(3.20)	86.95(0.17)	0.44(0.45)
328.15	0.1	278.25(0.56)	21.46(1.32)	88.68(0.19)	1.24(0.45)
377.11	10.4			91.94(0.12)	0.87(0.34)
426.37	10.4			94.96(0.19)	-0.17(0.47)
475.83	10.5			96.94(0.14)	0.11(0.37)
529.09	10.4			96.57(0.15)	1.22(0.39)
			$Na_2T(aq)$		
283.15	0.1	-153.33(1.28)	165.27(4.31)	50.43(0.08)	5.24(0.27)
298.15	0.1	-27.79(0.99)	91.22(3.16)	56.99(0.09)	3.78(0.27)
313.15	0.1	23.96(1.02)	61.79(3.26)	60.53(0.19)	2.91(0.61)
328.15	0.1	34.55(5.46)	47.04(16.18)	62.51(0.33)	2.55(0.98)
377.06	10.5			59.74(0.31)	1.75(0.31)
426.38	10.5			50.52(0.40)	-0.62(0.39)
477.73	10.5			24.84(0.91)	-2.41(0.84)
529.02	10.4			-36.72(1.70)	-5.41(1.55)

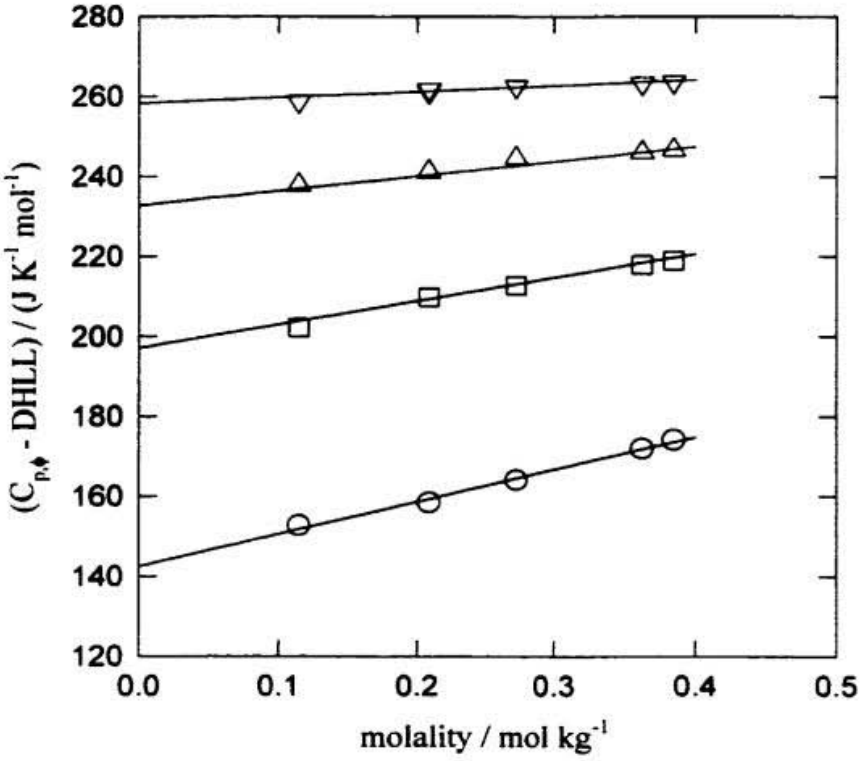

Figure V.1a. Apparent molar heat capacities of $H_2Tar(aq)/NaHTar(aq)$ plotted against molality after subtracting the Debye-Hückel limiting law (DHLL) term according to equation (V.7): ○, T = 283 K □, T = 298 K; △, T = 313 K; ▽, T = 328 K. Symbols are experimental results and lines represent the global least-squares fits to equations (V.7), (V.11) and (V.12).

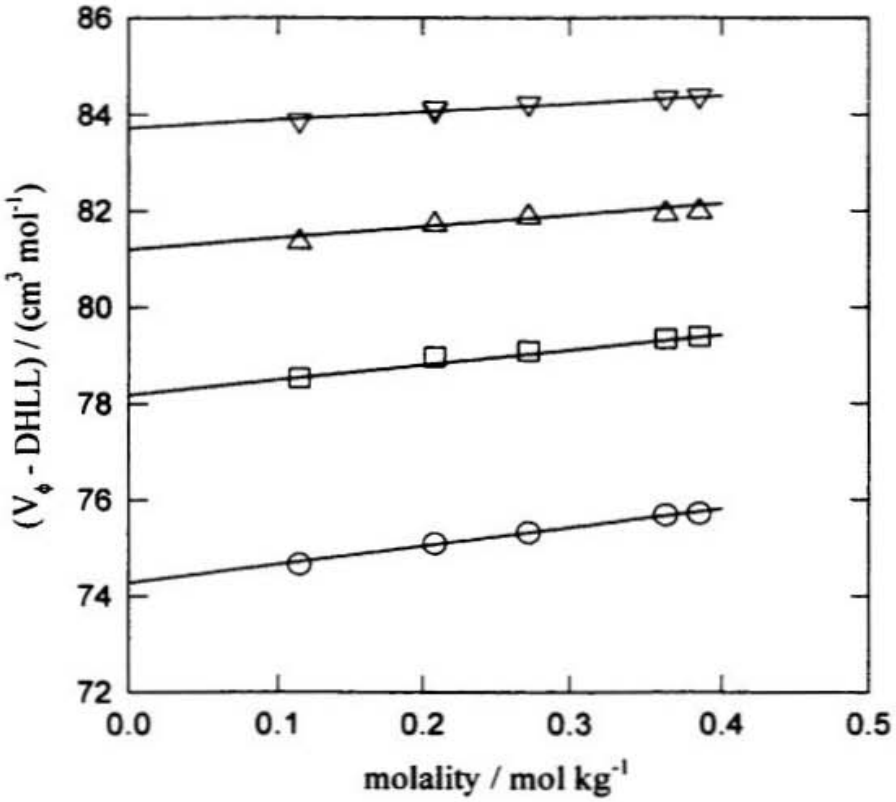

Figure V.1b. Apparent molar volumes of $H_2Tar(aq)/NaHTar(aq)$ plotted against molality after subtracting the Debye-Hückel limiting law (DHLL) term according to equation (V.6): ○, T = 283 K □, T = 298 K; △, T = 313 K; ▽, T = 328 K. Symbols are experimental results and lines represent the global least-squares fits to equations (V.6), (V.10) and (V.12).

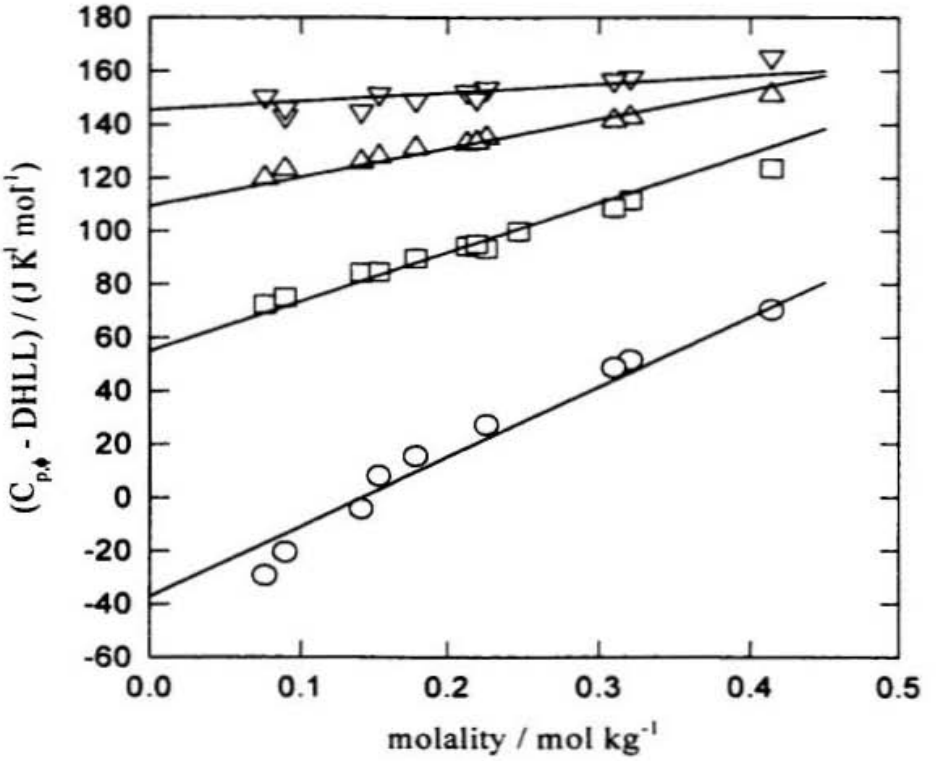

Figure V.2a. Apparent molar heat capacities of NaHTar(aq)/Na_2Tar(aq) plotted against molality after subtracting the Debye-Hückel limiting law (DHLL) term according to equation (V.7): ○, T = 283 K □, T = 298 K; △, T = 313 K; ▽, T = 328 K. Symbols are experimental results and lines represent the global least-squares fits to equations (V.7), (V.11) and (V.12).

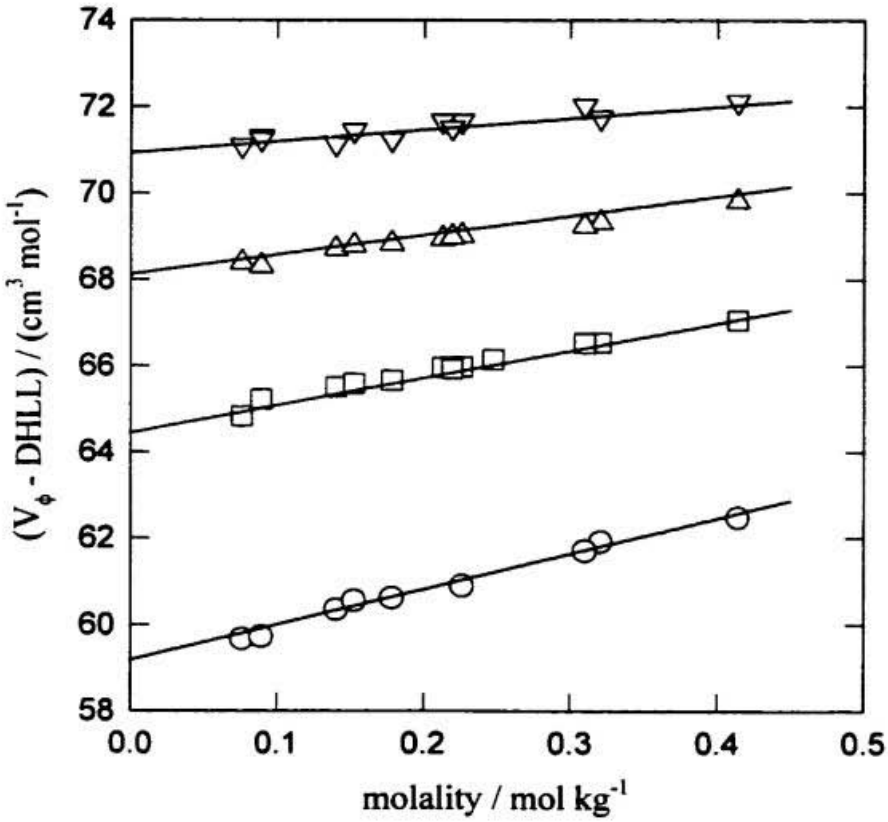

Figure V.2b. Apparent molar volumes of NaHTar(aq)/Na_2Tar(aq) plotted against molality after subtracting the Debye-Hückel limiting law (DHLL) term according to equation (V.6): ○, T = 283 K □, T = 298 K; △, T = 313 K; ▽, T = 328 K. Symbols are experimental results and lines represent the global least-squares fits to equations (V.6), (V.10) and (V.12).

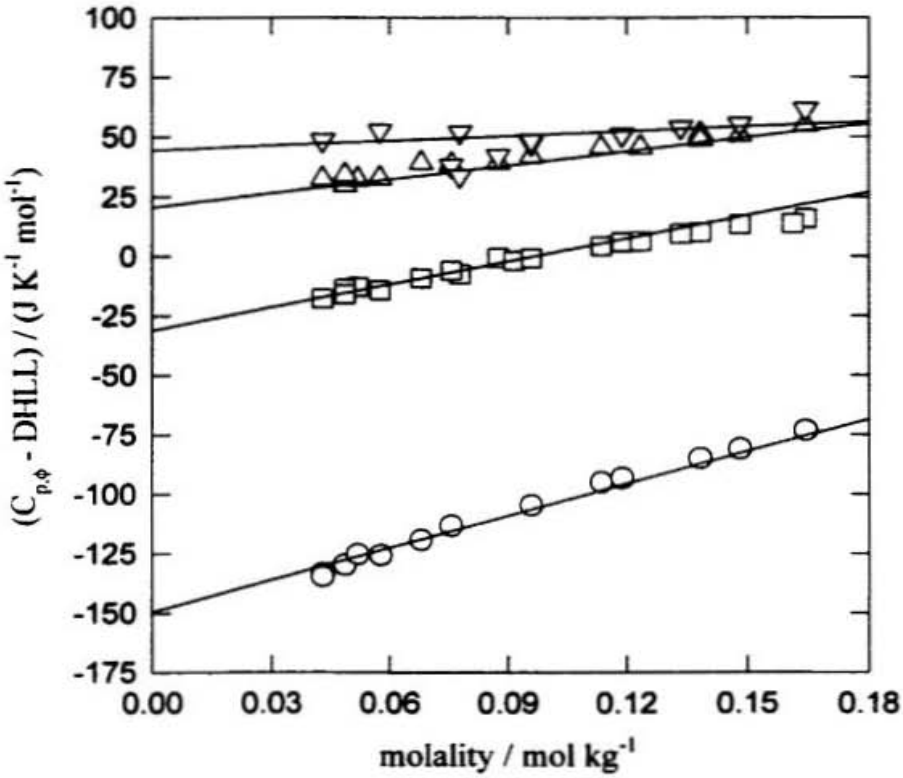

Figure V.3a. Apparent molar heat capacities of $Na_2Tar(aq)$ plotted against molality after subtracting the Debye-Hückel limiting law (DHLL) term according to equation (V.7): ○, T = 283 K □, T = 298 K; △, T = 313 K; ▽, T = 328 K. Symbols are experimental results and lines represent the global least-squares fits to equations (V.7), (V.11) and (V.12).

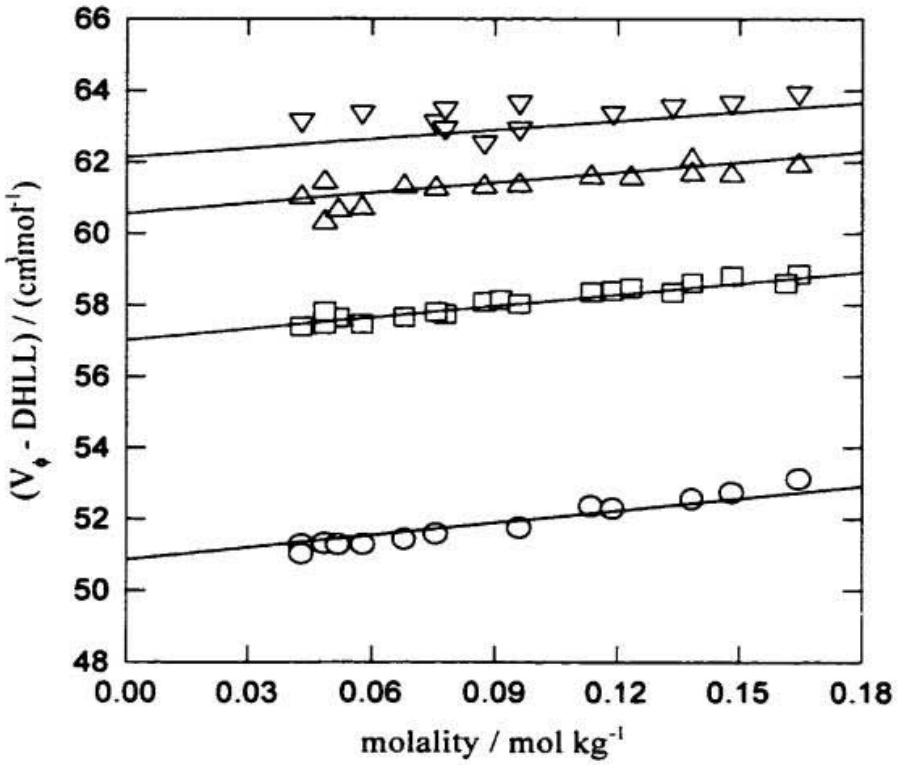

Figure V.3b. Apparent molar volumes of $Na_2Tar(aq)$ plotted against molality after subtracting the Debye-Hückel limiting law (DHLL) term according to equation (V.6): ○, T = 283 K □, T = 298 K; △, T = 313 K; ▽, T = 328 K. Symbols are experimental results and lines represent the global least-squares fits to equations (V.6), (V.10) and (V.12).

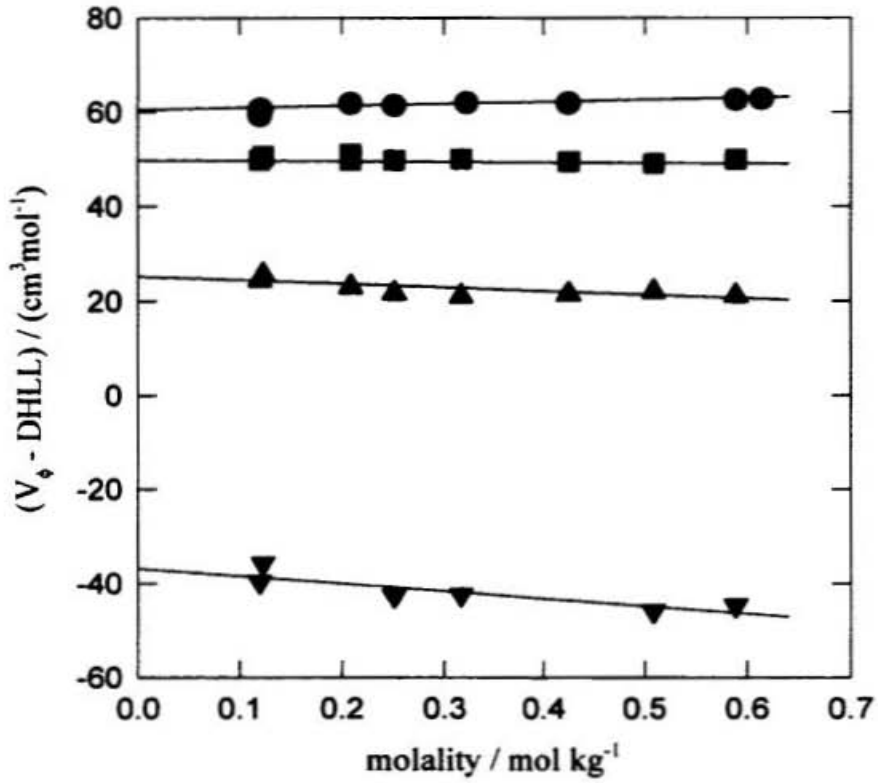

Figure V.3c. Apparent molar volumes of $Na_2Tar(aq)$ plotted against molality after subtracting the Debye-Hückel limiting law (DHLL) term according to equation (V.6): ●, T = 377 K ■, T = 426 K; ▲, T = 477 K; ▼, T = 529 K. Symbols are experimental results and lines represent the global least-squares fits to equations (V.6), (V.10) and (V.12).

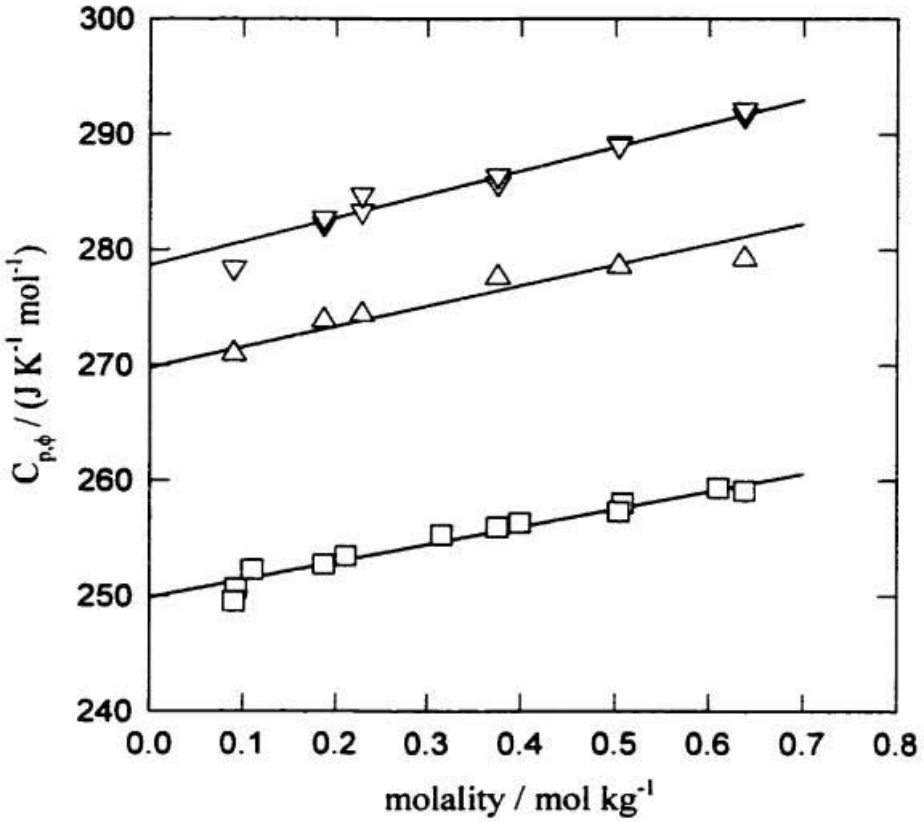

Figure V.4a. Apparent molar heat capacities of $H_2Tar(aq)$ plotted against molality: □, T = 298 K; △, T = 313 K; ▽, T = 328 K. Symbols are experimental results and lines represent the global least-squares fits to equations (V.9), (V.11) and (V.12).

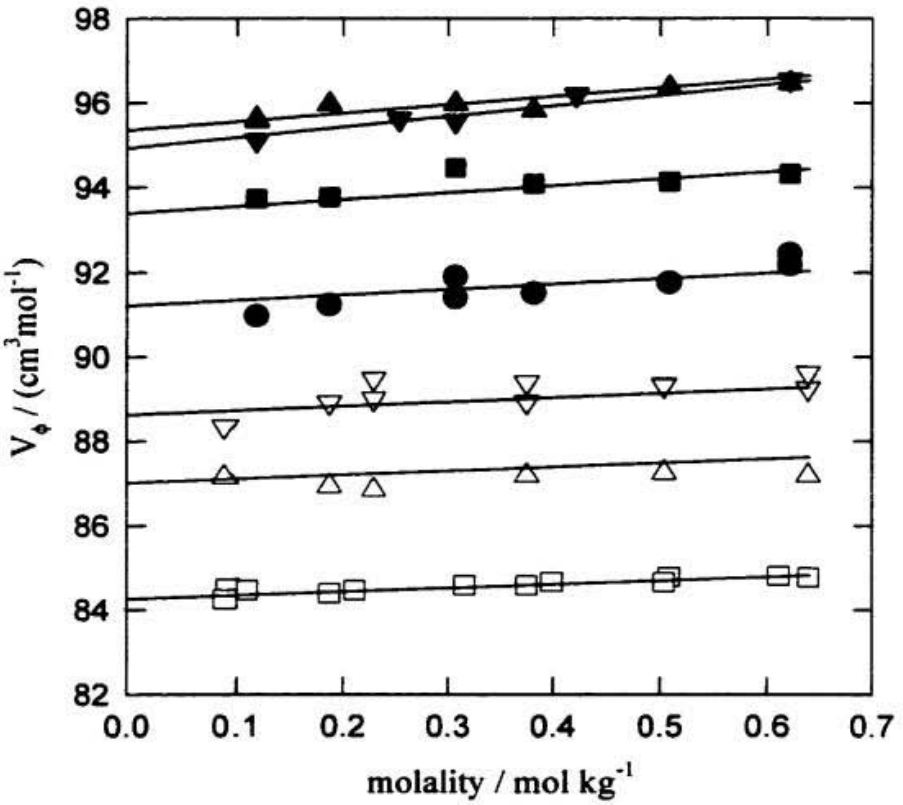

Figure V. 4b. Apparent molar volumes of $H_2Tar(aq)$ plotted against molality: □, T = 298 K; △, T = 313 K; ▽, T = 328 K; ●, T = 377 K ■, T = 426 K; ▲, T = 475 K; ▼, T = 529 K. Symbols are experimental results and lines represent the global least-squares fits to equations (V.8), (V.12) and (V.13).

An empirical equation was successfully used to describe the temperature dependence of V_2^o for aqueous morpholine over a wide temperature range by Tremaine *et al.*, (1997). A similar equation was used here to represent the behaviour of V_2^o (H_2Tar, aq) over the experimental temperature range:

$$V_2^o = v_1 + v_2/T^{1/2} + v_3/(T\text{-}228) + v_4/T^{3/2} - v_5 R\beta_1^* \qquad (V.13)$$

where the v_i terms are adjustable parameters, β_1^* is the compressibility coefficient of the solvent water, and R is the gas constant. Equations (V.8), (V.12) and (V.13) were fitted to the experimental values of $V_{\phi,2}$ (H_2Tar, aq) at all temperatures and molalities, and the resulting parameters are listed in Table V.4. The overall standard deviation of $V_{\phi,2}$ for L-tartaric acid is about 0.22 $cm^3\ mol^{-1}$. The calculated values of $V_{\phi,2}$ (H_2Tar, aq) are compared with the experimental data in Figure V.4, and the deviations between calculated and experimental values of $V_{\phi,2}$ are shown in Figure V.6.

Very recently, empirical equations based on the density model of Mesmer *et al.* (1991) were introduced by Clarke and Tremaine (1998) to express the standard partial molar volumes V_2^o of amino acids, such as glycine, α-alanine and proline, at elevated temperatures and pressures:

$$V_2^o = v_1 + (v_2/T + v_3 + v_4 T)R\beta_1^* \qquad (V.14)$$

$$B_V = b_1 + b_2 RT\beta_1^* \qquad (V.15)$$

where v_i and B_i terms are adjustable parameters, and β_1^* and R have the same definitions as in equation (V.13). The experimental results of $V_{\phi,2}$ (H_2Tar, aq) and $V_{\phi,2}$ (Na_2Tar, aq) were also examined with equations (V.14) and (V.15). The parameters and standard deviations are listed in Table V.4.

Equation (V.14) yielded an overall standard deviation for Na_2Tar(aq) and H_2Tar(aq) of 1.42 $cm^3 \cdot mol^{-1}$ and 0.44 $cm^3 \cdot mol^{-1}$, respectively, which is twice as large as that obtained by fitting equation (V.10) and equation (V.13), respectively. However, equation (V.14) has the advantages of fewer parameters and a universal approach to both aqueous electrolytes and non-electrolytes. In the case of V_2^o (H_2Tar, aq), it seems that the extra parameters in equation (V.13) describes the low temperature behavior better than that of equation (V.14).

Table V.3. The Global-Fitting Parameters from Equations (V.11) and (V.12) for the Apparent Molar Heat Capacities of Aqueous Tartrate Systems.

parameter	$H_2Tar(aq)$	$H_2Tar(aq)$/ NaHTar(aq)	NaHTar(aq)/ $Na_2Tar(aq)$	$Na_2Tar(aq)$
$c_1/(J\ K^{-1}mol^{-1})$	2.638×10^{2}	3.910×10^{2}	2.992×10^{2}	1.642×10^{2}
$c_2/(J\ K\ mol^{-1})$	-4.800×10^{5}	-2.423×10^{5}	-5.593×10^{5}	-1.207×10^{6}
$c_3/(J\ K^{-2}mol^{-1})$	2.216×10^{9}	-3.833×10^{9}	-3.462×10^{9}	5.240×10^{9}
$b_1/(J\ kg\ K^{-1}mol^{-2})$	-3.612×10^{1}	9.954×10^{2}	8.548×10^{2}	9.560×10^{2}
$b_2/(J\ kg\ K^{-2}mol^{-2})$	1.723×10^{-1}	-2.944×10^{0}	-2.556×10^{1}	-2.846×10^{1}
$\sigma/(cm^3\ mol^{-1})$	0.79	0.95	4.11	3.47

Table V.4. The Global-Fitting Parameters for the Apparent Molar Volumes of Aqueous Tartrate Systems.

	$H_2Tar(aq)$		$Na_2Tar(aq)$		Buffer 1[a]	Buffer 2[b]
parameter	Eq (V.13)	Eq (V.14)	Eq (V.10)	Eq (V.14)	Eq (V.10)	Eq (V.10)
v_1	4.318×10^{2}	7.855×10^{1}	9.256×10^{1}	9.740×10^{1}	5.977×10^{1}	6.573×10^{1}
v_2	-9.791×10^{3}	-7.750×10^{6}	-2.446×10^{3}	-9.274×10^{6}	-6.474×10^{2}	-1.159×10^{3}
v_3	-3.403×10^{3}	4.283×10^{4}	-1.280×10^{-2}	3.876×10^{4}	9.270×10^{-2}	5.110×10^{-2}
v_4	1.403×10^{6}	-5.069×10^{1}	1.215×10^{5}	-6.178×10^{1}	-	-
v_5	1.305×10^{3}		4.600×10^{1}		-	-
b_1	6.662×10^{-1}	6.928×10^{-1}	2.843×10^{0}	2.101×10^{0}	3.518×10^{1}	2.138×10^{1}
b_2	-2.900×10^{-3}	3.542×10^{-1}	2.490×10^{-2}	-1.250×10^{0}	-9.720×10^{-2}	-6.110×10^{-2}
b_3	1.175×10^{-5}		-7.629×10^{-5}		-	-
σ	0.22	0.44	0.69	1.42	0.08	0.14

[a] Buffer 1, $H_2Tar(aq)/NaHTar(aq)$; [b] buffer 2, $NaHTar(aq)/Na_2Tar(aq)$.

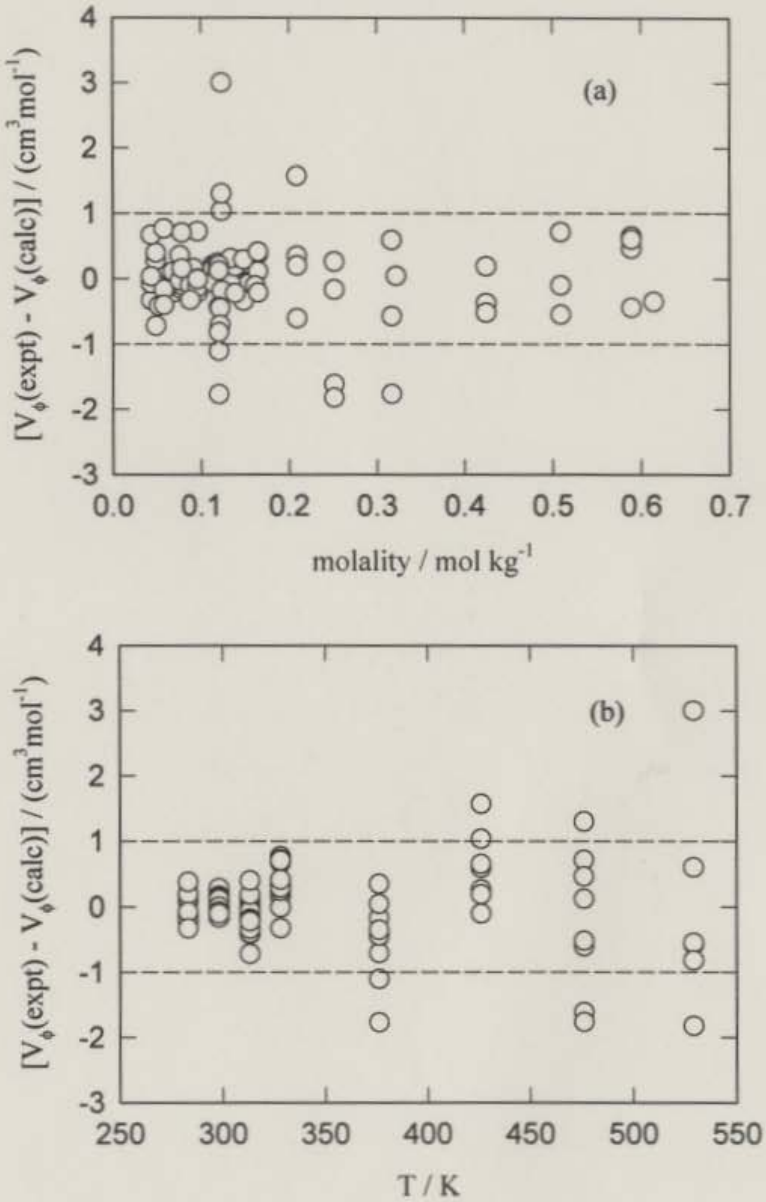

Figure V.5. $V_{\phi,2}$ (observed) minus $V_{\phi,2}$ (calculated) from equations (V.6), (V.10) and (V.12) plotted against molality and temperature: a, molality; b, temperature.

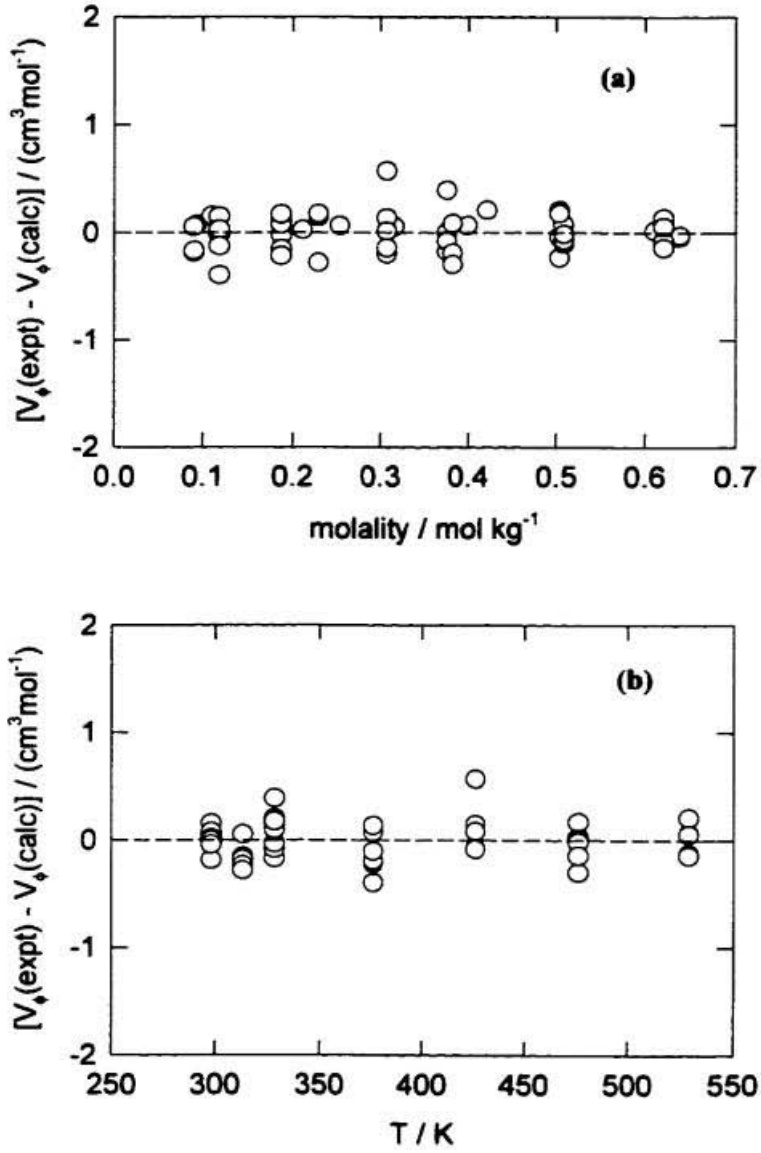

Figure V.6. $V_{\phi,2}$ (observed) minus $V_{\phi,2}$ (calculated) from equations (V.8), (V.12) and (V.13) plotted against molality and temperature: a, molality; b, temperature.

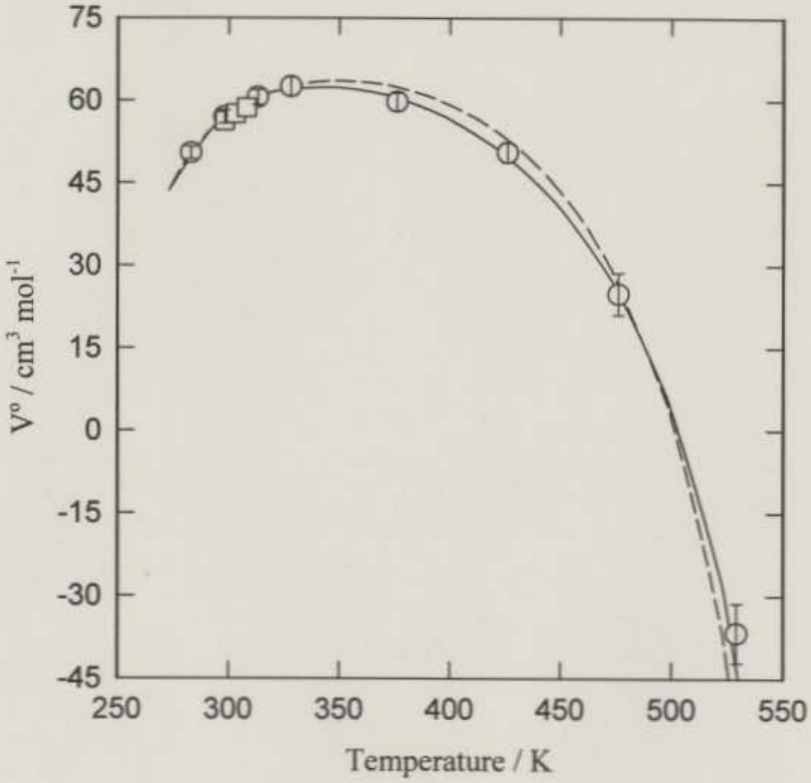

Figure V.7. Plots of V° against temperature for $Na_2Tar(aq)$: ○, this work; □, Høiland's result; —, equation (V.10); ---, HKF extrapolation

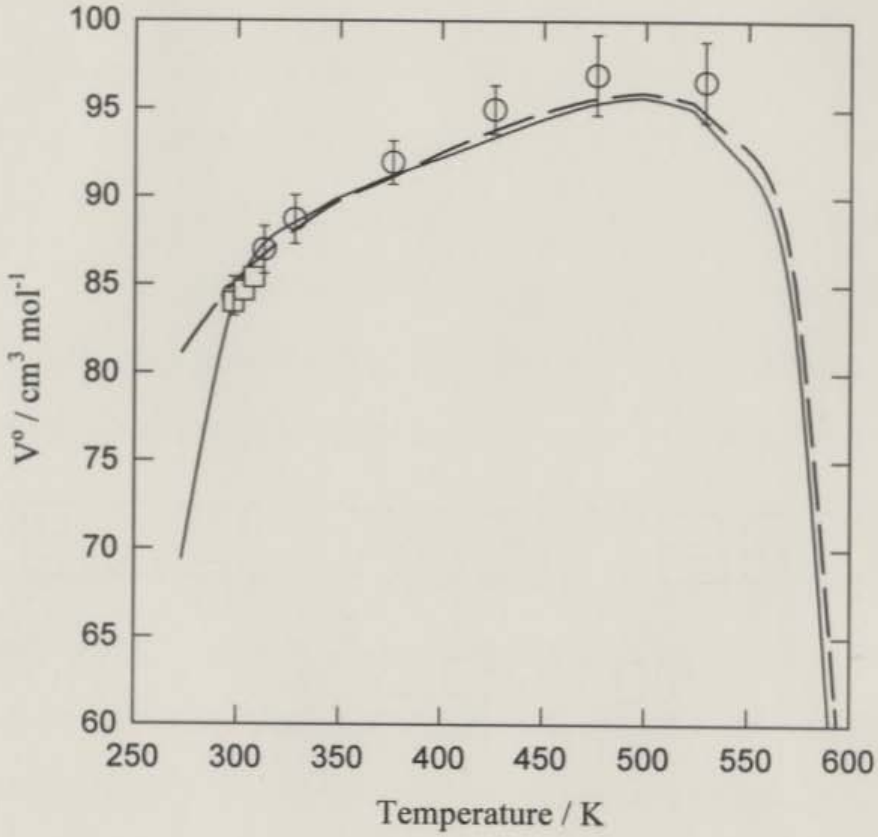

Figure V.8. Plots of V° against temperature for $H_2Tar(aq)$: ○, this work; □, Høiland's result; —, equation (V.13); ---, equation (V.14).

V.4 Discussion

V.4.1 Comparison with Literature Data

The apparent molar volumes of aqueous $H_2Tar(aq)$ and $Na_2Tar(aq)$ at T = 298.15 K from Apelblat and Manzurola (1990) can be compared with our results. The experimental values of $V_{\phi,2}$ (H_2Tar, aq) in our work are systematically higher than Apelblat and Manzurola's (1990) results by 0.5 $cm^3 \cdot mol^{-1}$ over the molality range of our experiments, and the extrapolated value based on equation (V.3.6) V_2^o (H_2Tar, aq) = 84.32 $cm^3 \cdot mol^{-1}$ differs from their value of 82.23 $cm^3 \cdot mol^{-1}$ by 2.09 $cm^3 \cdot mol^{-1}$. Our value of V_2^o (H_2Tar, aq) agrees well with the values reported by Høiland and Vikingstad (1975), V_2^o (H_2Tar, aq) = 83.99 $cm^3 \cdot mol^{-1}$; and Sijpkes *et al.* (1989), V_2^o (H_2Tar, aq) = 83.4 $cm^3 \cdot mol^{-1}$. The discrepancies are apparently not coming from the accuracy of the measurements, but because of differences in the data treatment. Our values for $V_{\phi,2}$ (Na_2Tar, aq) agree well with Apelblat and Manzurola's (1990) data at m > 0.1 $mol \cdot kg^{-1}$. The value V_2^o (Na_2Tar, aq) obtained by extrapolating our data to infinite dilution is 56.99 $cm^3 \cdot mol^{-1}$, compared with that of Apelblat and Manzurola (1990), V_2^o (Na_2Tar, aq) = 57.87 $cm^3 \cdot mol^{-1}$. The value of V_2^o (Na_2Tar, aq) reported by Høiland and Vikingstad (1975) at T = 298.15 K is 56.26 $cm^3 \cdot mol^{-1}$.

There are not many studies on the apparent molar heat capacities of tartaric acid and its salts at 298.15 K. The value of $C_{p,2}^o$ (H_2Tar, aq) = 251 $J \cdot K^{-1} \cdot mol^{-1}$ reported by Sijpkes *et al.* (1989) is in good agreement with our value of 249.6 $J \cdot K^{-1} \cdot mol^{-1}$. Bates and Canham (1951) studied the dissociation constants of tartaric acid from 273.15 to 323.15

K by an emf method, and derived the heat capacity change ΔC_p^o for the second dissociation step of tartaric acid averaged over the temperature range. Values of ΔV^o and ΔC_p^o can be calculated from our results using the values for V^o (Na^+, aq) and C_p^o (Na^+, aq) in Table III.5. Bates and Canham's value for the second stepwise dissociation reaction of H_2Tar (aq), $\Delta C_p^o = -220 \pm 10$ $J \cdot K^{-1} \cdot mol^{-1}$, is in excellent agreement with our experimental value, -216 ± 7 $J \cdot K^{-1} \cdot mol^{-1}$. For the ΔC_p^o of the first stepwise dissociation reaction, there is a large difference between the value from Bates and Canham, -170 ± 20 $J \cdot K^{-1} \cdot mol^{-1}$, and our experimental data, -146 ± 7 $J \cdot K^{-1} \cdot mol^{-1}$. The value of Bates and Canham may be of even lower accuracy than the authors estimate because it was obtained from the second temperature derivative of log K_1 instead of from direct experimental measurements. The comparison between the experimental results from the current study and those from the literature is shown in Table V.

V.4.2 Temperature Dependence of Partial Molar Volumes

The values of V_2^o (Na_2Tar, aq) obtained by fitting equations (V.6), (V.10) and (V.12) to the entire array of the experimental data are shown in Figure V.7, while values for V_2^o (H_2Tar, aq) obtained by fitting equations (V.8), (V.12) and (V.13) are shown in Figure V.8. The individual points are the values of V_2^o obtained by fitting equations (V.6) and (V.8), respectively, to the isobaric data at each temperature. As the pressure dependence of V_2^o is small and less than the uncertainty of the measurements, no corrections were made to convert the low temperature range data at p = 0.1 MPa to p =

10.4 MPa in the entire matrix of data curve fitting. The behavior of V_2^o (Na_2Tar, aq) over the whole temperature range is typical of all electrolytes. It has been shown in many studies that V_2^o of aqueous electrolytes first increases to a maximum, which is in the vicinity of T = 373 K or below, then decreases toward negative infinity as the temperature is raised toward the critical point of water. The reasons are well known (Wheeler, 1972; Sengers and Sengers, 1986; Debenedetti and Mohamed, 1989; Hnedkovsky *et al.*, 1995). It is interesting to note that V_2^o (H_2Tar, aq) increases with increasing temperature, as is often observed for the other aqueous non-electrolytes at elevated temperatures, but unlike most non-electrolytes, a maximum appears at about 480 K, after which V^o begins to decrease. This unusual behavior may reflect the attractive interactions between tartaric acid molecules and water because of the strong hydrogen-bonding. Similar behavior is observed in boric acid which forms strong hydrogen bonds with water and whose V^o diverges to negative infinity as the critical point is approached (Hnedkovsky *et al.*, 1995).

V.4.3 Extrapolation to Elevated Temperatures

The HKF equation of state (Helgeson *et al.*, 1981, 1988, 1992) has been used with some success to extrapolate the standard partial properties of aqueous electrolytes to temperatures as high as 573 K by Tremaine *et al.* (1986) and Conti *et al.* (1992). In the current work, the standard partial molar volumes V_2^o (Na_2Tar, aq) were extrapolated to high temperature by fitting the HKF equation to the values from the isothermal fit at T ≤ 328.15 K, the results were plotted in Figure V.7. The agreement between the HKF

extrapolation and the experimental results strongly supports the HKF approach to the aqueous electrolytes.

Table V.5. Standard Partial Molar Heat Capacities and Volumes of Aqueous Tartrate Species at 298.15 K.

Solute	C_p^o	Lit. values	V^o	Lit. values
	$J \cdot K^{-1} \cdot mol^{-1}$		$cm^3 \cdot mol^{-1}$	
H_2T (aq)	249.63(0.46)	251(2)[a]	84.32(0.05)	83.4(0.1)[a], 83.99,[b] 82.23[c]
NaHT (aq)*	145.57(2.12)		72.10(0.15)	70.83,[b] 71.01[d]
Na_2T (aq)	-27.79(0.99)		56.99(0.09)	56.26(0.1),[b] 57.87[d]

* Average values from two buffer solutions. [a] Sijpkes et al. (1989), [b] Høiland and Vikingstad (1975), [c] Manzurola and Apelblat (1985), [d] Apelblat and Manzurola (1990).

Bibliography and References

Abraham, M. H. and Marcus, Y. M. (1986), The Thermodynamics of Solvation of Ions Part I. The heat Capacity of Hydration at 298.15 K, *J. Chem. Soc. Faraday Trans. I.*, **82**, 3255-3274.

Albert, H. J. and Wood, R. H. (1984), High-Precision Flow Densimeter for Fluids at Temperatures to 700 K and Pressures to 40 MPa, *Rev. Sci. Instrum.*, **55**, 589-593.

Anderegg, G. and Malik, S. C. (1976), Komplexone XLVII. The Stability of Palladium (II) Complexes with Aminopolycarboxylate Anions, *Helv. Chim. Acta*, **59**, 1498-1511.

Anderson, G. M., Castet, S., Schott, J. and Mesmer, R. E. (1991), The Density Model for Estimation of Thermodynamic Parameters of Reactions at High Temperatures and Pressures, *Geochim. Cosmochim. Acta*, **55**, 1769-1779.

Angell, C. A. (1982), In *Water. A Comprehensive Treatise*: Vol. 7., F. Franks, ed., (Plenum Press, New York).

Apelblat, A. and Manzurola, E. (1990), Apparent Molar Volumes of Organic Acids and Salts in Water at 298.15 K, *Fluid Phase Equilibria*, **60**, 157-171.

Archer, D. G. (1992), Thermodynamic Properties of NaCl + H_2O System II. Thermodynamic Properties of NaCl(aq), NaCl-$2H_2O$(cr), and Phase Equilibria, *J. Phys. Chem. Ref. Data*, **21**, 793-821.

Archer, D. G. and Wang, P. (1990), The Dielectric Constant of Water and Debye-Hückel Limiting Law Slopes, *J. Phys. Chem. Ref. Data*, **19**, 371-411.

Barbero, J. A., Hepler, L. G., McCurdy, K. G. and Tremaine, P. R. (1983), Thermodynamics of Aqueous Carbon Dioxide and Sulfur Dioxide: Heat Capacities, Volumes and Temperature Dependence of Ionization, *Can. J. Chem.*, **61**, 2509-2519.

Barron, L. D., Gargaro, A. R., Hecht, L., Polavarapu, P. L. and Sugeta, H. (1992), Experimental and ab initio Theoretical Vibrational Raman Optical Activity of tartaric Acid, *Spectrochimica Acta*, 48A, **8**, 1051-1066.

Bates, R. G. and Canham, R. G. (1951), Resolution of the Dissociation Constants of d-Tartaric Acid from 0° to 50°C, *J. Res. Natl. Bur. Std.*, **47**, 343-348.

Bhattacharjee, R., Jain, Y. S. and Bist, H. D. (1989), Laser Raman and Infrared Spectra of Tartaric Acid Crystals, *Journal of Raman Spectroscopy*, **20**, 91-97.

Blomqvist, K. and Still, E. R. (1984), Solution Studies of Systems with Polynuclear Complex Formation. 5. Copper(II) and Cadmium(II) D-(+)-Tartrate System, *Inorg. Chem.*, **23**, 3730-3734.

Born, V. M. (1920), Volumen and Hydratationswärme der Ionen. *Z. Phys.*, **1**, 45-48.

Boscolo, P., Porcelli, G., Minini, E., and Finelli, V. N. (1983), EDTA Plus Zinc as Therapy of Lead Intoxication: Preliminary Results, *Med. Lav.*, **74**, 370-375.

Chaberek, S., Frost, A. E., Doran, M. A. and Bicknell, N. J. (1959), Interaction of some Divalent Metal Ions with Diethylenetriaminepentaacetic Acid, *J. Inorg. Nucl. Chem.*, **11**, 184-196.

Choppin, G. R., Biasden, P. A. and Khan, S. A. (1979), Nuclear Magnetic Resonance Studies of Diamagnetic Metal-Diethylenetriaminepentaacetate Complexes, *Inorg. Chem.*, **18**, 1330-1332.

Clarke, R. and Tremaine, P. R. (1999), Amino Acids Under Hydrothermal Conditions: Apparent Molar Volumes of Aqueous α-Alanine, β-Alanine, and Proline at Temperatures from 298 to 523 K and Pressures up to 20 MPa, *J. Phys. Chem.*, in press.

Cobble, J. W. and Murray, R. C. (1977), Unusual Ion Solvation Energies in High Temperature Water, *Faraday Soc. Discuss.*, 64-144.

Conti, G., Gianni, P. G. and Matteoli, E. (1992), Apparent Molar Heat Capacity of Aqueous Hydrolyzed and Non-Hydrolyzed $AlCl_3$ between 50-150°C, *Geochim. Cosmochim. Acta*, **56**, 4125-4133.

Corti, H. R., Fernandez-Prini, R. and Svarc, F. (1990), Densities and Partial Molar Volumes of Aqueous Solutions of Lithium, Sodium, Potassium Hydroxides up to 250°C, *J. Solution Chem.*, **19**, 793-809.

Criss, C. M. and Wood, R. H. (1996), Apparent Molar Volumes of Aqueous Solutions of some Organic Solutes at the pressure 28 MPa and Temperatures to 598 K, *J. Chem. Thermodynamics*, **28**, 723-741.

Creagh, D. C. and Hubbell, J. H. (1992), *International Tables for X-Ray Crystallgraphy*, Vol. C, (Kluwer Academic Publishers, Boston).

Creagh, D. C. and McAuley, W. J. (1992), *International Tables for X-Ray Crystallgraphy* , Vol. C, (Kluwer Academic Publishers, Boston).

Cromer, D. T. and Waber, J. T. (1974), *International Tables for X-Ray Crystallgraphy*, Vol. IV, (The Kynoch Press, Birmingham, England).

Debenedetti, P. G. and Mohamed, R. S. (1989), Attractive, Weakly Attractive, and Repulsive Near-critical Systems, *J. Chem. Phys.*, **90**, 4528-4541.

Debye, P. and Hückel, E. (1923), Theory of Electrolytes II. The Limiting Law of Electrical Conductivity, *Physik. Z. Leipzig*, **v.24**, 305-325.

Desnoyers, J. E., de Visser, C., Perron, G. and Picker, P. (1976), Re-examination of the Heat Capacities Obtained by Flow Microcalorimetry. Recommendation for the Use of a Chemical Standard, *J. Solution Chem.*, **5**, 605-616.

Finnen, D. C., Pinkerton, A., Dunham, W. R., Sand, R.H. and Max O. Funk, Jr. (1991), Structures and Spectroscopic Characteristics of Iron(III) Diethylenetriaminepentaacetic Acid Complexes. A Non-Heme Iron(III) Complex with Relevance to the Iron Environment in Lipoxygenases, *Inorg. Chem.*, **30**, 3960-3964.

Franck E.U. (1956) Hochverdichteter Wasserdampf II. Ionendissociation von KCl in H_2O bis 750°C. *Z. Phys. Chem.* **8**, 107-126.

Franck E.U. (1961) Überkritisches Wasser als electrolytisches Lösungsmittel. *Angew. Chem.* **73**, 309-322.

French, R. N. and Criss, C. M. (1982), Effect of Charge on the Standard Partial Molar Volumes and Heat Capacities of Organic Electrolytes in Methanol and Water, *J. Solution Chem.*, **11**, 625-648.

Harvie, C. E. and Weare, J. H. (1980), The Prediction of Mineral Solubilities in Natural Waters: the Na-K-Mg-Ca-Cl-SO_4-H_2O System from Zero to High Concentration at 25°C, *Geochim. Cosmochim. Acta*, **44**, 981-987.

Helgeson, H. C. and Kirkham, D. H. (1976), Theoretical Predictions of the Thermodynamic Behavior of Aqueous Electrolytes at High Pressures and Temperatures. III. Equation of State for Aqueous Species at Infinite Dilution, *Am. J. Sci.*, **276**, 97-240.

Helgeson, H. C., Kirkham, D. H. and Flowers, G. C. (1981), Theoretical Predications of the Thermodynamic Behavior of Aqueous Electrolytes at High Pressures and Temperatures. Calculation of Activity Coefficient, Osmotic Coefficients, and Apparent

Molar and Standard and Relative Partial Molar Properties to 600°C and 5 kb, *Am. J. Sci.*, **281**, 1249-1516.

Higginson, W. C. E. and Samuel, B. (1970), Structures of the Ethylenediaminetetra-acetate Complexes of some Bivalent Cations in Aqueous Solution, *J. Chem. Soc.*, **A**, 1579-1586.

Hill, P. G. (1990), A Unified Fundamental Equation for the Thermodynamic Properties of H_2O, *J. Phys. Chem. Ref. Data*, **19**, 1233-1274.

Hnedkovsky, L., Majer, V. and Wood, R. H. (1995), Volumes and Heat Capacities of H_3BO_3(aq) at Temperatures from 298.15 K to 705 K and at Pressures to 35 MPa, *J. Chem. Thermodynamics*, **27**, 801-814.

Høiland, H. and Vikingstad, E. (1975), Partial Molar Volumes and Volumes of Ionization of Hydroxycarboxylic Acids in Aqueous Solution at 25, 30 and 35°C, *J. Chem. Soc. Faraday Trans.*, **71**, 2007-2016.

Hovey, J. K. (1988), *Thermodynamics of Aqueous Solutions*, Ph.D Thesis, University of Alberta.

Hovey, J. K., Hepler, L. G. and Tremaine, P. R. (1986), Thermodynamics of aqueous EDTA Systems: Apparent and Partial Molar Heat Capacities and Volumes of Aqueous Strontium and Barium EDTA, *J. Solution Chem.*, **15**, 977-987.

Hovey, J. K., Hepler, L. G. and Tremaine, P. R. (1988a), Thermodynamics of Aqueous Aluminate Ion: Standard Partial Molar Heat Capacities and Volumes of $Al(OH)_4^-$ from 10 to 55°C, *J. Phys. Chem.*, **92**, 1323-1332.

Hovey, J. K., Hepler, L. G. and Tremaine, P. R. (1988b), Thermodynamics of Aqueous EDTA Systems: Apparent and Partial Molar Heat Capacities and Volumes of Aqueous $EDTA^{4-}$, $HEDTA^{3-}$, H_2EDTA^{2-}, $NaEDTA^{3-}$, and $KEDTA^{3-}$ at 25°C. Relaxation Effects in Mixed Aqueous Electrolyte Solutions and Calculations of Temperature Dependence Equilibrium Constants, *Can. J. Chem.*, **66**, 881-896.

Hovey, J. K. and Tremaine, P. R. (1985), Thermodynamics of the Complexes of Aqueous Iron(III), Aluminum, and Several Divalent Cations with EDTA: Heat Capacities, Volumes, and Variations in Stability with Temperature, *J. Phys. Chem.*, **89**, 5541-5549.

Hovey, J. K. and Tremaine, P. R. (1986), Thermodynamics of Aqueous Aluminum: Standard Partial Molar Heat Capacities of Al^{3+} from 10 to 55°C, *Geochim. Cosmochim. Acta*, **50**, 453-459.

Inglese, A., Sedlbauer, J. and Wood, R. H. (1996), Apparent Molar Heat Capacities of aqueous Solutions of Acetic, Propanoic and Succinic Acids, Sodium Acetate and Sodium Propanoate from 300 to 525 K and a Pressure of 28 MPa, *J. Solution Chem.*, **25**, 849-865.

Inglese, A. and Wood, R. H. (1996), Apparent Molar Heat Capacities of Aqueous Solutions of 1-Propanol, Butane-1,4-diol, and Hexane-1,6-diol at Temperatures from 300 K to 525 K and a Pressure of 28 MPa, *J. Chem. Thermodynamics*, **28**, 1059-1070.

Jeffery, G. H., Bassett, J., Mendham, J. and Denney, R. C. (1989), *Vogel's Textbook of Quantitative Chemical Analysis*, Fifth edition, (Longman Press, England).

Jezowska-Trzebiatowska, B., Latos-Grazynski, L. and Kozlowski, H. (1977), PMR Studies of Nickel(II)-DTPA Complexes Aqueous Solutions. *Inorganica Chimica Acta*, **21**, 145-150.

Johnson, J. W., Oelkers, E. H. and Helgeson, H. C. (1992), Supcrt92: A Software Package for Calculating the Standard Molar Thermodynamic Properties of Minerals, Gases, Aqueous Species, and Reactions from 1 to 5000 Bar and 0 to 1000°C, *Computers and Geosciences*, **18**, 899-947.

Kaneko, N., Kaneko, M. and Takahashi, H. (1984), Infrared and Raman Spectra and Vibrational Assignment of some Metal Tartrates, *Spectrochimica Acta*, Vol. 40A, No. **1**, 33-42.

Kennard, C. H. L. (1967), The Crystal Structure of (Hydrogen Ethylenediaminetetra-acetato)aquoferrate (III) and Gallate (III), *Inorg. Chim. Acta*, **1**, 347-354.

Latos-Grazynski, L. and Jezowska-Trzebiatowska, B. (1980), Nuclear Magnetic Resonance Studies of the Configuration and Ligand Rearrangement in Complexes of Nickel(II) and Cobalt(II) with Diethylenetriaminepentaacetic Acid and Triethylenetetraaminehexaacetic Acid, *J. Coord. Chem.*, **10**, 159-169.

Letkeman, P. and Martell, A. E. (1979), Nuclear Magnetic Resonance and Potentiometric Protonation Study of Polyaminopolyacetic Acids Containing from Two to Six Nitrogen Atoms, *Inorg. Chem.*, **18**, 1284-1289.

Lopez-Alcala, J. M., Puerat-Vizcaino, M. C., Gonzalea-Vilchez, F., Duesler, E. N. and Tapscott, R. E. (1984), A redetermination of Sodium Aqua [ethylenediaminetetra-acetato(4-)]ferrate (III) Dihydrate, $Na[Fe(C_{10}H_{12}N_2O_8)(H_2O)]\cdot 2H_2O$ *Acta Crystallogr.*, **C40**, 939-941.

Mains, G. J., Larson, J. W. and Hepler, L. G. (1984), General Thermodynamic Analysis of the Contributions of Temperature-Dependent Chemical Equilibria to Heat Capacities of Ideal Gases and Ideal Associated Solutions, *J. Phys. Chem.*, **88**, 1257.

Majer, V., Crovetto, R. and Wood, R. H. (1991), A new Version of Vibrating-Tube Flow Densitometer for Measurements at Temperatures up to 730 K, *J. Chem. Thermodynamics*, **23**, 333-344.

Manzurola, E. and Apelblat, A. (1985), Apparent Molar Volumes of Citric, Tartaric, Malic, Succinic, Maleic, and Acetic Acids in Water at 298.15 K, *J. Chem. Thermodynamics*, **17**, 579-584.

Marcus, Y. (1985), *Ion Solvation*, (Wiley Press, New York).

Martell, A. E., Motekaitis, R. J., Fried, A. R., Wilson, J. S. and MacMillan, D. T. (1975), Thermal Decomposition of EDTA, NTA, and Nitrilotrimethylenephosphonic Acid in Aqueous Solution, *Can. J. Chem.*, **53**, 3471-3476.

Martell, A. E. and Smith, R. M. (1982), *Critical Stability Constants*, Vol. 5, (Plenum Press, New York).

Mehdi, G. H. and Budesinsky, B. W. (1974), Proronated Metal Complexes of Diethylenetriaminepentaacetic Acid (DTPA), *J. Coord. Chem.*, **3**, 287-292.

Mesmer, R. E. (1985), A Model for Estimmation of Thermodynamic Quantities for Reactions-Uncertainties from such Predictions: Paper Presented at Second International Symposium on Hydrothermal Reactions at The Pennsylvania State University.

Millero, F. J. (1979), *In Activity Coefficients in Electrolyte Solutions*: Vol. 2, Pytkowicz, M. ed., (CRC Press, Boca Raton, FL).

Milyukov, P. M. and Polenova, N. V. (1981), Temperature Dependence of Thermodynamic Functions of the Stepwise Dissociation of Diethylenetriaminepentaacetic Acid in Aqueous Solution, *Russian J. Phys. Chem.*, **55(9)**, 1360-1362.

Motekaitis, R. J., Hayes, D., Martell, A. E. and Frenier, W. W. (1979), Hydrolysis and Ammonolysis of EDTA in Aqueous Solution, *Can. J. Chem.*, **57**, 1018-1024.

Nakamoto, K., Morimoto, Y. and Martell, A. E. J. (1963), Infrared Spectra of Aqueous Solutions. III. Ethylenediaminetetraacetic Acid, N-Hydroxyethylethylenediaminetri-acetic Acid and Diethylenetriaminepentaacetic Acid, *Amer. Chem. Soc.*, **85**, 309-313.

Oakes, C. S., Simonson, J. M. and Bondnar, R. J. (1995), Apparent Molar Volumes of Aqueous Calcium Chloride to 250°C, 400 Bars, and from Molalities of 0.242 to 6.150, *J. Solution Chem.*, **24**, 897-916.

Oakes, J. and Smith, E. G. (1983), Nuclear Magnetic Resonance Studies of Transition-metal Complexes of Ethylenediaminetetra-acetic Acid (EDTA) in Aqueous Solution, *J. Chem. Soc. Faraday Trans. I*, **79**, 543-552.

Peiper, J. C. and Pitzer, K. S. (1982), Thermodynamics of Aqueous Carbonate Solutions Including Mixtures of Sodium Carbonate, Bicarbonate, and Chloride, *J. Chem. Thermodyn.*, **14**, 613.

Peters, J.A. (1988), Multinuclear NMR Study of Lanthanide (III) Complexes of Diethylenetriaminepentaacetate, *Inorg. Chem.*, **27**, 4686-4691.

Pettit, L. D. and Powell, K. J. (1997), *IUPAC: Stability Constants Database SC-Database for Windows and A Database of Selected Stability Constants, Mini-SCDatabase*, Academic Software.

Picker, P., Leduc, P. A., Philip, P. R. and Desnoyers, J. E. (1971), Heat Capacity of Solutions by Flow Microcalorimetry, *J. Chem. Thermodyn.*, **3**, 631-642.

Picker, P., Tremblay, E. and Jolicoeur, C. (1974), A High-Precision Digital Readout Flow Densimeter for Liquids, *J. Solution Chem.*, **3**, 377-384.

Pitzer, K. S. (1973), Thermodynamics of Electrolytes. I. Theoretical basis and General Equations, *J. Phys. Chem.*, **77**, 268.

Pitzer, K. S. (1979), Theory: Ion Interaction Approach, in R.M. Pytowicz, ed., *Activity Coefficients in Electrolyte Solutions* v. **1**: Boca Raton, CRC Press, 157-208.

Pitzer, K. S. (1986), Theoretical Considerations of Solubility with Emphasis on Mixed Aqueous Electrolytes, *Pure & Appl. Chem.*, **58**, 1599-1610.

Pitzer, K. S. (1987), A Thermodynamic Model for Aqueous Solutions of Liquid-like Density: in I.S.E. Carmichael and H.P. Eugster, eds., Thermodynamic Modelling of Geological Materials: Minerals, Fluids and Melts, v **17**, Reviews in Mineralogy, *Mineral. Soc. Amer.*, 97-142.

Pitzer, K. S. (1989), Fluids, Both Ionic and Non-ionic, over Wide Ranges of Temperature and Composition, *J. Chem. Thermodyn.*, **21**, 1-17.

Pitzer, K. S. (1991), *Activity Coefficients in Electrolyte Solutions*, 2nd Edition, (CRC Press, Boca Raton).

Pitzer, K. S., Brewer, L., Lewis, G. N. and Randall, M. (1961), *Thermodynamics*, 2nd ed., (McGraw-Hill Press, New York).

Pitzer, K. S., Roy, R. N. and Silvester, L. F. (1977), Thermodynamics of Electrolyte. VII. Sulfuric Acid, *J. Am. Chem. Soc.*, **99**, 4930.

Pitzer, K. S. and Silvester, L. F. (1976), Thermodynamics of Electrolyte. VI. Weak Electrolytes Including H_3PO_4, *J. Solution Chem.*, **5**, 269.

Reilly, P. J. and Wood, R. H. (1969), The Prediction of the Properties of Mixed Electrolytes from measurements on Common Ion Mixtures, *J. Phys. Chem.*, **73**, 4292-4297.

Roux, A. H., Perron, G. and Desnoyers, J. E. (1984), Capacités Calorifiques, Volumes, Expansibilités et Compressibilités des Solutions Aqueous Concentrées de LiOH, NaOH et KOH, *Can. J. Chem.*, **62**, 878-885.

Seccombe, R. C., Lee, B. and Henry, G. M. (1975), Crystal and Molecular Structure of Trihydrogen Diethylenetriaminepentaacetatocuprate(II) Monohydrate ($H_3CuDTPA{\cdot}H_2O$), *Inorganic Chemistry*, **14**, 1147-1154.

Sengers, J. V. and Levelt Sengers, J. M. H. (1986), Thermodynamic Behavior of Fluids Near the Critical Point, *Ann. Rev. Phys. Chem.*, **37**, 189-222.

Shock, E. L., Oelkers, E. H., Johnson, J. W., Sverjensky, D. A. and Helgeson, H. C. (1992), Calculation of the Thermodynamic Properties of Aqueous Species at High Pressures and Temperatures, *J. Chem. Soc. Faraday Trans.*, **88**, 803-826.

Sievers, R. E. and Bailar Jr., J. C. (1962), Some Metal Chelates of Ethylenediaminetetraacetic Acid, Diethylenetriaminepentaacetic Acid, and Triethylenetetraminehexaacetic Acid, *Inorg. Chem.*, **1**, 174-182.

Sijpkes, A. H., Rossum, P. V., Raad, J. S. and Somsen, G. (1989), Heat Capacities and Volumes of some Polybasic Carboxylic Acids in Water at 298.15 K, *J. Chem. Thermodynamics*, **21**, 1061-1067.

Simonson, J. M., Oakes, C. S. and Bondnar, R. J. (1994), Densities of NaCl(aq) to the temperature 523 K at Pressures to 40 MPa Measured with a New Vibrating-Tube Densitometer, *J. Chem. Thermodynamics.*, **26**, 345-359.

Smith, R. M. and Martell, A. E. (1997), *NIST Standard Reference database 46: NIST Critically Selected Stability Constants of Metal Complexes Database*, Version 4.0.

Smith-Magowan, D. and Wood, R. H. (1981), Heat Capacities of Aqueous Sodium Chloride from 320 to 600 K Measured with a New Flow Calorimeter, *J. Chem. Thermodynamics*, **13**, 1047-1073.

Tanger, J. C. and Helgeson, H. C. (1988), Calculation of the Thermodynamic and Transport Properties of Aqueous Species at High Pressures and Temperatures: Revised Equation of State for the Standard Partial Molar properties of Ions and Electrolytes, *Amer. J. Sci.*, **288**, 19-98.

Tremaine, P. R., Shvedov, D. and Xiao, C. (1997), Thermodynamic Properties of Aqueous Morpholine and Morpholonium Chloride and temperature Dependence of Ionization, *J. Phys. Chem.*, **101**, 409-419.

Tremaine, P. R., Sway, K. and Barbero, J. A. (1986), The Apparent Molar Heat Capacity of Aqueous hydrochloric Acid from 10 to 140°C, *J. Solution Chem.*, **15**, 1-22.

Wang, Z. (1998), Apparent Molar Heat Capacities and Volumes of Aqueous Chelating Agents: EDTA and NTA, MSc Thesis, Memorial University of Newfoundland.

Weare, J. H. (1987), Models of Mineral Solubility in Concentrated Brines with Application to Field Observations: Chapter 5 in I.S.E. Carmichael and H.P. Eugster, eds., Thermodynamic Modelling of Geological Materials: Minerals, Fluids and Melts, v. **17**, Reviews in Mineralogy, *Mineral. Soc. Amer.*, 143-176.

Wedeen, R. P., Batuman, V. and Landy, E. (1983), The Safety of the EDTA Lead-Mobilization Test, *Env. Res.*, **30**, 58-62.

Weiser, H. B., Milligan, W. D. and Cook, E. L. (1942), Hydrous Cupric Hydroxides and Basic Cupric Sulfates, *J. Am. Chem. Soc.*, **64**, 503-508.

Wheeler, J. C. (1972), Behavior of a Solute Near the Critical Point of an Almost Pure Solvent, *Ber. Bunsenges. Phys. Chem.*, **76**, 308-318.

White, D. E. and Wood, R. H. (1982), Absolute Calibration of Flow Calorimeters Used for Measuring Differences in Heat Capacities. A Chemical Standard for Temperatures between 325 and 600 K, *J. Solution Chem.*, **11**, 223-236.

Woolley, E. M. and Hepler, L. G. (1977), Heat Capacities of Weak Electrolyte and Ion Association Reactions: Method and Application to Aqueous $MgSO_4$ and HIO_3 at 298 K, *Can. J. Chem.*, **55**, 158-163.

Xiao, C. (1997), Thermodynamics Of Aqueous Electrolytes and Hydrogen-Bonded Non-electrolytes over a Wide Range of Temperature and Pressure: The Aqueous Trivalent Lanthanide Cations and the Methanol-Water System, *Ph.D Thesis*, Memorial University of Newfoundland.

Xiao, C., Bianchi, H. and Tremaine, P. R. (1997), Excess Molar Volumes and Densities of (Methanol + Water) at Temperatures between 323 K and 573 K and Pressures of 7.0 MPa and 13.5 MPa, *J. Chem. Thermodynamics*, **29**, 261-286.

Xiao, C. and Tremaine, P. R. (1996), Apparent Molar Heat Capacities and Volumes of $LaCl_3$(aq), $La(ClO_4)_3$(aq) and $Gd(ClO_4)_3$(aq) from 283 to 338 K, *J. Chem. Thermodynamics*, **28**, 43-66.

Xiao, C. and Tremaine, P. R. (1997), Apparent Molar Volumes of Aqueous Sodium Trifluoromethanesulfonate and Trifluoromethanesulfonic Acid from 283 K to 600 K and Pressures up to 20 MPa. *J. Solution Chem.* **26**, 277-294.

Xie, W. and Tremaine, P. R. (1999), Thermodynamics of Aqueous Diethylenetriaminepentaacetic Acid(DTPA) Systems: Apparent and Partial Molar Heat Capacities and Volumes of Aqueous H_2DTPA^{3-}, $DTPA^{5-}$, $CuDTPA^{3-}$, and Cu_2DTPA^- from 10 to 55°C, *J. Solution Chem.*, **28**, 291-325.

Yaeger, L. L. (1983), Electrolytic Scission of Hexadentate Aluminum Bonds, *Rejuvenation*, **11**, 76-80.

Young, T. F. and Smith, M. B. (1954), Thermodynamic Properties of Mixtures of Electrolytes in Aqueous Solutions, *J. Phys. Chem.*, **58**, 716-724.

Appendices

Appendix A: Tables of Experimental Results

Table A.III.1. Experimental Apparent molar Volumes V_ϕ and Heat Capacities $C_{p,\phi}$ for $Na_3H_2DTPA(aq)$ from 283.15 to 328.15 K.

m	$10^2(\rho-\rho_1^*)$	V_ϕ	$10^2(c_p\rho/c_{p,1}^*\rho_1^*-1)$	$C_{p,\phi}$
$mol \cdot kg^{-1}$	$g \cdot cm^{-3}$	$cm^{-3} \cdot mol^{-1}$		$J \cdot K^{-1} \cdot mol^{-1}$
		T = 283.15 K		
0.06855	1.6817	210.49	-1.238	114.22
0.10362	2.5130	211.55	-1.810	138.15
0.15402	3.6645	213.65	-2.492	194.42
0.22930	5.3199	215.92	-3.402	251.73
0.31597	7.1359	218.02	-4.279	306.57
0.32224	7.2611	218.24	-4.335	310.65
0.41140	9.0226	220.23	-5.072	359.04
0.51510	10.9597	222.29	-5.732	411.48
0.73314	14.6910	225.85	-6.765	495.51
		T = 298.15 K		
0.06855	1.6269	219.76	-1.009	285.61
0.10362	2.4274	221.03	-1.465	311.22
0.15402	3.5476	222.42	-2.059	343.77
0.22930	5.1502	224.47	-2.839	386.31
0.31597	6.9189	226.01	-3.599	426.87
0.32224	7.0459	226.04	-3.665	427.20
0.41140	8.7648	227.61	-4.328	463.16
0.73369	14.3010	232.41	-5.950	568.01

Table A.III.1. Continued

		T = 298.15 K (Solution 2)		
0.09299	2.1893	220.40	-1.325	304.98
0.10236	2.3996	220.91	-1.445	311.75
0.24209	5.4186	224.63	-2.954	393.42
0.43777	9.2469	228.27	-4.483	476.04
0.51794	10.6959	229.54	-4.961	504.40
		T = 313.15 K		
0.06855	1.5939	226.75	-0.871	386.10
0.10362	2.3776	227.96	-1.270	406.38
0.15402	3.4788	228.98	-1.796	431.13
0.22930	5.0563	230.62	-2.505	462.81
0.31597	6.7897	232.12	-3.208	494..50
0.32224	6.9096	232.29	-3.257	496.54
0.41140	8.5981	233.65	-3.877	525.16
0.51510	10.4562	235.13	-4.489	555.29
0.73369	14.0654	237.52	-5.475	608.51

Table A.III.1. Continued.

		T = 328.15 K		
0.06855	1.5957	229.42	-0.803	420.65
0.10362	2.3650	232.12	-1.144	457.70
0.22930	4.9802	236.79	-2.218	525.44
0.32224	6.7942	238.66	-2.881	558.38
0.41140	8.4427	240.17	-3.439	584.21
0.51510	10.2484	241.85	-4.000	611.33
0.73314	13.7587	244.21	-4.902	658.68

Table A.III.2. Experimental Apparent Molar Volumes V_ϕ for {Na_5DTPA + NaOH}(aq) from 283.15 to 328.15 K.

m_2	m_3	$10^2(\rho-\rho_1^*)$	V_ϕ^{exp}	$F_3V_{\phi,3}$	$V_{\phi,2}$
$mol \cdot kg^{-1}$	$mol \cdot kg^{-1}$	$g \cdot cm^{-3}$	$cm^{-3} \cdot mol^{-1}$	$cm^{-3} \cdot mol^{-1}$	$cm^{-3} \cdot mol^{-1}$
		T = 283.15 K			
0.06059	0.01000	1.8424	173.30	-0.61	204.89
0.09994	0.00927	2.9458	188.58	-0.28	208.28
0.09994	0.00928	2.9423	188.90	-0.28	208.66
0.15109	0.00828	4.3203	199.08	-0.12	211.84
0.15109	0.00828	4.3259	199.44	-0.12	212.23
0.20120	0.00732	5.6326	205.28	-0.06	214.40
0.25852	0.00621	7.0738	210.27	-0.03	216.86
0.31145	0.00518	8.3567	213.84	-0.02	218.89
0.43883	0.00272	11.2415	220.95	-0.01	223.76
		T = 298.15 K			
0.06059	0.01000	1.7866	181.05	-0.42	213.29
0.09994	0.00927	2.8568	196.56	-0.24	216.66
0.11335	0.00901	3.2137	199.91	-0.22	217.60
0.15109	0.00828	4.2009	206.75	-0.19	219.78
0.20120	0.00732	5.4722	212.79	-0.18	222.17
0.25852	0.00621	6.8725	217.70	-0.18	224.57
0.31145	0.00518	8.1188	221.20	-0.17	226.55

Table A.III.2. Continued.

		T = 313.15 K			
0.06059	0.01000	1.7528	185.46	-0.21	217.67
0.09994	0.00927	2.8078	200.71	-0.04	220.47
0.11335	0.00901	3.1605	203.94	-0.02	221.23
0.15109	0.00828	4.1286	211.01	0.02	223.54
0.20120	0.00732	5.3795	216.99	0.04	225.75
0.25852	0.00621	6.7543	221.97	0.05	228.11
0.31145	0.00518	7.9820	225.36	0.04	229.88
0.43883	0.00272	10.7609	231.65	0.02	233.83
		T = 328.15 K			
0.06059	0.01000	1.7383	187.11	0.13	219.22
0.09994	0.00927	2.7824	202.69	0.01	222.38
0.11335	0.00901	3.1315	205.97	0.02	223.18
0.15109	0.00828	4.0862	213.38	0.05	225.84
0.20120	0.00732	5.3258	219.33	0.06	227.98
0.25852	0.00621	6.6936	224.07	0.06	230.08
0.31145	0.00518	7.9119	227.42	0.06	231.81
0.43883	0.00272	10.6739	223.56	0.03	235.58

Table A.III.3. Experimental Apparent Molar Heat Capacities $C_{p,\phi}^{exp}$ for {Na_5DTPA + NaOH}(aq) from 283.15 to 328.15 K.

m_2	m_3	$10^2(c_p\rho/c_{p,1}^*\rho_1^* - 1)$	$C_{p,\phi}^{exp}$	$F_3C_{p,\phi,3}$	$C_{p,\phi,2}$
$mol \cdot kg^{-1}$	$mol \cdot kg^{-1}$		$J \cdot K^{-1} \cdot mol^{-1}$	$J \cdot K^{-1} \cdot mol^{-1}$	$J \cdot K^{-1} \cdot mol^{-1}$
		T = 283.15 K			
0.06059	0.01000	-1.089	72.57	-12.06	105.34
0.09994	0.00927	-1.616	157.43	-1.25	183.36
0.09994	0.00928	-1.579	173.36	-4.55	201.86
0.15109	0.00828	-2.211	231.81	-4.55	251.55
0.15109	0.00828	-2.211	235.89	-1.25	256.08
0.20120	0.00732	-2.710	292.38	-0.17	308.93
0.25852	0.00621	-3.171	351.30	0.17	365.57
0.31145	0.00518	-3.516	399.47	0.17	412.43
0.43883	0.00272	-4.091	499.93	-0.06	511.15
		T = 298.15 K			
0.06059	0.01000	-0.792	280.07	-5.93	344.71
0.09994	0.00927	-1.207	347.15	-1.79	390.76
0.11335	0.00901	-1.336	365.71	-1.10	404.90
0.15109	0.00828	-1.677	407.39	0.01	437.81
0.20120	0.00732	-2.067	454.15	0.56	477.53
0.25852	0.00621	-2.444	499.22	0.68	517.50
0.31145	0.00518	-2.738	535.11	0.61	550.18
0.43883	0.00272	-3.258	609.03	0.27	619.21

Table A.III.3. Continued.

		T = 313.15 K			
0.06059	0.01000	-0.636	388.00	-2.86	467.27
0.09994	0.00927	-0.988	446.05	-0.35	497.47
0.11335	0.00901	-1.098	461.40	0.05	507.12
0.15109	0.00828	-1.384	499.78	0.67	534.78
0.20120	0.00732	-1.719	539.61	0.93	565.80
0.25852	0.00621	-2.049	577.83	0.93	597.70
0.31145	0.00518	-2.310	607.76	0.81	623.60
0.43883	0.00272	-2.792	669.27	0.41	678.97
		T = 328.15 K			
0.06059	0.01000	-0.625	396.24	-1.07	473.04
0.09994	0.00927	-0.901	483.19	0.55	536.91
0.11335	0.00901	-0.982	505.00	0.79	553.52
0.15109	0.00828	-1.239	543.67	1.11	580.84
0.20120	0.00732	-1.521	585.32	1.18	613.29
0.25852	0.00621	-1.759	629.36	1.06	650.87
0.31145	0.00518	-2.064	645.38	0.89	662.06
0.43883	0.00272	-2.492	702.61	0.43	712.75

Table A.III.4. Experimental Apparent Molar Volumes V_ϕ for {$Na_3CuDTPA$ + NaOH}(aq) from 283.15 to 328.15 K.

m_2	m_3	$10^2(\rho-\rho_1^*)$	V_ϕ^{exp}	$F_3V_{\phi,3}$	$V_{\phi,2}$
$mol \cdot kg^{-1}$	$mol \cdot kg^{-1}$	$g \cdot cm^{-3}$	$cm^{-3} \cdot mol^{-1}$	$cm^{-3} \cdot mol^{-1}$	$cm^{-3} \cdot mol^{-1}$
		T = 283.15 K			
0.05710	0.00741	1.7359	212.77	-0.74	213.05
0.07511	0.00665	2.2658	214.06	-0.48	214.25
0.09009	0.00791	2.7035	214.68	-0.45	214.87
0.10776	0.00938	3.2161	215.22	-0.43	215.41
0.12154	0.01626	3.6122	215.54	-0.63	215.83
0.13851	0.01838	4.0966	215.91	-0.59	216.20
0.15345	0.02199	4.5189	216.25	-0.61	216.57
		T = 298.15 K			
0.04339	0.00390	1.2923	219.75	-0.36	219.96
0.05352	0.00479	1.5877	220.28	-0.35	220.48
0.07511	0.00665	2.2098	221.35	-0.31	221.55
0.09009	0.00791	2.6366	221.94	-0.30	222.14
0.10776	0.00938	3.1361	222.46	-0.28	222.65
0.12154	0.01626	3.5215	222.80	-0.41	223.11
0.13851	0.01838	3.9931	223.18	-0.40	223.48
0.15345	0.02199	4.4044	223.51	-0.42	223.83
0.15346	0.01379	4.4025	223.74	-0.26	223.94

Table A.III.4. Continued.

		T = 298.15 K (Solution 2)			
0.08239	0.00006	2.4394	220.50	-0.22	220.67
0.10707	0.00008	3.1454	221.22	-0.23	221.39
0.13324	0.00010	3.8809	221.95	-0.25	222.12
0.15835	0.00012	4.5796	222.50	-0.26	222.71
		T = 313.15 K			
0.04339	0.00390	1.2474	223.35	-0.26	223.56
0.05352	0.00479	1.5634	224.40	-0.24	224.60
0.05710	0.00741	1.6647	224.68	-0.35	224.98
0.07511	0.00665	2.1764	225.41	-0.21	225.61
0.09009	0.00791	2.5959	226.10	-0.19	226.30
0.01078	0.00938	3.0856	226.79	-0.17	226.99
0.12154	0.01626	3.4669	226.95	-0.24	227.26
0.13851	0.01838	3.9298	227.42	-0.22	227.73
0.15345	0.02199	4.3348	227.73	-0.21	228.05

Table A.III.4. Continued.

		T = 328.15 K			
0.04339	0.00390	1.2612	226.04	-0.19	226.25
0.05710	0.00740	1.6542	226.09	-0.25	226.38
0.07511	0.00664	2.1588	227.35	-0.15	227.56
0.09009	0.00791	2.5747	228.06	-0.14	228.26
0.10776	0.00938	3.0632	228.50	-0.12	228.70
0.12154	0.01626	3.4414	228.68	-0.16	228.99
0.13851	0.01837	3.9069	228.71	-0.14	229.01
0.15345	0.02199	4.3057	229.27	-0.13	229.60

Table A.III.5. Experimental Apparent Molar Heat Capacities $C_{p,\phi}^{exp}$ for {$Na_3CuDTPA$ + NaOH}(aq) from 283.15 to 328.15 K.

m_2	m_3	$10^2(c_p\rho/c_{p,1}^*\rho_1^* - 1)$	$C_{p,\phi}^{exp}$	$F_3C_{p,\phi,3}$	$C_{p,\phi,2}$
$mol \cdot kg^{-1}$	$mol \cdot kg^{-1}$		$J \cdot K^{-1} \cdot mol^{-1}$	$J \cdot K^{-1} \cdot mol^{-1}$	$J \cdot K^{-1} \cdot mol^{-1}$
		T = 283.15 K			
0.15345	0.02199	-2.6709	153.68	-0.12	154.02
0.13851	0.01838	-2.4530	141.43	-0.12	141.73
0.12154	0.01626	-2.1942	127.90	-0.13	128.20
0.10776	0.00938	-1.9785	115.32	-0.09	115.51
0.09009	0.00791	-1.6887	99.69	-0.10	99.87
0.07511	0.00665	-1.4335	85.14	-0.10	85.32
0.05710	0.00741	-1.1157	64.03	-0.16	64.28
		T = 298.15 K			
0.15346	0.01379	-2.2001	313.20	-0.04	313.52
0.15345	0.02199	-2.2009	312.32	-0.06	312.82
0.13851	0.01838	-2.0167	303.55	-0.06	304.02
0.12154	0.01626	-1.7976	294.47	-0.07	294.93
0.10776	0.00938	-1.6135	286.76	-0.05	287.06
0.09009	0.00791	-1.3724	276.00	-0.05	276.30
0.07511	0.00665	-1.1589	267.38	-0.06	267.67
0.05352	0.004788	-0.8460	250.00	-0.06	250.29
0.04339	0.003902	-0.6949	240.51	-0.07	240.79

Table A.III.5. Continued.

		T = 298.15 K (Solution 2)			
0.15835	0.00012	-2.2646	308.84	-0.03	309.16
0.13324	0.00010	-1.9557	293.85	-0.04	294.11
0.10707	0.00008	-1.6088	279.25	-0.04	279.51
0.08239	0.00006	-1.2711	263.24	-0.05	263.49
		T = 313.15 K			
0.15345	0.02199	-1.9036	408.57	-0.03	409.18
0.13851	0.01838	-1.7390	402.57	-0.03	403.14
0.12154	0.01626	-1.5475	395.08	-0.03	395.64
0.10776	0.00938	-1.3894	388.97	-0.03	389.34
0.09009	0.00791	-1.1814	378.93	-0.03	379.29
0.07511	0.00665	-0.9970	371.17	-0.03	371.53
0.05710	0.00741	-0.7756	357.66	-0.05	358.18
0.05352	0.00479	-0.7298	354.49	-0.04	354.84
0.04339	0.00390	-0.5979	345.43	-0.04	345.78

Table A.III.5. Continued.

		T = 328.15 K			
0.15345	0.02199	-1.7239	459.61	-0.01	460.34
0.13851	0.01838	-1.5763	452.59	-0.01	453.21
0.12154	0.01626	-1.4037	447.12	-0.02	447.74
0.10776	0.00938	-1.2623	440.57	-0.01	440.97
0.09009	0.00791	-1.0751	431.39	-0.02	431.78
0.07511	0.00665	-0.9111	421.89	-0.02	422.28
0.05710	0.00741	-0.7016	412.38	-0.03	412.94
0.04339	0.00390	-0.5524	394.90	-0.03	395.28

Table A.III.6. Experimental Apparent Molar Volumes V_ϕ for {$NaCu_2DTPA$ + NaOH} (aq) from 283.15 to 328.15 K.

m_2	m_3	$10^2(\rho-\rho_1^*)$	V_ϕ^{exp}	$F_3V_{\phi,3}$	$V_{\phi,2}$
$mol \cdot kg^{-1}$	$mol \cdot kg^{-1}$	$g \cdot cm^{-3}$	$cm^{-3} \cdot mol^{-1}$	$cm^{-3} \cdot mol^{-1}$	$cm^{-3} \cdot mol^{-1}$
		T = 283.15 K			
0.19512	0.03001	5.5157	242.00	-0.96	242.38
0.16429	0.02565	4.6933	241.03	-0.99	241.41
0.14712	0.00310	4.2195	241.31	-0.14	241.36
0.11385	0.01823	3.2969	240.48	-1.05	240.88
0.09348	0.01513	2.7267	239.77	-1.08	240.16
0.07267	0.00159	2.1359	239.24	-0.15	239.30
0.06344	0.00139	1.8674	239.42	-0.15	239.47
		T = 298.15 K			
0.19512	0.03001	5.4193	246.85	-0.65	247.24
0.16429	0.02565	4.6015	246.52	-0.68	246.92
0.14712	0.00300	4.1396	246.66	-0.94	246.72
0.11385	0.01823	3.2374	245.63	-0.73	246.03
0.09348	0.01513	2.6730	245.43	-0.76	245.84
0.07267	0.00159	2.0920	245.23	-0.10	245.28
0.06344	0.00139	1.8326	244.87	-0.11	244.92

Table A.III.6. Continued.

		T = 313.15 K			
0.19512	0.03001	5.3529	250.10	-0.47	250.49
0.16429	0.02565	4.5421	249.97	-0.50	250.37
0.14712	0.00310	4.0877	250.02	-0.68	250.07
0.11385	0.01823	3.1942	249.22	-0.54	249.63
0.09348	0.01513	2.6381	248.95	-0.56	249.36
0.07267	0.00159	2.0647	248.74	-0.78	248.80
0.06344	0.00139	1.8072	248.63	-0.79	248.69
		T = 328.15 K			
0.16429	0.02565	4.5040	252.14	-0.38	252.54
0.14712	0.00310	4.0511	252.35	-0.05	252.40
0.11385	0.01823	3.1636	251.73	-0.41	252.14
0.09348	0.01513	2.6106	251.71	-0.43	252.12
0.07267	0.00159	2.0453	251.22	-0.06	251.27
0.06344	0.00139	1.7904	251.06	-0.06	251.12

Table A.III.7. Experimental Apparent Heat Capacities $C_{p,\phi}^{exp}$ for {$NaCu_2DTPA$ + NaOH}(aq) from 283.15 to 328.15 K.

m_2	m_3	$10^2(c_p\rho/c_{p,1}^{*}\rho_1^{*}-1)$	$C_{p,\phi}^{exp}$	$F_3C_{p,\phi,3}$	$C_{p,\phi,2}$
$mol \cdot kg^{-1}$	$mol \cdot kg^{-1}$		$J \cdot K^{-1} \cdot mol^{-1}$	$J \cdot K^{-1} \cdot mol^{-1}$	$J \cdot K^{-1} \cdot mol^{-1}$
		T = 283.15 K			
0.19512	0.03001	-2.5971	431.03	-0.21	431.91
0.16429	0.02565	-2.2511	414.18	-0.22	415.05
0.14712	0.00310	-2.0486	407.29	-0.03	407.40
0.11385	0.01823	-1.6405	388.57	-0.24	389.43
0.09348	0.01513	-1.3775	374.62	-0.24	375.47
0.07267	0.00159	-1.0947	360.78	-0.03	360.89
0.06344	0.00139	-0.9677	354.85	-0.03	354.97
		T = 298.15 K			
0.19512	0.03001	-2.1569	545.23	-0.12	546.19
0.16429	0.02565	-1.8592	535.99	-0.12	536.95
0.14712	0.00310	-1.6868	531.49	-0.02	531.62
0.11385	0.01823	-1.3412	518.26	-0.13	519.22
0.09348	0.01513	-1.1218	510.53	-0.14	511.49
0.07267	0.00159	-0.8881	502.18	-0.02	502.30
0.06344	0.00139	-0.7819	497.39	-0.02	497.52

Table A.III.7. Continued.

		T = 313.15 K			
0.19512	0.030011	-1.8287	626.85	-0.07	627.88
0.16429	0.025653	-1.571	621.07	-0.08	622.12
0.14712	0.0031	-1.4231	617.64	-0.01	617.78
0.11385	0.018232	-1.1271	608.59	-0.08	609.64
0.09348	0.015127	-0.9419	602.07	-0.09	603.13
0.07267	0.00159	-0.7439	596.03	-0.01	596.17
0.06344	0.001395	-0.6521	594.78	-0.01	594.92
		T = 328.15 K			
0.16429	0.025653	-1.3257	688.56001	-0.05	689.69
0.14712	0.0031	-1.2182	681.29	-0.01	681.44
0.11385	0.018232	-0.9626	674.62	-0.06	675.76
0.09348	0.015127	-0.8041	670.1	-0.06	671.25
0.07267	0.00159	-0.6303	666.43	-0.01	666.58
0.06344	0.001395	-0.5637	657.68	-0.01	657.84

Table A.III.8. Contribution of Speciation and Relaxation to the Apparent Molar Heat Capacities of Na_3H_2DTPA (aq) from 283.15 to 328.15 K.

m_2	$C^{exp}_{p,\phi}$	$\alpha\times10^3$	$C^{rel}_{p,\phi,\alpha}$	$\beta\times10^3$	$C^{rel}_{p,\phi,\beta}$	$C_{p,\phi,2}$
$mol\cdot kg^{-1}$	$J\cdot K^{-1}\cdot mol^{-1}$		$J\cdot K^{-1}\cdot mol^{-1}$		$J\cdot K^{-1}\cdot mol^{-1}$	$J\cdot K^{-1}\cdot mol^{-1}$
			T = 283.15 K			
0.73314	495.51	6.7470	1.8754	6.7466	0.6739	499.82
0.51510	411.18	6.7471	1.8754	6.7465	0.6739	414.63
0.41140	359.04	6.7472	1.8755	6.7465	0.6739	361.48
0.32220	310.65	6.7473	1.8755	6.7464	0.6739	312.42
0.31597	306.57	6.7473	1.8755	6.7464	0.6739	308.29
0.22930	251.73	6.7474	1.8755	6.7462	0.6739	252.69
0.15402	194.42	6.7477	1.8756	6.7459	0.6738	194.61
0.10362	138.15	6.7481	1.8757	6.7455	0.6738	137.57
0.06855	114.22	6.7488	1.8759	6.7448	0.6738	113.31
			T = 298.15 K			
0.73369	568.01	7.7312	1.7804	7.7307	0.3339	572.10
0.51510	500.52	7.7313	1.7804	7.7306	0.3339	503.55
0.41140	463.16	7.7314	1.7805	7.7305	0.3339	465.61
0.32224	427.20	7.7315	1.7805	7.7304	0.3339	429.08
0.31597	426.87	7.7315	1.7805	7.7304	0.3339	428.74

Table A.III.8. Continued.

0.22930	386.31	7.7318	1.7806	7.7301	0.3338	387.55
0.15402	343.77	7.7322	1.7807	7.7297	0.3338	344.35
0.10362	311.22	7.7328	1.7808	7.7219	0.3336	311.28
0.06855	285.61	7.7339	1.7811	7.7282	0.3338	285.27
			T = 298.15 K (Solution 2)			
0.51794	504.40	7.7313	1.7805	7.7306	0.3339	507.49
0.43777	476.04	7.7314	1.7805	7.7305	0.3339	478.69
0.24209	393.42	7.7317	1.7806	7.7302	0.3338	394.77
0.10236	311.75	7.7328	1.7808	7.7291	0.3338	311.82
0.09299	304.98	7.7330	1.7809	7.7289	0.3338	304.94
			T = 313.15 K			
0.73369	608.51	7.9085	1.5195	7.9078	0.0718	612.30
0.51510	555.29	7.9086	1.5195	7.9078	0.0718	558.23
0.41140	525.16	7.9087	1.5195	7.9077	0.0718	527.62
0.32224	496.54	7.9088	1.5195	7.9075	0.0718	498.54
0.31597	494.50	7.9088	1.5195	7.9075	0.0718	496.46
0.22930	462.81	7.9091	1.5196	7.9072	0.0718	464.26
0.15402	431.13	7.9096	1.5197	7.9068	0.0718	432.08
0.10362	406.38	7.9103	1.5198	7.9061	0.0717	406.93
0.06855	386.10	7.9113	1.5200	7.905	0.0717	386.32

Table A.III.8. Continued.

			T = 328.15 K			
0.73314	658.68	8.6583	1.3844	8.6576	0.0003	663.31
0.51510	611.33	8.6584	1.3844	8.6574	0.0003	615.12
0.41140	584.21	8.6585	1.3844	8.6573	0.0003	587.52
0.32224	558.38	8.6587	1.3844	8.6571	0.0003	561.24
0.22930	525.44	8.6591	1.3845	8.6567	0.0003	527.72
0.15402	489.35	8.6597	1.3846	8.6562	0.0003	490.99
0.10362	457.70	8.6605	1.3847	8.6554	0.0003	458.78
0.06855	420.65	8.6618	1.3849	8.6541	0.0003	421.08

Table A.III.9. **Relaxation Contributions to Apparent Molar Heat Capacities of {Na_5DTPA + NaOH} (aq) from 283.15 to 328.15 K.**

m_2	α	$C_{p,\phi}^{rel}$	$C_{p,\phi}^{exp}$	$C_{p,\phi}^{exp}-C_{p,\phi}^{rel}$	$C_{p,\phi,2}$
$mol \cdot kg^{-1}$		$J \cdot K^{-1} \cdot mol^{-1}$	$J \cdot K^{-1} \cdot mol^{-1}$	$J \cdot K^{-1} \cdot mol^{-1}$	$J \cdot K^{-1} \cdot mol^{-1}$
		T = 283.15 K			
0.43883	0.03010	12.222	499.93	487.71	511.15
0.31145	0.03523	12.913	399.47	386.56	412.43
0.25852	0.03831	13.316	351.30	337.98	365.57
0.20120	0.04291	13.847	292.38	278.53	308.93
0.15109	0.04866	14.439	235.89	221.45	256.08
0.15109	0.04866	14.439	231.81	217.37	251.55
0.09994	0.05840	15.117	173.36	158.24	201.86
0.09994	0.05840	15.117	157.43	142.31	183.36
0.06059	0.07198	15.564	72.57	57.01	105.34
		T = 298.15 K			
0.43883	0.02504	6.868	609.03	602.17	619.21
0.31145	0.02925	7.138	535.11	527.97	550.18
0.25852	0.03177	7.305	499.22	491.91	517.50
0.20120	0.03553	7.526	454.15	446.63	477.53

Table A.III.9. Continued.

0.15109	0.04022	7.775	407.39	399.61	437.81
0.11335	0.04534	7.999	365.71	357.72	404.90
0.09994	0.04812	8.043	347.15	339.10	390.76
0.06059	0.05903	8.182	280.07	271.89	344.71
		T = 313.15 K			
0.43883	0.01924	3.370	669.27	665.90	678.97
0.31145	0.02239	3.406	607.76	604.35	623.60
0.25852	0.02427	3.443	577.83	574.39	597.70
0.20120	0.02706	3.494	539.61	536.12	565.80
0.15109	0.03050	3.556	499.78	496.23	534.78
0.11335	0.03420	3.611	461.40	457.78	507.12
0.09994	0.03629	3.611	446.05	442.44	497.47
0.06059	0.04409	3.607	388.00	384.39	467.27
		T = 328.15 K			
0.43883	0.01574	1.591	702.61	701.02	712.75
0.31145	0.01825	1.569	645.38	643.81	662.06
0.25852	0.01973	1.569	629.36	627.80	650.87
0.20120	0.02194	1.572	585.32	583.75	613.29

Table A.III.9. Continued.

0.15109	0.02462	1.581	543.67	542.09	580.84
0.11335	0.02746	1.589	505.00	503.41	553.52
0.09994	0.02914	1.581	483.19	481.61	536.91
0.06059	0.03505	1.557	396.24	394.68	473.04

Table A.IV.1. Experimental Apparent Molar Volumes V_{ϕ}^{exp} for {$Na_3NiDTPA$+ NaOH} (aq) at 298.15 K and 0.1MPa.

m_2	10^2m_3	$10^2(\rho - \rho_1^*)$	V_{ϕ}^{exp}	$V_{\phi,2}$
$mol \cdot kg^{-1}$	$mol \cdot kg^{-1}$		$cm^{-3} \cdot mol^{-1}$	$cm^{-3} \cdot mol^{-1}$
0.05913	0.2810	1.7327	210.79	220.99
0.06955	0.3514	2.0437	210.61	221.43
0.08387	0.3937	2.4381	211.61	221.71
0.09732	0.4539	2.8165	212.10	222.14
0.12922	0.5934	3.7013	213.15	223.07

Table A.IV.2. Experimental Apparent Molar Heat Capacities $C_{p,\phi}^{exp}$ for {$Na_3NiDTPA$ + NaOH}(aq) at 298.15 K and 0.1MPa.

m_2	10^2m_3	$10^2(c_p\rho/c_{p,1}^*\rho_1^* - 1)$	$C_{p,\phi}^{exp}$	$C_{p,\phi,2}$
$mol \cdot kg^{-1}$	$mol \cdot kg^{-1}$		$J \cdot K^{-1} \cdot mol^{-1}$	$J \cdot K^{-1} \cdot mol^{-1}$
0.05913	0.2810	-0.9325	241.02	255.69
0.06955	0.3514	-1.0792	244.49	260.08
0.08387	0.3937	-1.3005	251.36	265.97
0.09732	0.4539	-1.4874	260.41	275.16
0.12922	0.5934	-1.9230	276.51	291.38

Table A.IV.3. Experimental Apparent Molar Volumes V_ϕ and Heat Capacities $C_{p,\phi}$ of $Na_2FeDTPA(aq)$ and NaFeHDTPA(aq) at 298.15 K and 0.1 MPa.

m	$10^2(\rho-\rho_1^*)$	V_ϕ	$10^2(c_p\rho/c_{p,1}^*\rho_1^* - 1)$	$C_{p,\phi}$
$mol \cdot kg^{-1}$		$cm^{-3} \cdot mol^{-1}$		$J \cdot K^{-1} \cdot mol^{-1}$
		$Na_2FeDTPA$ (aq)		
0.01544	0.3953	234.42	-0.2409	311.74
0.01546	0.3961	234.59	-0.2428	316.92
0.02849	0.7253	235.27	-0.4464	314.86
0.03643	0.9253	235.40	-0.5748	309.66
0.04303	1.0898	235.74	-0.6710	317.91
0.05472	1.3800	236.15	-0.8491	321.16
0.10093	2.5090	237.03	-1.5185	338.06
		NaFeHDTPA (aq)		
0.01975	0.4437	243.78	-0.2828	409.10
0.02856	0.6386	244.36	-0.4154	400.57
0.04324	0.9621	244.70	-0.6224	406.45
0.05480	1.2145	244.95	-0.7800	412.59
0.07205	1.5908	244.86	-1.0173	414.62

Table A.V.1. Experimental Apparent Molar Volumes V_ϕ and Heat Capacities $C_{p,\phi}$ for Tartrate Systems from Temperatures 283.15 to 328.15 K and Pressure 0.1 MPa.

m	$10^2(\rho-\rho_1^*)$	V_ϕ	$10^2(c_p\rho/c_{p,1}^*\rho_1^*-1)$	$C_{p,\phi}$
$mol \cdot kg^{-1}$	$g \cdot cm^{-3}$	$cm^{-3} \cdot mol^{-1}$		$J \cdot K^{-1} \cdot mol^{-1}$
		$H_2Tar(aq)/NaHTar(aq)$, T = 283.15 K		
0.11456	1.7302	74.82	0.7248	155.15
0.20838	2.5106	75.31	0.3970	161.63
0.27229	3.0330	75.56	0.1998	167.61
0.36250	3.7551	75.94	-0.0523	175.91
0.38492	3.9342	75.98	-0.1058	178.21
		$NaHTar(aq)/Na_2Tar(aq)$, T = 283.15 K		
0.07609	1.6776	60.64	0.6679	-14.64
0.08932	1.8369	60.76	0.6028	-4.95
0.14089	2.4475	61.58	0.3374	14.12
0.15319	2.5905	61.82	0.3102	27.14
0.17872	2.8915	61.96	0.2039	35.57
0.22609	3.4425	62.34	0.0183	49.06
0.30977	4.3898	63.31	-0.2509	72.81
0.32067	4.5078	63.54	-0.2832	75.93
0.41414	5.5458	64.23	-0.5173	96.80

Table A.V.1. Continued.

		$Na_2Tar(aq)$, T = 283.15 K		
0.04305	0.6082	52.39	-0.3418	-113.97
0.04861	0.6849	52.74	-0.3808	-108.16
0.05187	0.7307	52.75	-0.4	-103.11
0.05783	0.8141	52.82	-0.4455	-102.54
0.06804	0.9557	53.06	-0.5125	-94.61
0.07581	1.0628	53.28	-0.5597	-87.55
0.09595	1.3408	53.6	-0.6859	-76.73
0.11361	1.5777	54.33	-0.7888	-65.33
0.11887	1.6508	54.29	-0.8181	-63.04
0.13844	1.9154	54.67	-0.9245	-53.17
0.14819	2.0457	54.9	-0.9762	-48.54
0.16453	2.2619	55.35	-1.0555	-39.62
		$H_2Tar(aq)$, T = 298.15 K		
0.09025	0.6032	83.2	-0.2331	236.3
0.09296	0.619	83.44	-0.2396	237.51
0.11008	0.7314	83.49	-0.2774	239.99
0.18712	1.2324	83.64	-0.4575	243.18
0.2112	1.3861	83.75	-0.5115	244.4
0.31591	2.0477	83.99	-0.7418	247.73

Table A.V.1. Continued.

0.37543	2.4199	84.04	-0.8681	249
0.39887	2.5624	84.13	-0.9191	249.55
0.50382	3.2066	84.18	-1.1349	251.19
0.50815	3.2273	84.3	-1.1411	251.94
0.61065	3.842	84.37	-1.3394	253.74
0.63864	4.0104	84.35	-1.3984	253.61
	$H_2Tar(aq)/NaHTar(aq)$, T = 298.15 K			
0.11456	0.9406	78.72	-0.3277	205.37
0.20838	1.6881	79.21	-0.5597	214.02
0.27229	2.1908	79.36	-0.7106	217.36
0.3625	2.8862	79.64	-0.9012	223.08
0.38492	3.0572	79.69	-0.9466	224.29
	$NaHTar(aq)/Na_2Tar(aq)$, T = 298.15 K			
0.07609	0.891	65.93	-0.3263	91.71
0.08932	1.0408	66.4	-0.3788	95.53
0.14089	1.6288	66.91	-0.5592	108.54
0.15319	1.7677	67.03	-0.6053	109.68
0.17872	2.056	67.18	-0.6799	116.27
0.21297	2.436	67.58	-0.7852	122.55
0.21949	2.5098	67.56	-0.8035	123.53
0.22609	2.5828	67.62	-0.8359	122.18

Table A.V.1. Continued.

0.24742	2.8167	67.85	-0.8768	129.42
0.30977	3.4958	68.36	-1.0279	140.59
0.32067	3.6151	68.39	-1.0403	143.78
0.41414	4.6113	69.07	-1.2218	158.4
		$Na_2Tar(aq)$, T = 298.15 K		
0.04305	0.5827	58.96	-0.2394	9.29
0.04861	0.657	59.09	-0.2645	14.74
0.04861	0.6553	59.45	-0.2688	12.53
0.04883	0.6565	59.8	-0.266	17.46
0.05187	0.6998	59.32	-0.2815	16.26
0.05761	0.7776	59.21	-0.3122	16.09
0.06804	0.9156	59.52	-0.3591	23.21
0.07581	1.018	59.74	-0.3935	27.71
0.07797	1.0472	59.7	-0.4065	26.54
0.08751	1.1709	60.13	-0.4421	35.04
0.09151	1.2233	60.22	-0.4646	34.29
0.09595	1.2831	60.14	-0.4822	36.07
0.11361	1.5122	60.61	-0.556	43.39
0.11887	1.5809	60.68	-0.5757	45.7
0.12345	1.6399	60.79	-0.5968	46.53
0.13361	1.7747	60.73	-0.6309	50.88
0.13844	1.8342	61.02	-0.654	51.95

Table.A.V.1. Continued.

0.14819	1.9584	61.27	-0.6884	56.18
0.16139	2.1333	61.14	-0.7409	57.82
0.16453	2.1699	61.41	-0.7502	60.21
		$H_2Tar(aq)$, T = 313.15 K		
0.06257	0.406	86.02	-0.1459	254.4
0.09025	0.5831	86.16	-0.1994	259.92
0.18712	1.1972	86.25	-0.3858	265.86
0.22921	1.4616	86.23	-0.4639	267.12
0.37543	2.3477	86.69	-0.7275	271.77
0.50382	3.1101	86.82	-0.9539	273.44
0.63864	3.8993	86.8	-1.1786	274.64
		$H_2Tar(aq)/NaHTar(aq)$, T = 313.15 K		
0.11456	0.1670	81.56	-1.3903	241.65
0.20838	0.8960	82.0	-1.5754	246.1
0.27229	1.3846	82.19	-1.6849	250.07
0.3625	2.0679	82.28	-1.8454	252.08
0.38492	2.2348	82.33	-1.8825	252.88
		$NaHTar(aq)/Na_2Tar(aq)$, T = 313.15 K		
0.07609	0.1192	69.67	-1.3945	142.27
0.08932	0.2693	69.68	-1.4276	147.05
0.14089	0.8428	70.32	-1.5744	154.27

Table A.V.1. Continued.

0.15319	0.9783	70.46	-1.6029	157.24
0.17872	1.2602	70.6	-1.6611	161.94
0.21297	1.6348	70.83	-1.7453	165.63
0.21949	1.7054	70.88	-1.761	166.34
0.22609	1.7769	70.93	-1.7695	168.4
0.30977	2.678	71.38	-1.938	178.39
0.32067	2.7926	71.48	-1.9559	180.1
0.41414	3.767	72.15	-2.1048	191.49
		$Na_2Tar(aq)$, T = 313.15 K		
0.04305	0.5696	62.82	-0.1935	63.94
0.04861	0.6459	62.2	-0.2167	62.8
0.04861	0.6405	63.32	-0.2172	67.04
0.05187	0.6872	62.59	-0.2289	66.22
0.05761	0.7621	62.74	-0.2524	68.11
0.06804	0.8945	63.48	-0.2887	76.82
0.07581	0.996	63.51	-0.3204	77.55
0.08751	1.1474	63.67	-0.3647	80.61
0.09595	1.2563	63.8	-0.3918	84.59
0.11361	1.4814	64.19	-0.4508	90.86
0.12345	1.6081	64.24	-0.486	92.28

Table A.V.1. Continued.

0.13844	1.793	64.86	-0.5292	99.55
0.14919	1.9235	64.49	-0.5584	100.25
0.16453	2.1271	64.87	-0.6024	106.19
		$H_2Tar(aq)$, T = 328.15 K		
0.09025	0.5793	87.56	-0.2758	224.44
0.18712	1.1769	88.32	-0.4117	263.03
0.18712	1.1769	88.32	-0.3495	277.15
0.22921	1.4331	88.9	-0.4925	265.53
0.22921	1.423	88.46	-0.4572	273.96
0.37543	2.316	88.95	-0.7033	276.62
0.37543	2.2994	88.5	-0.6703	282.29
0.50382	3.0512	88.93	-0.8922	282.25
0.50382	3.0525	88.95	-0.8558	285.3
0.63864	3.8263	88.91	-1.0736	285.29
0.63864	3.804	89.26	-1.0458	288.7
		$H_2Tar(aq)/NaHTar(aq)$, T= 328.15 K		
0.11456	0.8997	84.12	-0.2019	262.91
0.20838	1.6176	84.4	-0.3532	266.57
0.20838	1.6166	84.46	-0.3514	267.16
0.27229	2.0974	84.59	-0.4523	268.53
0.3625	2.7659	84.74	-0.592	269.99
0.38492	2.9295	84.79	-0.625	270.52

Table A.V.1. Continued.

		NaHTar(aq)/Na_2Tar(aq), T = 328.15 K		
0.07609	0.8559	72.6	-0.1996	175.48
0.08932	1.0011	72.9	-0.249	169.8
0.08932	1.0016	72.84	-0.2421	172.81
0.14089	1.5712	73.03	-0.3708	176.65
0.15319	1.7012	73.4	-0.3814	184.13
0.17872	1.9828	73.3	-0.4444	183.72
0.21297	2.3448	73.87	-0.5139	189.06
0.21949	2.4184	73.72	-0.5381	186.82
0.22609	2.4859	73.91	-0.5357	191.02
0.30977	3.3659	74.52	-0.6983	198.12
0.32067	3.4897	74.26	-0.7033	199.63
0.41414	4.4515	74.85	-0.8206	210.8
		Na_2Tar(aq), T = 328.15 K		
0.04305	0.5645	65.28	-0.1744	83.87
0.05761	0.7526	65.76	-0.1996	92.18
0.07581	0.9885	65.76	-0.3134	82
0.07797	1.0232	65.76	-0.3215	78.2
0.07797	1.0135	66.16	-0.2987	96.42

Table A.V.1. Continued.

0.0875	1.144	65.32	-0.3442	88.45
0.09595	1.2492	65.8	-0.364	96.32
0.09595	1.2582	66.54	-0.355	95.19
0.11887	1.5372	66.48	-0.4407	102.62
0.13361	1.7219	66.8	-0.4827	107.83
0.14819	1.9046	67.02	-0.5266	111.14
0.16453	2.106	67.4	-0.5588	119.28

Table A.V.2. Experimental Apparent Molar Volumes V_ϕ for $H_2Tar(aq)$ and $Na_2Tar(aq)$ from Temperatures 377 to 529 K and Pressure 10 MPa.

m	$10^2(\rho-\rho_1^*)$	V_ϕ	m	$10^2(\rho-\rho_1^*)$	V_ϕ
$mol \cdot kg^{-1}$	$g \cdot cm^{-3}$	$cm^{-3} \cdot mol^{-1}$	$mol \cdot kg^{-1}$	$g \cdot cm^{-3}$	$cm^{-3} \cdot mol^{-1}$
		$H_2Tar(aq)$			
T = 377.11 K, p = 10.43 MPa			T = 426.37 K, p = 10.41 MPa		
0.11837	0.7122	90.38	0.11837	0.6885	93.73
0.18688	1.1031	91.23	0.18688	1.0801	93.77
0.30713	1.7896	91.41	0.30713	1.7395	94.45
0.30713	1.8	91.03	0.38176	2.1603	94.09
0.38176	2.2058	91.51	0.50865	2.8458	94.14
0.50865	2.8974	91.76	0.62124	3.4346	94.31
0.62124	3.4818	92.17			
0.62124	3.4672	92.43			
T = 475.83 K, p = 10.47 MPa			T = 529.09 K, p = 10.42 MPa		
0.11837	0.6826	95.57	0.11837	0.6947	95.1
0.11837	0.6834	95.62	0.30713	1.7682	95.56
0.18688	1.0667	95.96	0.25336	1.4638	95.6
0.30713	1.7357	95.97	0.42153	2.3897	96.18
0.38176	2.1489	95.82	0.62124	3.4567	96.53
0.50865	2.8135	96.36			
0.62124	3.4007	96.46			

Table A.V.2. Continued.

$Na_2Tar(aq)$					
T = 377.06 K, p = 10.48 MPa			T = 426.38 K, p = 10.47 MPa		
0.12003	1.5135	64.33	0.12003	1.5325	59.05
0.12003	1.4985	65.67	0.12314	1.5624	59.97
0.12003	1.506	65	0.20877	2.5964	62.2
0.12144	1.5159	65.68	0.25128	2.621	61.51
0.12144	1.5188	65.43	0.31681	3.9043	62.63
0.20878	2.5488	67.88	0.42442	5.1771	63.22
0.25128	3.0594	67.91	0.58914	7.0291	64.97
0.32206	3.8722	68.93			
0.42442	5.0484	69.44			
0.58914	6.853	70.88			
0.61424	7.1166	71.17			
T = 477.73 K, p = 10.45 MPa			T = 529.02 K, p = 10.42 MPa		
0.12003	1.6267	42.54	0.12003	1.8378	4.17
0.12314	1.6568	43.85	0.12314	1.8252	8.43
0.20878	2.7843	44.82	0.25128	3.6659	13.3
0.25128	3.3461	44.8	0.31681	4.5272	17.59
0.31681	4.1828	45.83	0.50891	7.0723	22.79
0.42442	5.4932	48.43	0.58914	8.0177	26.68
0.50891	6.4851	50.39			
0.58914	7.4698	50.64			

Appendix B: Dissociation Contribution Calculation

The ionization reactions for L-tartaric acid in aqueous solution can be expressed as

$$\begin{array}{llll} H_2Tar(aq) & \rightleftharpoons & H^+(aq) + & HTar^-(aq) \\ (1 - \alpha_1 - \alpha_2)m & & (\alpha_1 + 2\alpha_2)m & \alpha_1 m \end{array} \qquad \text{(B1)}$$

$$\begin{array}{llll} HTar^-(aq) & \rightleftharpoons & H^+(aq) + & Tar^{2-}(aq) \\ \alpha_1 m & & (\alpha_1 + 2\alpha_2)m & \alpha_2 m \end{array} \qquad \text{(B2)}$$

Here α_1 and α_2 are the degree of dissociation. The experimental apparent molar heat capacities $C_{p,\phi}^{expt}$ of $H_2Tar(aq)$ are considered to result from the sum of the contributions from each species in solution, plus an additional term to correct for the shift in the degree of hydrolysis caused by the temperature increment in the heat capacity measurement, the so-called "chemical relaxation effect". In the current experimental conditions, the degree of the secondary step of dissociation is so small that it can be neglected. According to equation (B1), the apparent molar heat capacity for $H_2Tar(aq)$ is expressed by

$$C_{p,\phi}^{expt}(H_2Tar, aq) = (1-\alpha_1)C_{p,\phi}(H_2Tar, aq) + \alpha_1 C_{p,\phi}(HTar^-, aq) + \alpha_1 C_{p,\phi}(H^+, aq) + C_{p,\phi}^{rel} \qquad \text{(B3)}$$

where the chemical relaxation contribution $C_{p,\phi}^{rel} = \Delta H_r(\partial\alpha_1/\partial T)_m$, and ΔH_r is the reaction enthalpy. The expression for V_ϕ^{expt} is similar with that of $C_{p,\phi}^{expt}$, but there is no

contribution from chemical relaxation. The equilibrium constant reported by Robinson and Stokes (1959) was used to calculate the degree of dissociation α_1 with the activity coefficient $\gamma_\pm$ according to the Pitzer ion interaction model (1991) based on the following equations

$$K(T, p) = \alpha_1^2 m \gamma_\pm^2/(1-\alpha_1) \tag{B4}$$

and

$$\ln\gamma_\pm = -|z_H z_{HTar}| A_\phi [I^{1/2}/(1+1.2I^{1/2}) + (2/1.2)\ln(1+1.2I^{1/2})] \tag{B5}$$

where A_ϕ is the osmotic slope in the Debye-Hückel limiting law from Archer and Wang (1991). Because the degree of dissociation is general small, the contributions from $C_{p,\phi}(HTar^-, aq)$ and $C_{p,\phi}(H^-, aq)$ can be approximately calculated from equation

$$C_{p,\phi}(HTar^-, aq) + C_{p,\phi}(H^-, aq) = C_p^o(HTar^-, aq) + C_p^o(H^-, aq) + \upsilon|z_H z_{HTar}|(A_J/2.4)(1 + 1.2I^{1/2}) \tag{B6}$$

where υ is the stoichiometric sum of the number of ions, and A_J is the Debye-Hückel limiting slope, calculated again from Archer and Wang (1991). The values of ΔH_r^o obtained by Bates and Canham(1951) were used to calculate the ΔH_r of reaction (B1). The standard partial molar heat capacities of $HTar^-(aq)$ ion were also calculated from $\Delta C_{p,r}^o$ (Bates and Canham, 1951) with the initial values of $C_p^o(H_2Tar, aq)$ obtained by

fitting the equation (V.3.7) without any corrections for ionization.

The equilibrium constants of $H_2Tar(aq)$ at high temperatures and p = 10 MPa were obtained from the density model of Anderson *et al.* (1991)

$$\ln K = \ln K_r - (1/R)\Delta H^\circ_r[(1/T) - (1/T_r)] + \Delta cr_r[(1/T)\ln(\rho^*_{l,r}/\rho) - \alpha^*_{l,r}(T - T_r)/T]/[RT_r(\partial\alpha^*_l/\partial T)_{Pr}] \qquad \text{(B7)}$$

where ρ^*_l is the density of water, α^*_l is the coefficient of the thermal expansion of water, and r refers to the reference state. It should be understood that K is equilibrium constant at T and p, K_r is the equilibrium constant at T_r and p_r. ΔH°_r at T_r = 298. 15 K and p_r = 0.1 MPa was obtained from Bates and Canham (1951), and ΔC°_{pr}(298.15 K, 0.1MPa) is from this study.

Appendix C: X-Ray Crystal Structure Determination of $H_3CuDTPA$

Single X-Ray Diffraction Structure Report for $H_3CuDTPA$

David O. Miller, Wei Xie and Peter Tremaine

Chemistry Department

Memorial University of Newfoundland

June 9, 1998

Introduction

Collection, solution and refinement all proceeded normally. Hydrogens were optimized by positional refinement with isotropic thermal parameters set twenty percent greater than those of their bonding partners at the time of their inclusion.

Experimental

Data Collection

A blue irregular crystal of $C_{14}H_{23}O_{11}N_3Cu$ having approximate dimensions of 0.20 x 0.05 x 0.42 mm was mounted on a glass fiber. All measurements were made on a Rigaku AFC6S diffractometer with graphite monochromated Mo-Kα radiation.

Cell constants and an orientation matrix for data collection, obtained from a least-squares refinement using the setting angles of 18 carefully centered reflections in the range $21.11 < 2\theta < 26.98^\circ$ corresponded to a primitive triclinic cell with dimensions:

a = 9.522(2) Å	α = 94.20(2)$^\circ$
b = 16.288(3) Å	β = 104.65(2)$^\circ$
c = 6.438(1) Å	γ = 101.30(2)
V = 939.3(4) Å^3	

For Z = 2 and F.W. = 472.90, the calculated density is 1.67 g/cm^3. Based on a statistical analysis of intensity distribution,and the successful solution and refinement of thestructure, the space group was determined to be:

Po($\bar{}$,1) (#2)

The data were collected at a temperature of 26 $\pm$ 1° C using the ω-2θ scan technique to a maximum 2θ value of 55.1° .Omega scans of several intense reflections, made prior to data collection, had an average width at half-height of 0.30° with a take-off angle of 6.0° . Scans of (1.10 + 0.35 tan θ)$^\circ$ were made at a speed of 4.0° /min (in ω). The weak reflections ($I < 10.0\sigma(I)$) were rescanned (maximum of 10 scans) and the counts were accumulated to ensure good counting statistics. Stationary background counts were recorded on each side of the reflection. The ratio of peak counting time to background counting time was 2:1. The diameter of the incident beam collimator was 1.0 mm, the crystal to detector distance was 400 mm, and the detector aperture was 4.5 x 3.0 mm

(horizontal x vertical).

Data Reduction

Of the 4608 reflections which were collected, 4346 were unique ($R_{int} = 0.030$); equivalent reflections were removed. The intensities of three representative reflection were measured after every 150 reflections. No decay correction was applied.

The linear absorption coefficient, μ, for Mo-Kα radiation is 12.3 cm^{-1}. An empirical absorption correction based on azimuthal scans of several reflections was applied which resulted in transmission factors ranging from 0.89 to 1.00. The data were corrected for Lorentz and polarization effects.

Structure Solution and Refinement

The structure was solved by direct methods[1] and expanded using Fourier techniques.[2] The non-hydrogen atoms were refined anisotropically. The hydrogen atom coordinates were refined but their isotropic B's were held fixed The final cycle of full-matrix least-squares refinement[3] was based on 3536 observed reflections ($I > 2.00\sigma(I)$) and 331 variable parameters and converged (largest parameter shift was 0.00 times its esd) with unweighted and weighted agreement factors of:

$$R = \Sigma \, ||Fo| - |Fc|| \, / \, \Sigma \, |Fo| = 0.042$$

$$R_w = [(\Sigma \, w \, (|Fo| - |Fc|)^2 \, / \, \Sigma \, w \, Fo^2)]^{1/2} = 0.042$$

The standard deviation of an observation of unit weight[4] was 1.99. The weighting schemewas based on counting statistics and included a factor ($p = 0.005$) to downweight the intense reflections. Plots of $\Sigma \, w \, (|Fo| - |Fc|)^2$ versus $|Fo|$,reflection order in data collection, $\sin \theta/\lambda$ and various classes of indices showed no unusual trends. The maximum and minimum peaks on the final difference Fourier map corresponded to 0.42 and -0.60 $e^-/Å^3$, respectively.

Neutral atom scattering factors were taken from Cromer and Waber.[5] Anomalous dispersion effects were included in Fcalc;[6] the values for $\Delta f'$ and $\Delta f''$ were those of Creagh and McAuley.[7] The values for the mass attenuation coefficients are those of Creagh and

Hubbell.[8] All calculations were performed using the teXsan[9] crystallographic software package of Molecular Structure Corporation.

References

(1) SIR92: Altomare, A., Cascarano, M., Giacovazzo, C., Guagliardi, A. (1993). J. Appl. Cryst., 26, 343.

(2) DIRDIF94: Beurskens, P.T., Admiraal, G., Beurskens, G., Bosman, W.P., de Gelder, R., Israel, R. and Smits, J.M.M.(1994). The DIRDIF-94 program system, Technical Report of the Crystallography Laboratory, University of Nijmegen, The Netherlands.

(3) Least Squares function minimized:

$\Sigma w(|F_o|-|F_c|)^2$ where

$$w = 1/[\sigma^2(Fo)] = [\sigma^2_c(Fo) + p^2Fo^2/4]^{-1}$$

$\sigma_c(Fo)$ = e.s.d. based on counting statistics

p = p-factor

(4) Standard deviation of an observation of unit weight:

$$[\Sigma w(|F_o|-|F_c|)^2/(N_o-N_v)]^{1/2}$$

where N_o = number of observations

N_v = number of variables

(5) Cromer, D. T. & Waber, J. T.; "International Tables for X-ray Crystallography", Vol. IV, The Kynoch Press, Birmingham, England, Table 2.2 A (1974).

(6) Ibers, J. A. & Hamilton, W. C.; Acta Crystallogr., 17, 781 (1964).

(7) Creagh, D. C. & McAuley, W.J .; "International Tables for Crystallography", Vol C, (A.J.C. Wilson, ed.), Kluwer Academic Publishers, Boston, Table 4.2.6.8, pages 219-222 (1992).

(8) Creagh, D. C. & Hubbell, J.H..; "International Tables for Crystallography", Vol C, (A.J.C. Wilson, ed.), Kluwer Academic Publishers, Boston, Table 4.2.4.3, pages 200-206 (1992).

(9) teXsan for Windows: Crystal Structure Analysis Package, Molecular Structure Corporation (1997).

EXPERIMENTAL DETAILS

A. Crystal Data

Empirical Formula	$C_{14}H_{23}O_{11}N_3Cu$
Formula Weight	472.90
Crystal Color, Habit	blue, irregular
Crystal Dimensions	0.20 X 0.05 X 0.42 mm
Crystal System	triclinic
Lattice Type	Primitive
No. of Reflections Used for Unit	
Cell Determination (2θ range)	18 (21.1 - 27.0°)
Omega Scan Peak Width	
at Half-height	0.30°
Lattice Parameters	a = 9.522(2)Å
	b = 16.288(3) Å
	c = 6.438(1) Å
	α = 94.20(2)°

	$\beta = 104.65(2)^{\circ}$
	$\gamma = 101.30(2)^{\circ}$
	$V = 939.3(4)$ Å^3
Space Group	Po($\bar{}$,1) (#2)
Z value	2
D_{calc}	1.672 g/cm^3
F_{000}	490.00
μ(MoKα)	12.29 cm^{-1}

B. Intensity Measurements

Diffractometer	Rigaku AFC6S
Radiation	MoKα (λ = 0.71069 Å)
	graphite monochromated
Take-off Angle	6.0°
Detector Aperture	4.5 mm horizontal
	3.0 mm vertical
Crystal to Detector Distance	400 mm
Voltage, Current	50kV, 27.5mA
Temperature	26.0°C

Scan Type	ω-2θ
Scan Rate	4.0°/min (in ω) (up to 10 scans)
Scan Width	$(1.10 + 0.35 \tan \theta)^{\circ}$
$2\theta_{max}$	55.1°
No. of Reflections Measured	Total: 4608
	Unique: 4346 ($R_{int} = 0.030$)
Corrections	Lorentz-polarization Absorption (trans. factors: 0.8897 - 1.0000)

C. Structure Solution and Refinement

Structure Solution	Direct Methods (SIR92)
Refinement	Full-matrix least-squares
Function Minimized	$\Sigma\, w\, (\lvert Fo\rvert - \lvert Fc\rvert)^2$
Least Squares Weights	$1/\sigma^2(Fo) = 4Fo^2/\sigma^2(Fo^2)$
p-factor	0.0046
Anomalous Dispersion	All non-hydrogen atoms
No. Observations ($I>2.00\sigma(I)$)	3536
No. Variables	331

Reflection/Parameter Ratio	10.68
Residuals: R; Rw	0.042 ; 0.042
Goodness of Fit Indicator	1.99
Max Shift/Error in Final Cycle	0.00
Maximum peak in Final Diff. Map	0.42 $e^-/Å^3$
Minimum peak in Final Diff. Map	-0.60 $e^-/Å^3$

Table C.1. Positional Parameters for $H_3CuDTPA{\cdot}H_2O$.

atom	x	y	z
Cu(1)	0.34325(3)	0.24857(2)	0.79019(5)
O(1)	-0.0835(2)	0.0999(1)	1.2107(4)
O(2)	-0.1229(2)	0.2187(1)	1.0921(3)
O(3)	0.0559(2)	0.3921(1)	0.5654(3)
O(4)	0.2610(2)	0.3438(1)	0.6770(3)
O(5)	0.6990(2)	0.4688(1)	0.8919(4)
O(6)	0.5770(2)	0.3383(1)	0.7411(3)
O(7)	0.7395(2)	0.1002(1)	0.6090(4)
O(8)	0.6135(2)	0.0195(1)	0.7985(3)
O(9)	0.2218(2)	0.1690(1)	0.5331(3)
O(10)	0.1431(2)	0.0324(1)	0.4175(3)
O(11)	0.8172(3)	0.4678(2)	0.5791(5)
N(1)	0.1434(2)	0.2482(1)	0.9453(3)
N(2)	0.4688(2)	0.3059(1)	1.0897(3)
N(3)	0.4498(2)	0.1506(1)	0.8452(3)
C(1)	-0.0488(3)	0.1666(2)	1.1111(4)
C(2)	0.0806(3)	0.1684(2)	1.0114(4)
C(3)	0.0397(3)	0.2782(2)	0.7736(4)
C(4)	0.1251(3)	0.3435(2)	0.6644(4)
C(5)	0.2171(3)	0.3147(2)	1.1316(4)
C(6)	0.3717(3)	0.3051(2)	1.2416(4)
C(7)	0.5425(3)	0.3939(2)	1.0758(4)

Table C.1 Continued.

atom	x	y	z
C(8)	0.6072(3)	0.3968(2)	0.8834(4)
C(9)	0.5829(3)	0.2553(2)	1.1644(4)
C(10)	0.5186(3)	0.1619(1)	1.0840(4)
C(11)	0.5609(3)	0.1560(2)	0.7197(4)
C(12)	0.6394(3)	0.0832(1)	0.7178(4)
C(13)	0.3271(3)	0.0749(1)	0.7591(4)
C(14)	0.2235(3)	0.0926(2)	0.5531(4)
H(1)	0.049(3)	0.129(2)	0.881(4)
H(2)	0.159(3)	0.148(2)	1.112(4)
H(3)	-0.024(3)	0.229(2)	0.662(4)
H(4)	-0.030(3)	0.302(2)	0.823(4)
H(5)	0.223(3)	0.366(2)	1.082(4)
H(6)	0.163(3)	0.319(2)	1.228(4)
H(7)	0.778(3)	0.068(2)	0.596(5)
H(8)	0.418(3)	0.347(2)	1.357(4)
H(9)	0.472(3)	0.427(2)	1.055(4)
H(10)	0.616(3)	0.420(2)	1.211(6)
H(11)	0.857(3)	0.516(2)	0.568(7)
H(12)	0.619(3)	0.263(2)	1.327(4)
H(13)	0.445(3)	0.142(2)	1.147(4)
H(14)	0.587(3)	0.128(2)	1.130(4)
H(15)	0.512(3)	0.161(1)	0.556(4)
H(16)	0.636(3)	0.205(2)	0.769(4)

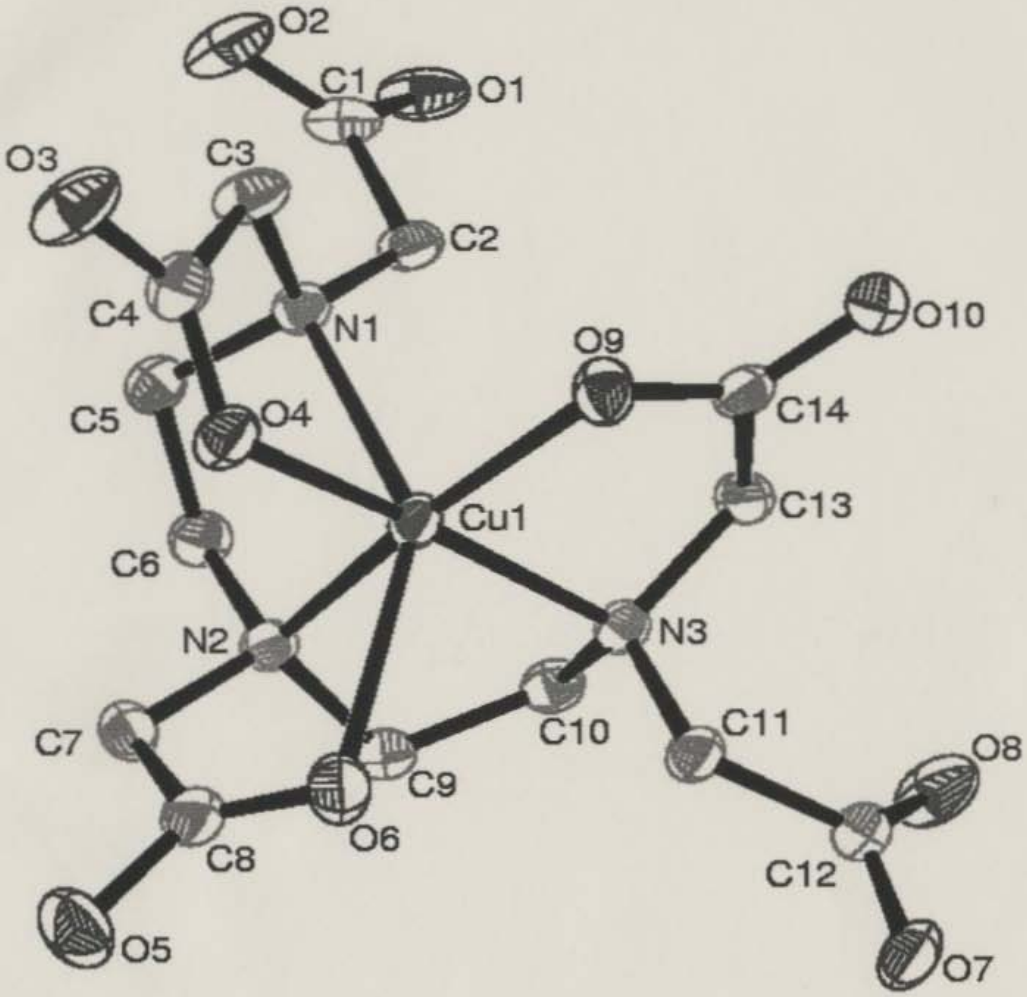

Figure C.1. An ORTEP plot of $H_3CuDTPA$